What's up in the dark side of the sky ?

Pierre Salati – Université de Savoie & **LAPTH**

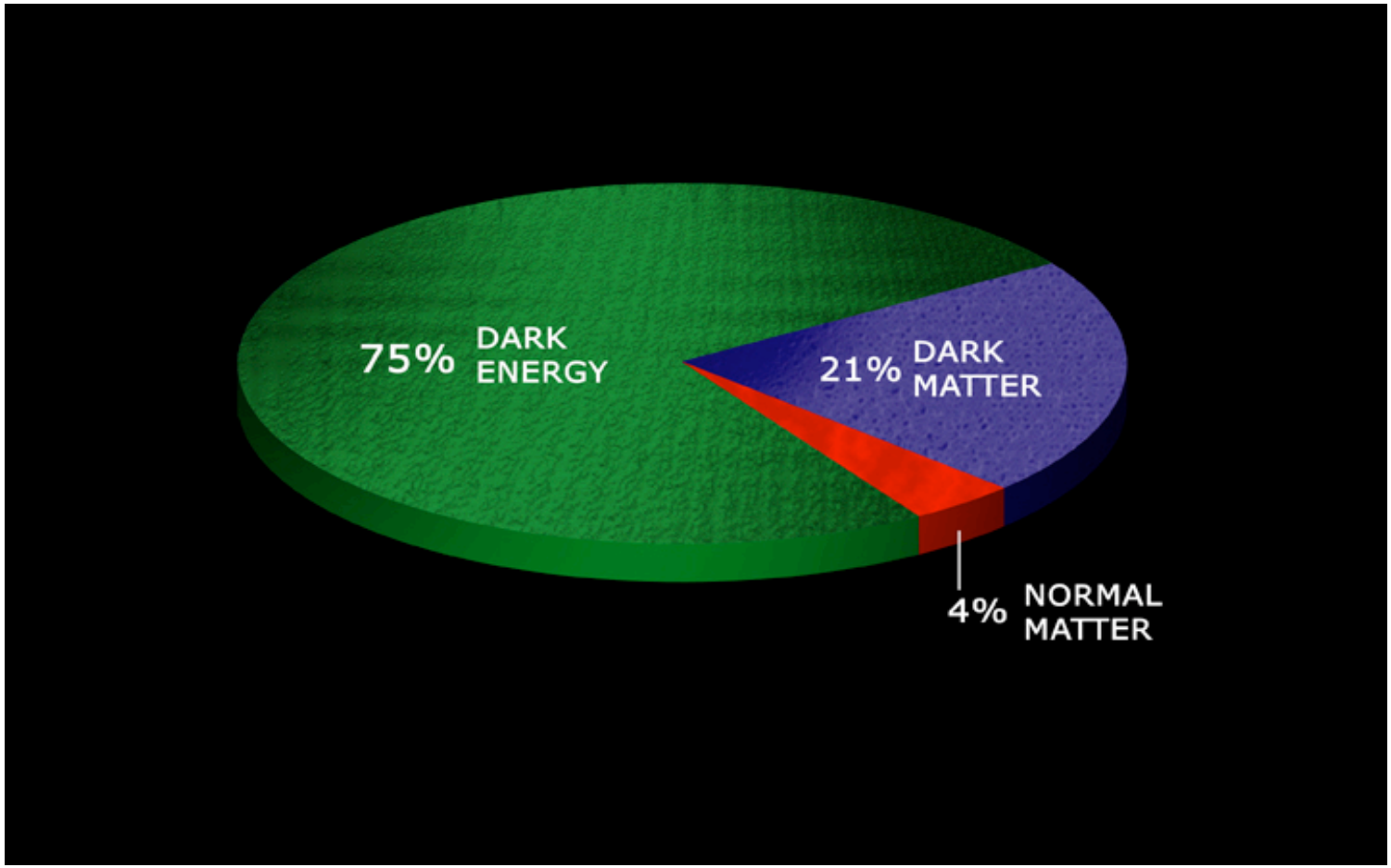

Rencontres de Physique des Particules – LPSC – 1 Mars 2007

Outline

1) Has MOND taken a bullet ?

2) Dark matter tomography – clumps & filaments

3) Computing the odds of the galactic lottery

4) Conclusions and perspectives

Rencontres de Physique des Particules – LPSC – 1 Mars 2007

1) Has MOND taken a bullet ?

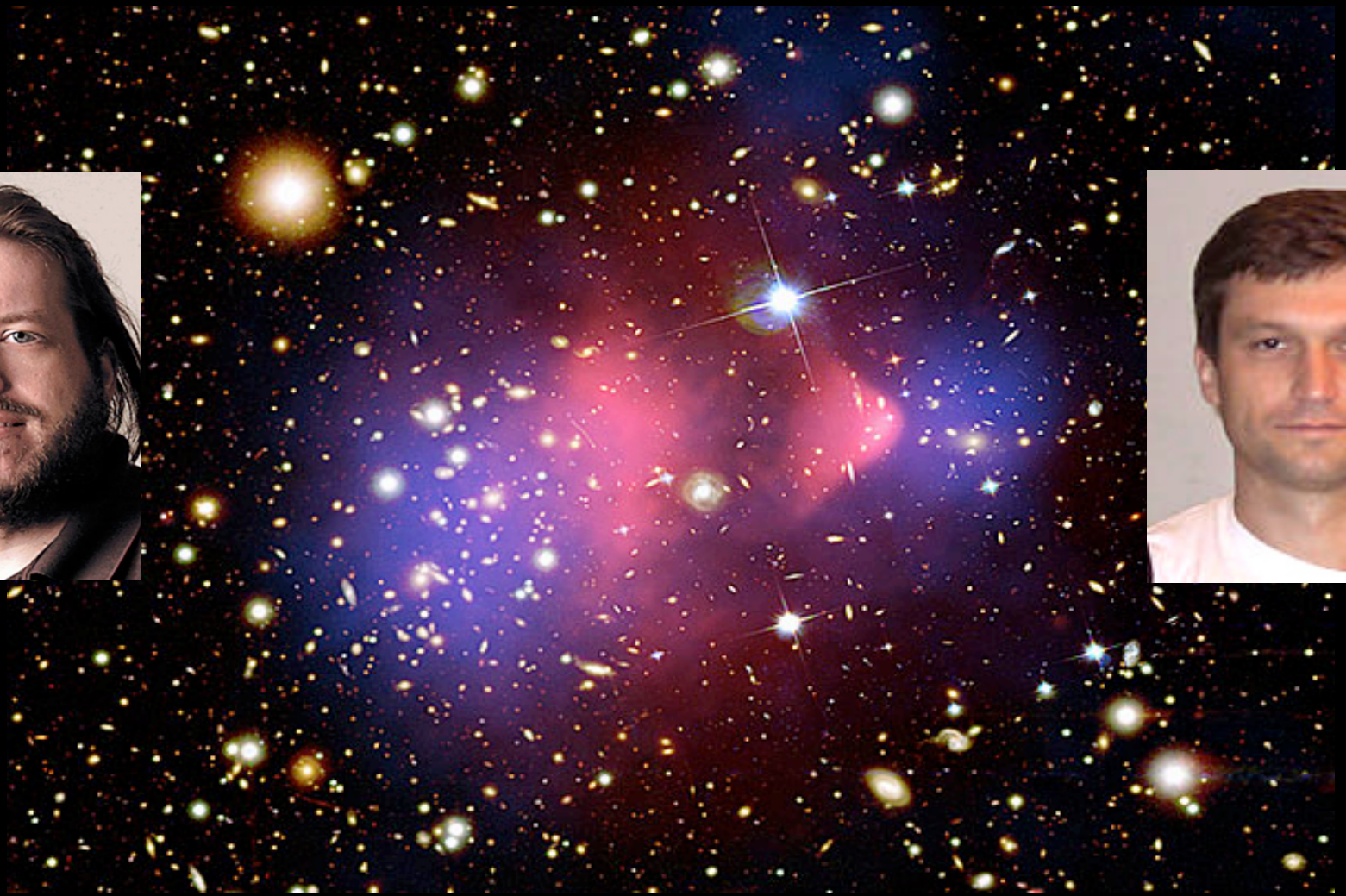

*BASED ON OBSERVATIONS MADE WITH THE NASA/ESA HUBBLE SPACE TELESCOPE, OBTAINED AT THE SPACE TELESCOPE SCIENCE INSTITUTE, WHICH IS OPERATED BY THE ASSOCIATION OF UNIVERSITIES FOR RESEARCH IN ASTRONOMY, INC., UNDER NASA CONTRACT NAS 5–26555, UNDER PROGRAM 10200, THE 6.5 METER MAGELLAN TELESCOPES LOCATED AT LAS CAMPANAS OBSERVATORY, CHILE, THE ESO TELESCOPES AT THE PARANAL OBSERVATORIES UNDER PROGRAM IDS 72.A-0511, 60.A-9203, AND 64.O-0332, AND WITH THE NASA CHANDRA X-RAY OBSERVATORY, OPERATED BY THE SMITHSONIAN ASTROPHYSICS OBSERVATORY UNDER CONTRACT TO NASA.

The bullet cluster : hot gas

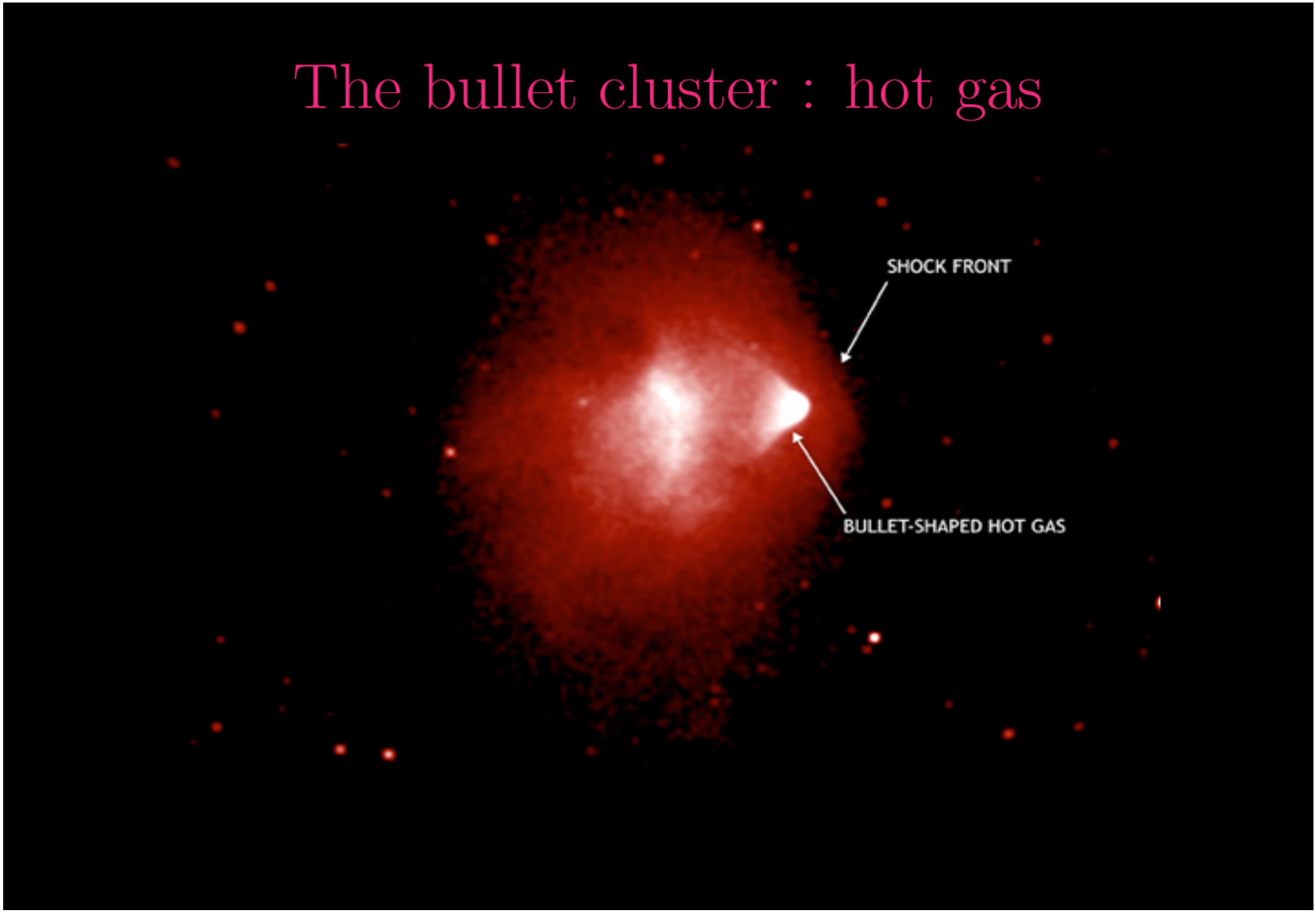

The bullet cluster : optical + dark matter

Dark matter and hot gas are different !

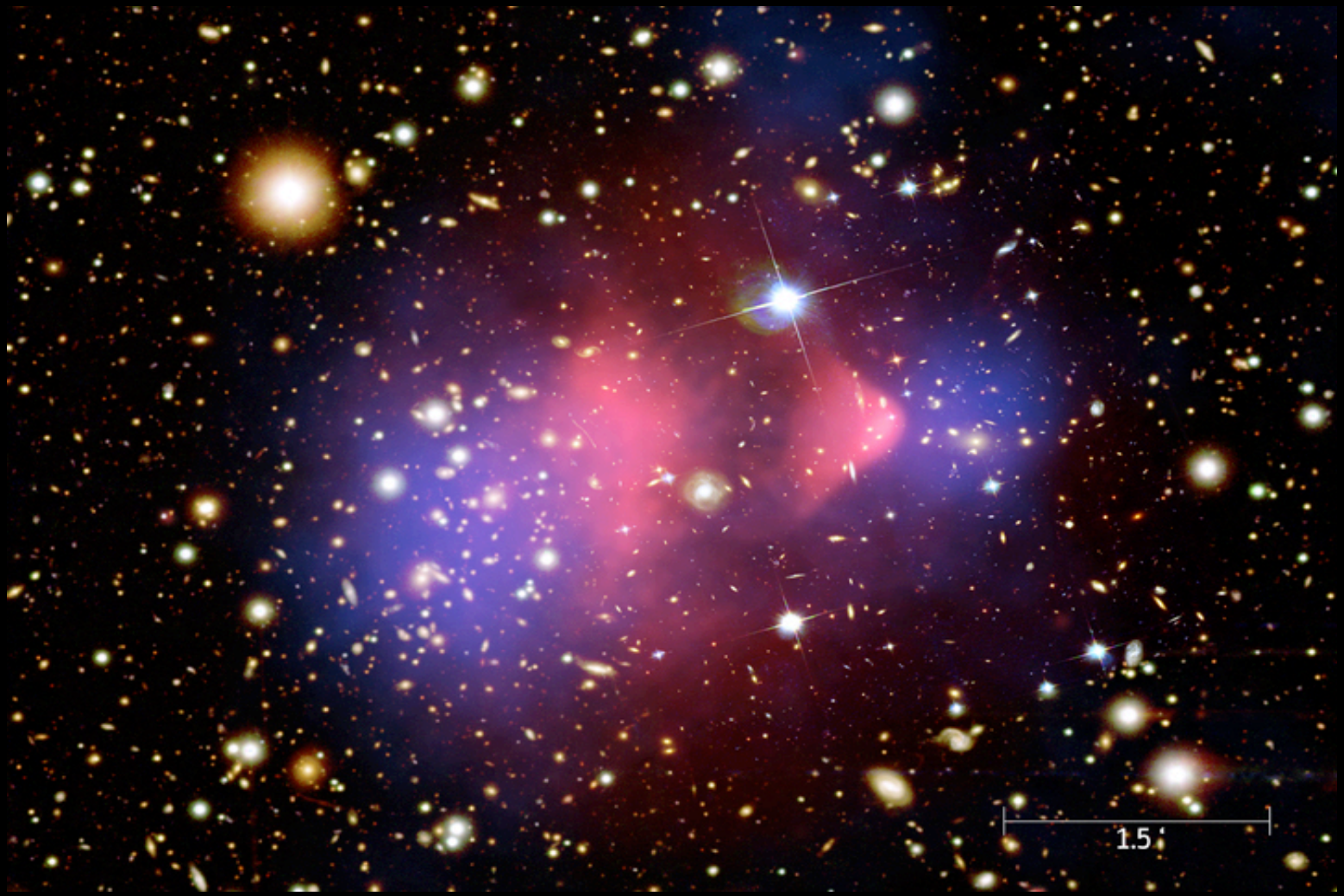

The two subclusters have collided 150 Myr ago

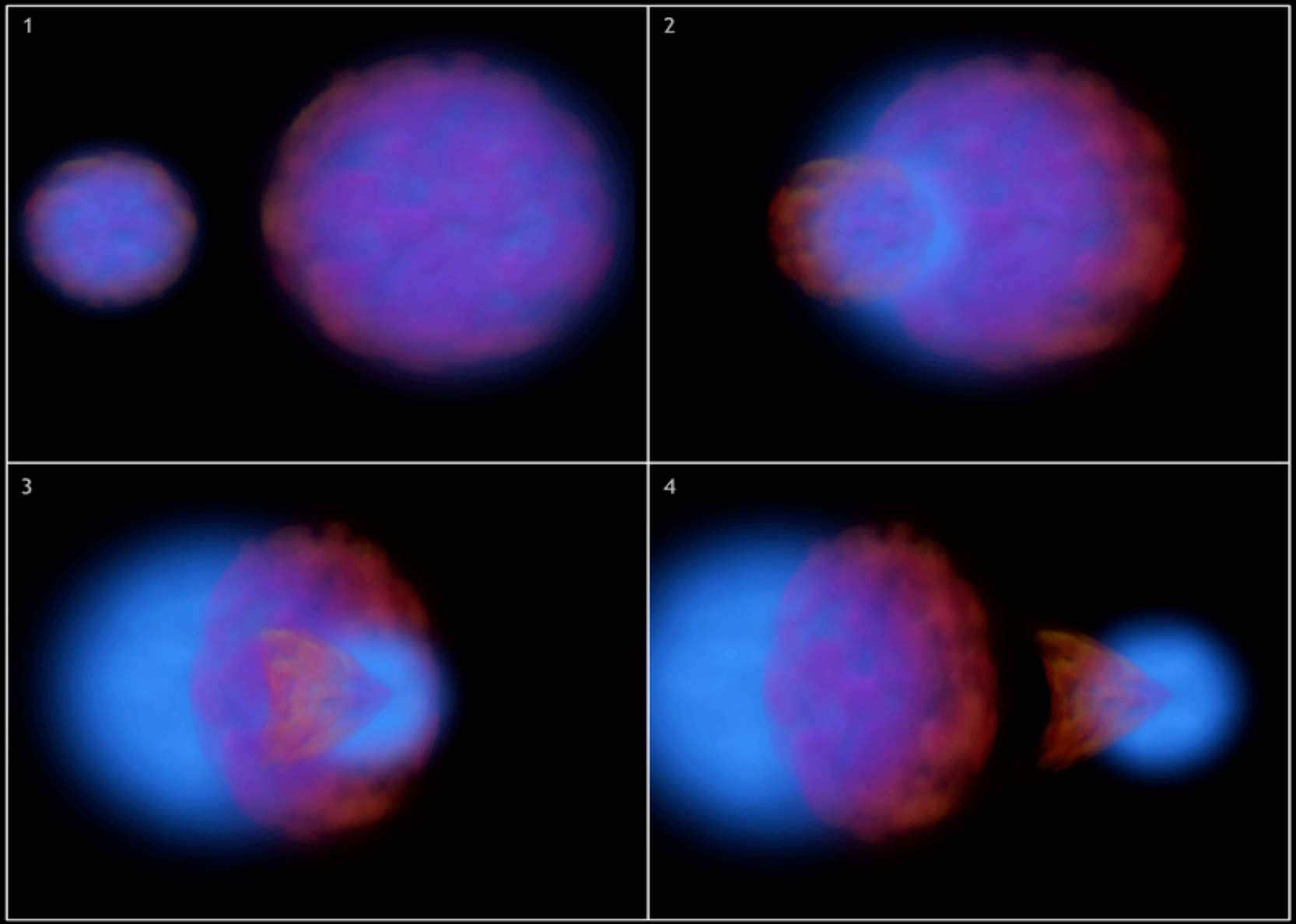

Optical Image with Chandra X–ray Contours

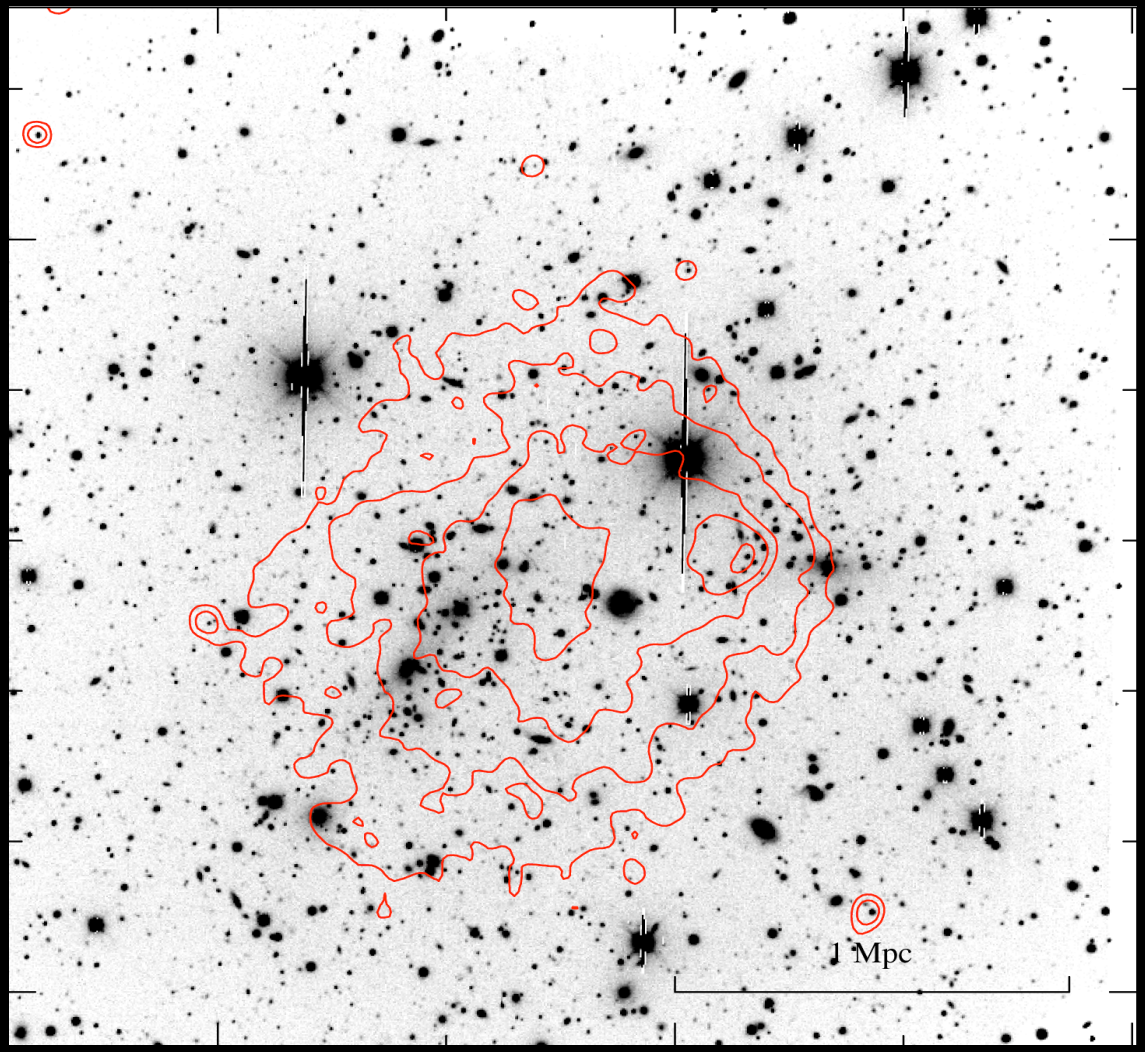

NASA Chandra

ESO NTT

HST Image with κ-Map Contours

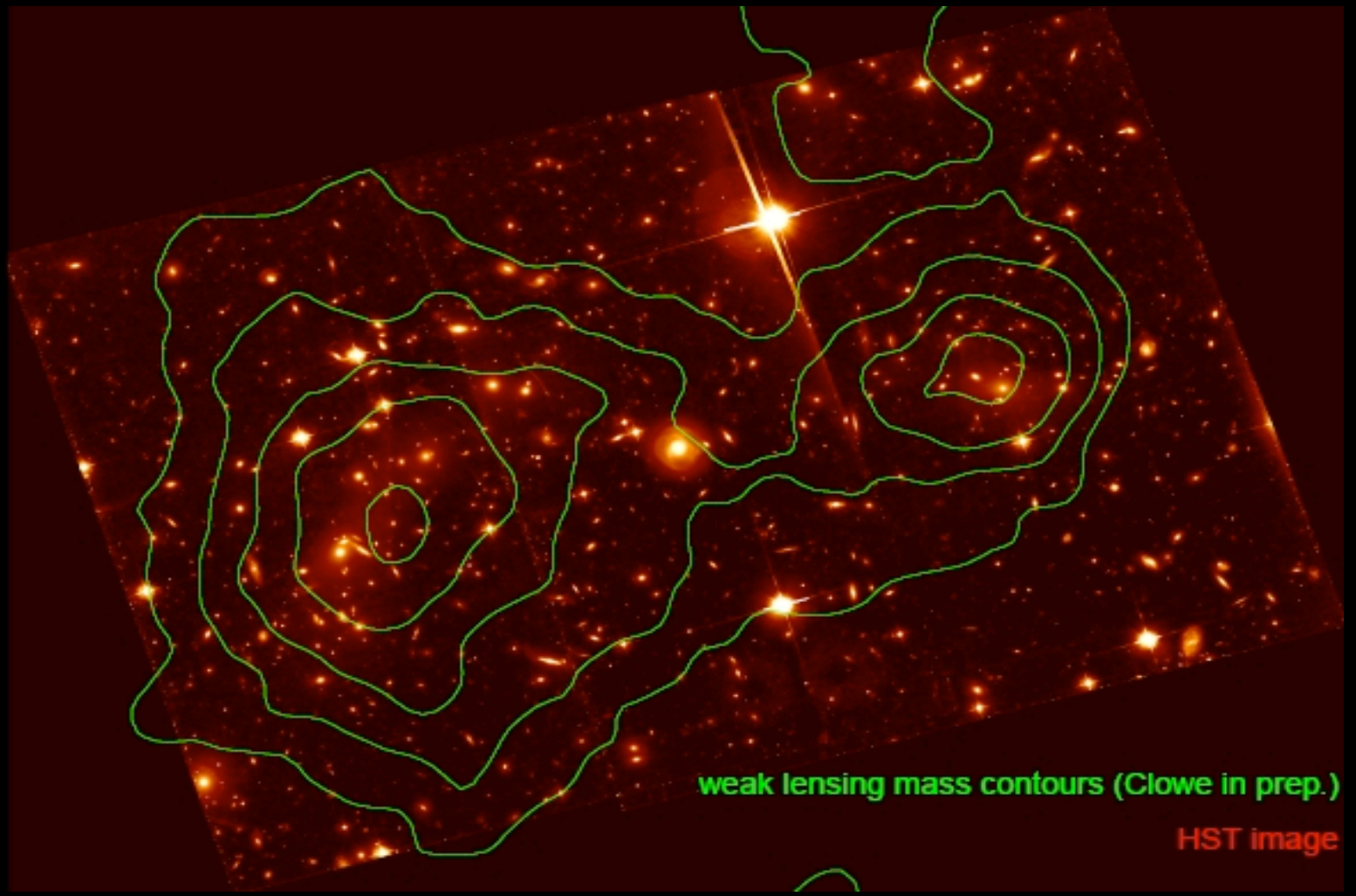

Gravitational Lensing : a Speaker's Digest

$$\frac{d\vec{e}}{ds} = -2\vec{\nabla}_{\perp}\Phi$$

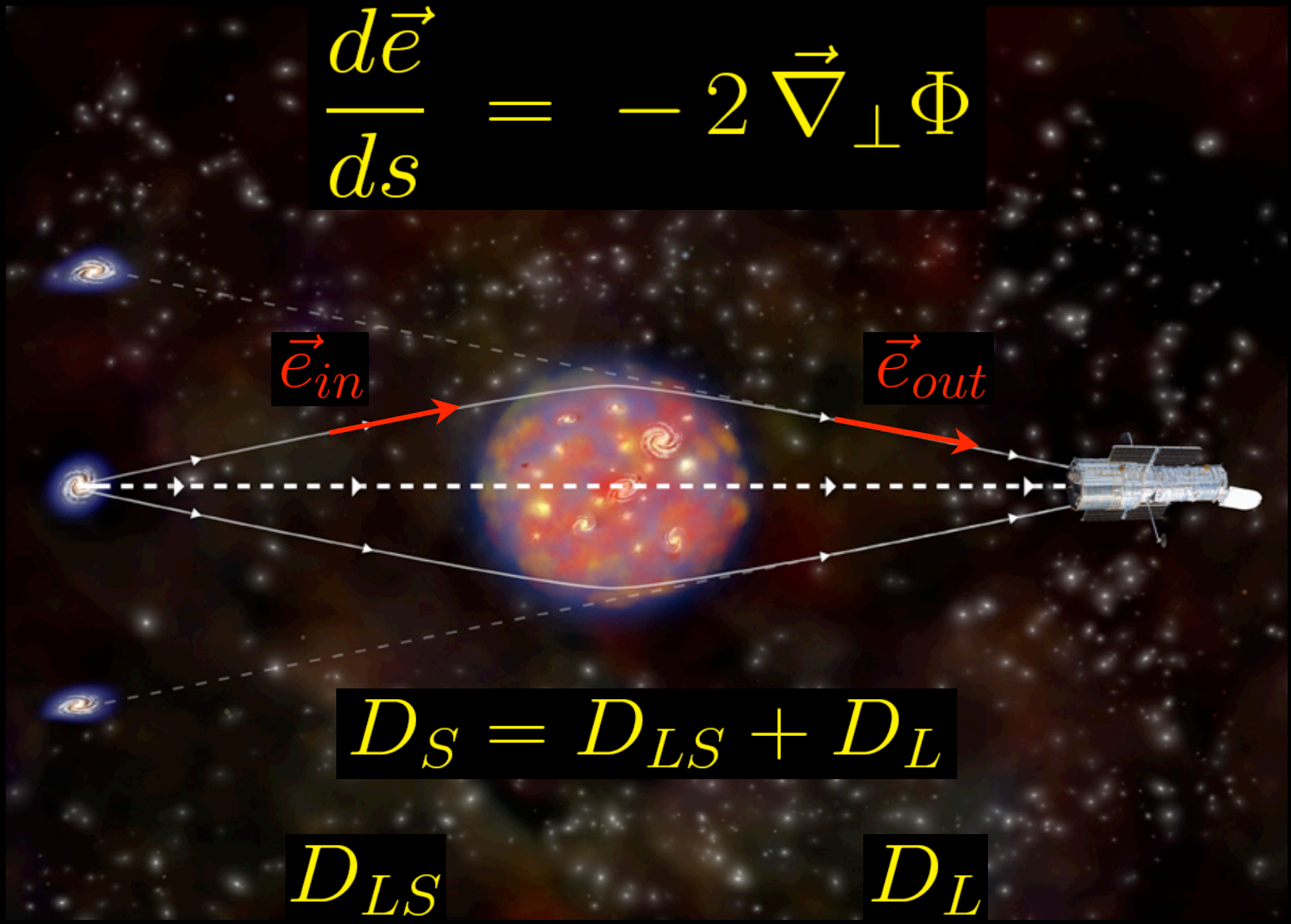

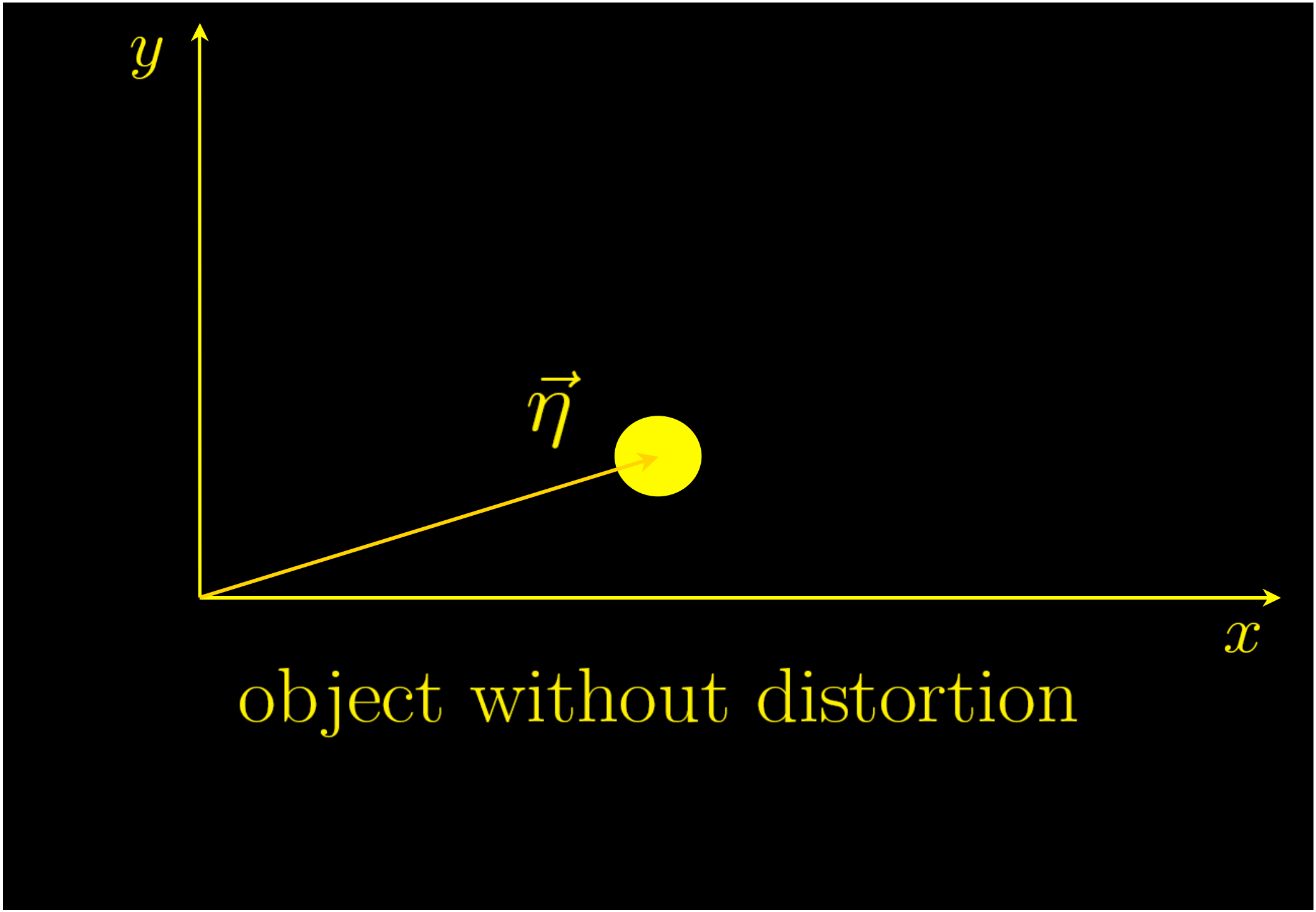
y
$\vec{\eta}$
x
object without distortion

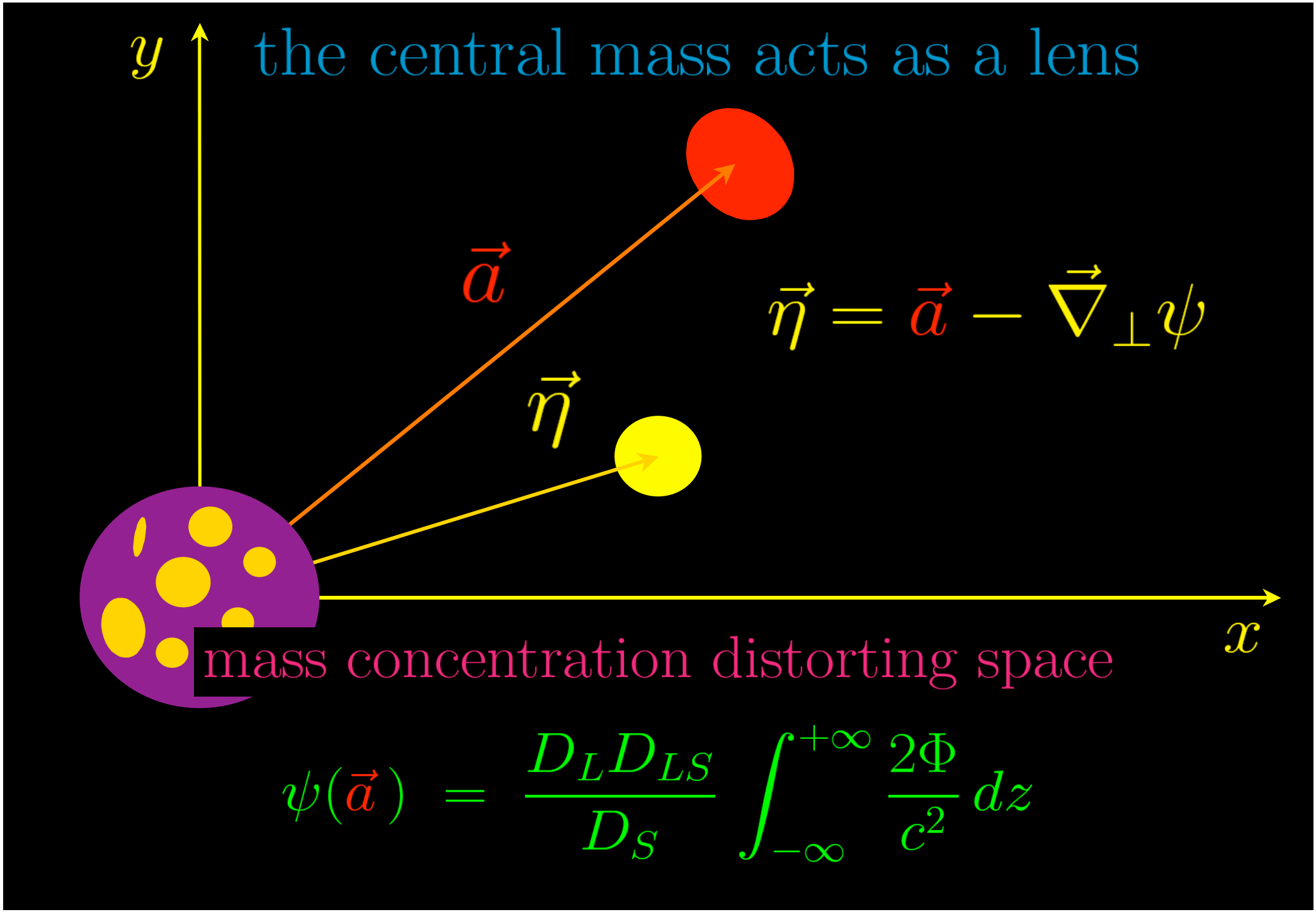
y
the central mass acts as a lens
$\vec{a}$
$\vec{\eta}$
$\vec{\eta} = \vec{a} - \vec{\nabla}_\perp \psi$
x
mass concentration distorting space
$\psi(\vec{a}) = \frac{D_L D_{LS}}{D_S} \int_{-\infty}^{+\infty} \frac{2\Phi}{c^2} dz$

Distortion Matrix $\mathcal{D}$

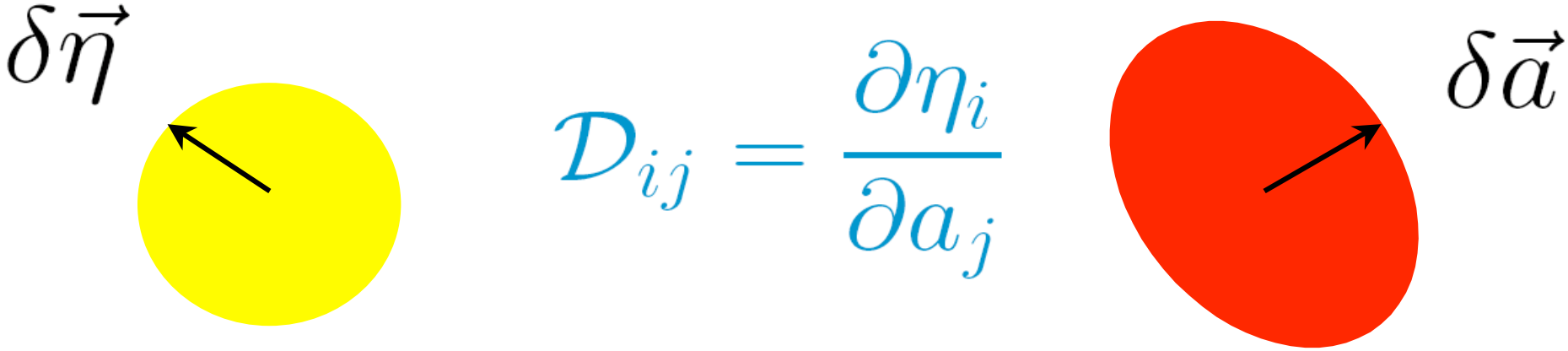

$$\mathcal{D}_{ij} = \delta_{ij} - \partial_i \partial_j \psi$$

$$\mathcal{D}_{ij} = (1-\kappa)\ \mathbb{I}_2 \ + \ \gamma \begin{Bmatrix} \cos 2\theta & \sin 2\theta \\ \sin 2\theta & -\cos 2\theta \end{Bmatrix}$$

Convergence

Shear

Convergence

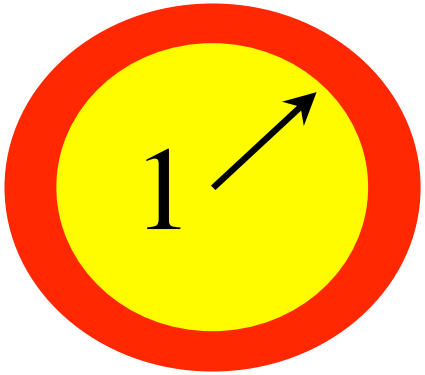

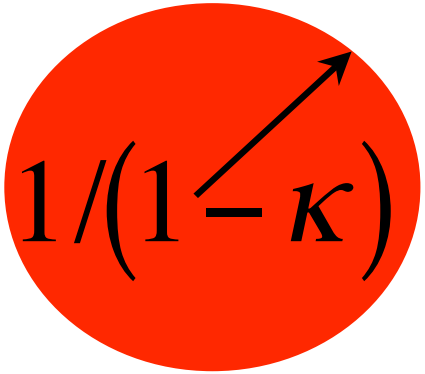

Shear

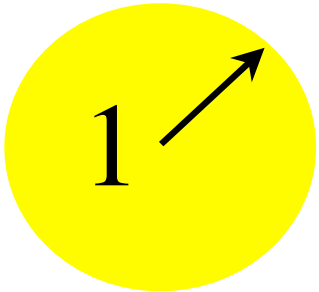

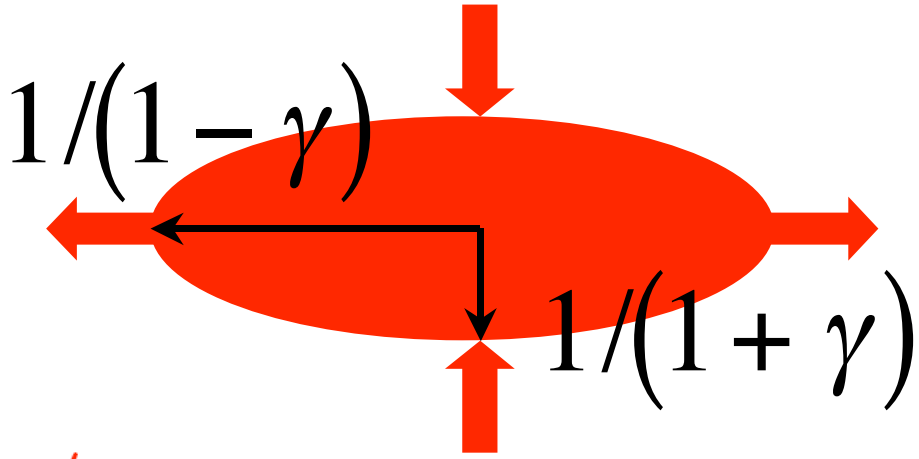

$\theta = \pi/2$

Poisson equation

$$\Delta\Phi \equiv \left\{ \vec{\nabla}_\perp \cdot \vec{\nabla}_\perp + \frac{\partial^2}{\partial z^2} \right\} \Phi = 4\pi G\,\rho$$

$$2\,\kappa = \Delta_\perp \psi \equiv \partial_x^2 \psi + \partial_y^2 \psi = 2\,\frac{\Sigma}{\Sigma_c}$$

where

$$\Sigma_c = \frac{c^2}{4\pi G}\,\frac{D_S}{D_L D_{LS}}$$

Relation between κ and $\Sigma = \int_{-\infty}^{+\infty} \rho\, dz$

$$\vec{g} = \vec{\gamma}/(1-\kappa)$$

$$\nabla \ln(1-\kappa) = \frac{1}{1-g_1^2-g_2^2} \begin{pmatrix} 1+g_1 & g_2 \\ g_2 & 1-g_1 \end{pmatrix} \begin{pmatrix} g_{1,1}+g_{2,2} \\ g_{2,1}-g_{1,2} \end{pmatrix}$$

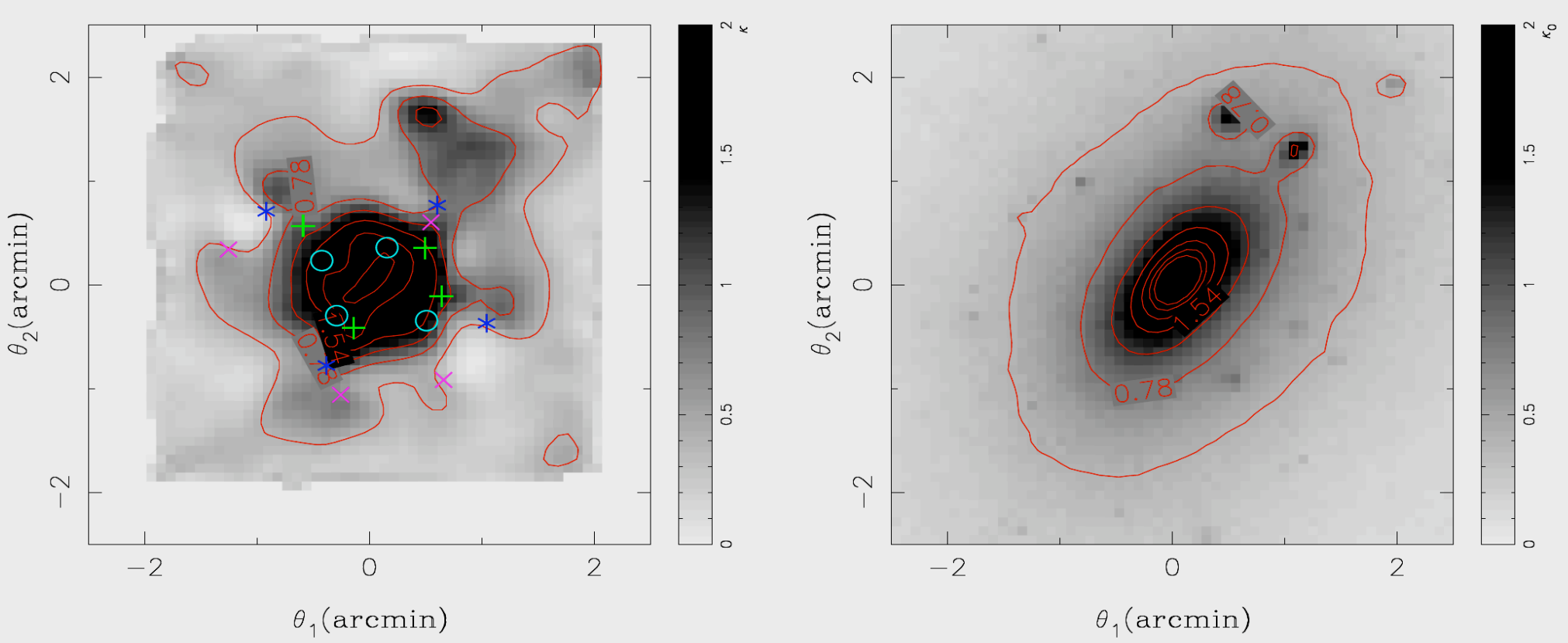

FIG. 3.— The reconstructed (left) and the original (right) surface mass density κ of the simulated cluster described in section 3. The symbols in the left panel denote the image positions of the four multiple-image systems at $z_s = \{0.8, 1.0, 3.0, 5.0\}$ which we use for the reconstruction. The contour levels, which are the same in both panels, are linearly spaced with $\Delta\kappa = 0.38$, starting at $\kappa = 0.4$ for a fiducial source at infinite redshift, $z_s \to \infty$.

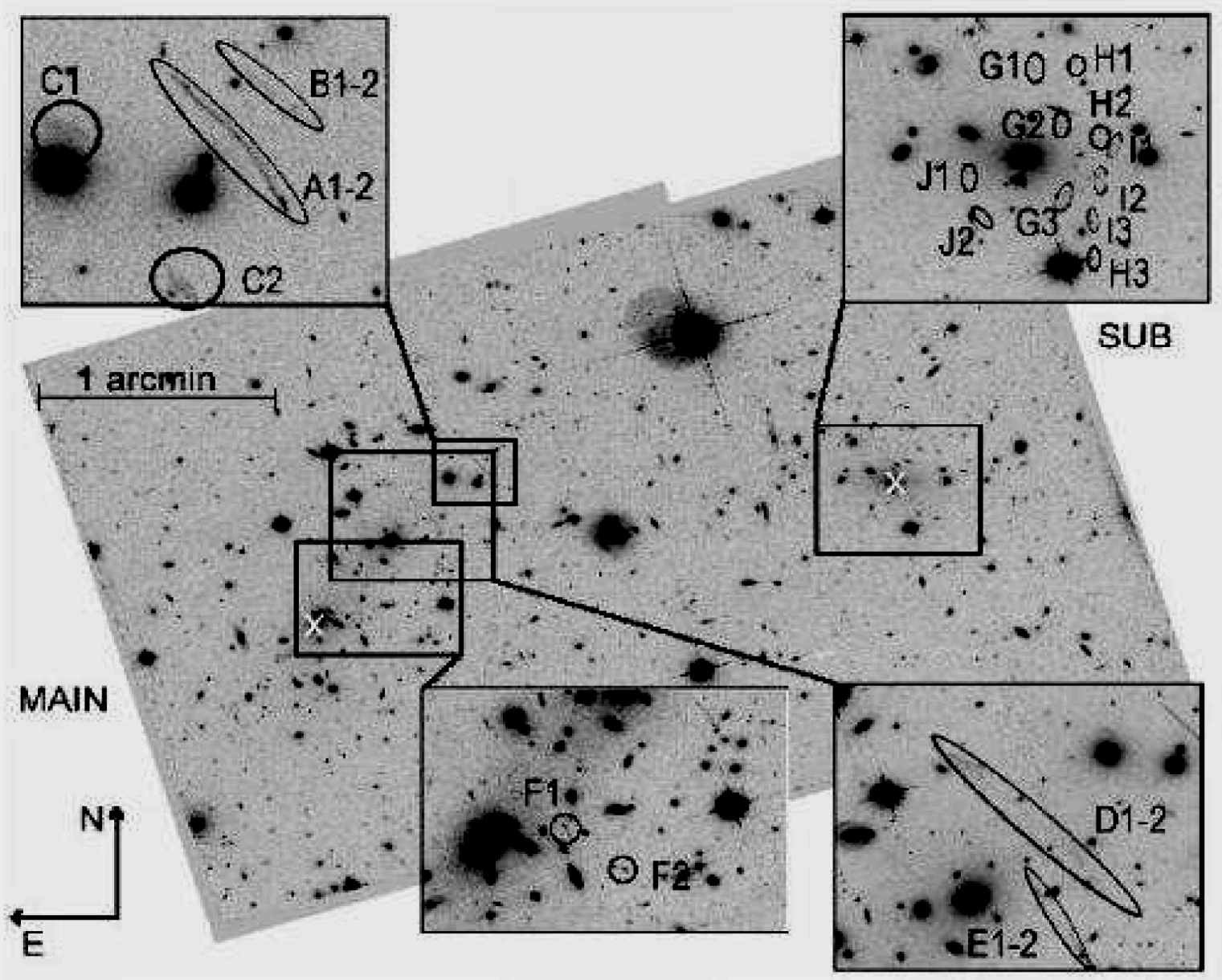

FIG. 1.— The two F606W pointings of the main and sub component region of 1E0657−56. Multiply imaged systems are marked and labeled (see also Table 1). White crosses denote the positions of the southern cD of the main and BCG of the subcluster.

A DIRECT EMPIRICAL PROOF OF THE EXISTENCE OF DARK MATTER *

Douglas Clowe[1], Maruša Bradač[2], Anthony H. Gonzalez[3], Maxim Markevitch[4,5], Scott W. Randall[4], Christine Jones[4], and Dennis Zaritsky[1]

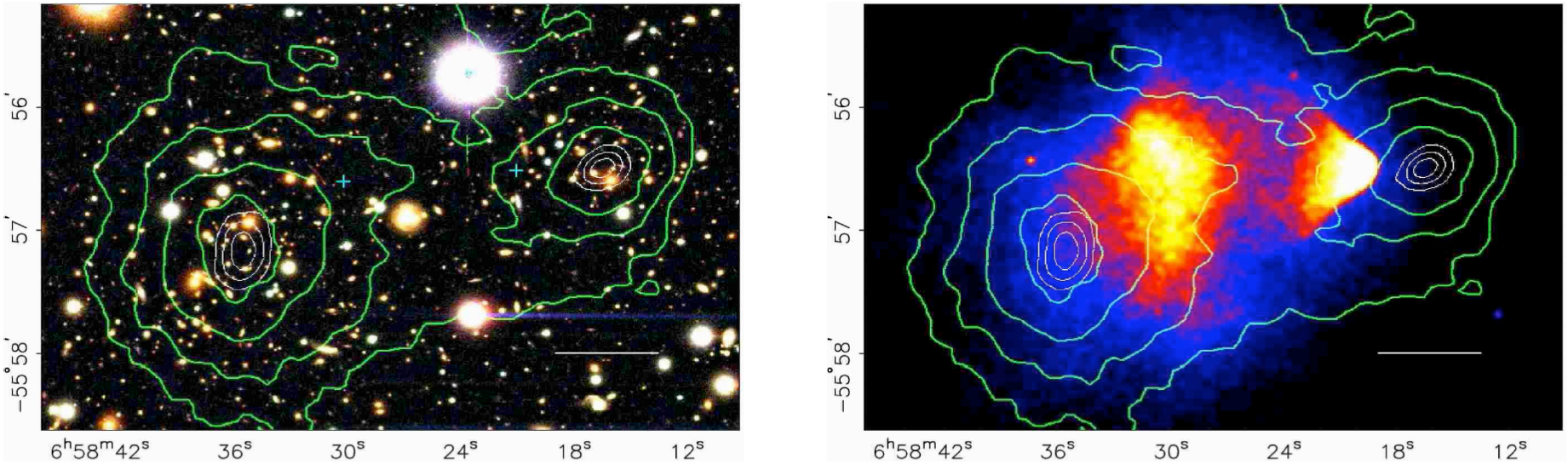

Fig. 1.— Shown above in the top panel is a color image from the Magellan images of the merging cluster 1E0657−558, with the white bar indicating 200 kpc at the distance of the cluster. In the bottom panel is a 500 ks Chandra image of the cluster. Shown in green contours in both panels are the weak lensing κ reconstruction with the outer contour level at $\kappa = 0.16$ and increasing in steps of 0.07. The white contours show the errors on the positions of the κ peaks and correspond to 68.3%, 95.5%, and 99.7% confidence levels. The blue +s show the location of the centers used to measure the masses of the plasma clouds in Table 2.

ON THE PROOF OF DARK MATTER, THE LAW OF GRAVITY AND THE MASS OF NEUTRINOS

Garry W. Angus[1], HuanYuan Shan[2,1], HongSheng Zhao[1,2], Benoit Famaey[3]

Draft version January 4, 2007

Modified Gravity where $\tilde{G} \neq G_{\rm N}$

$$\frac{G_{\rm N}}{\tilde{G}(x)} = \mu(x) = 1 - \left\{ \frac{1+\alpha x}{2} + \sqrt{\left(\frac{1-\alpha x}{2}\right)^2 + x} \right\}^{-1}$$

$$\text{where} \quad x \equiv \frac{|\nabla\Phi|}{a_0}$$

$$a_0 \sim 1 \text{Å s}^{-2}$$

$$\kappa = \frac{\Sigma}{\Sigma_c} \quad \text{where} \quad \Sigma_c = \frac{c^2}{4\pi\tilde{G}(\mathbf{r})} \frac{D_S}{D_L D_{LS}}$$

ON THE PROOF OF DARK MATTER, THE LAW OF GRAVITY AND THE MASS OF NEUTRINOS

Garry W. Angus[1], HuanYuan Shan[2,1], HongSheng Zhao[1,2], Benoit Famaey[3]

Draft version January 4, 2007

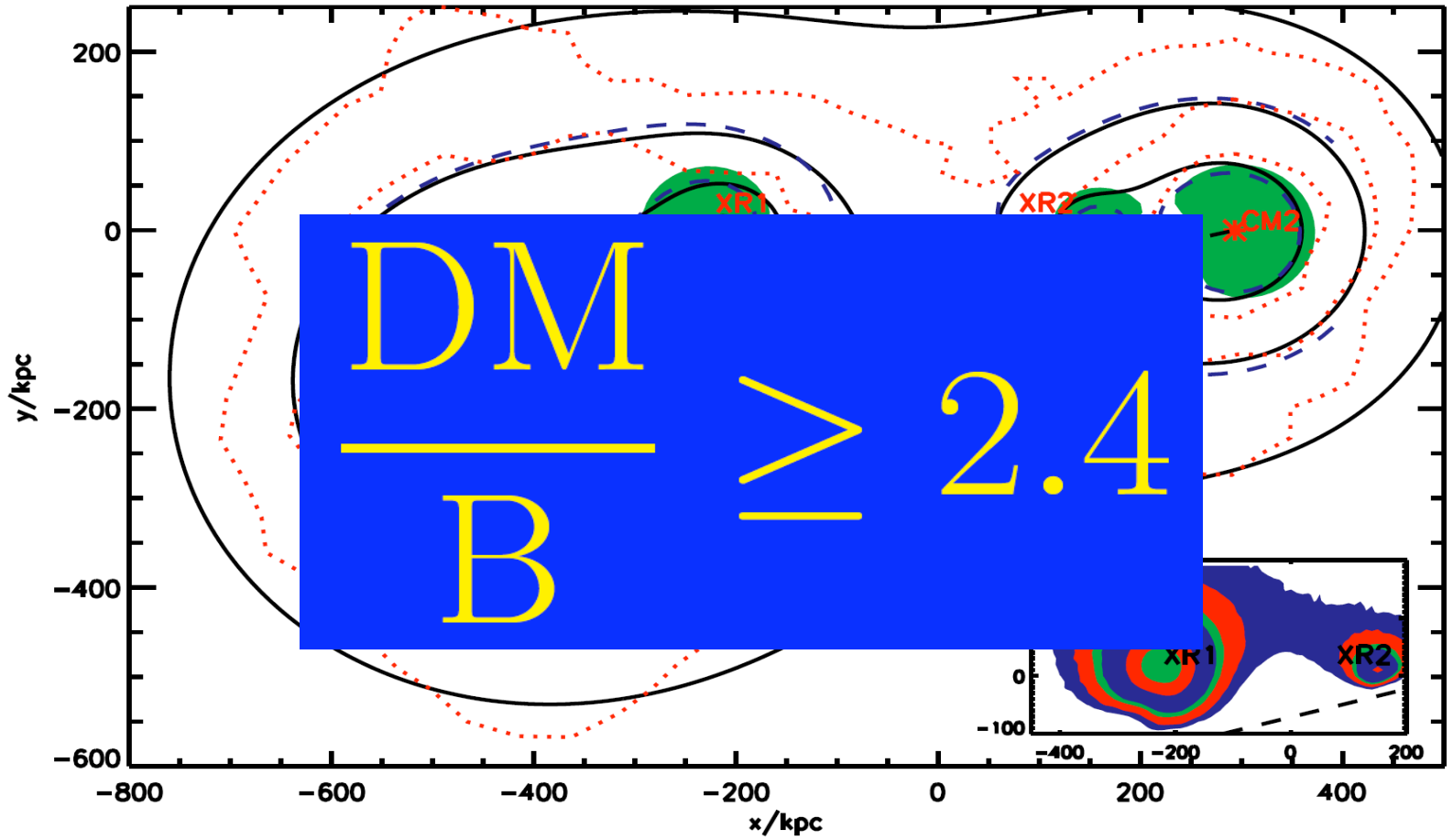

$$\frac{DM}{B} \geq 2.4$$

FIG. 1.— Our fitted converger dotted red lines) with x and y axes in kpc. The contours are fr ve used are the red stars which are labelled. Also overplotted (b c^{-2} for the MOND standard μ function; note slight distortions c ity is above $1.8\times10^{-3}M_{\odot}\,\mathrm{pc}^{-3}$ and correspond to the clustering er predicted by our collisionless matter subtraction method for t $M_{\odot}pc^{-2}$. The origin in RA and dec is [$06^h58^m24.38^s$,-$55^o56'.32$]

$$m_\nu \geq 2 \text{ eV}$$

2) Dark matter tomography – clumps & filaments

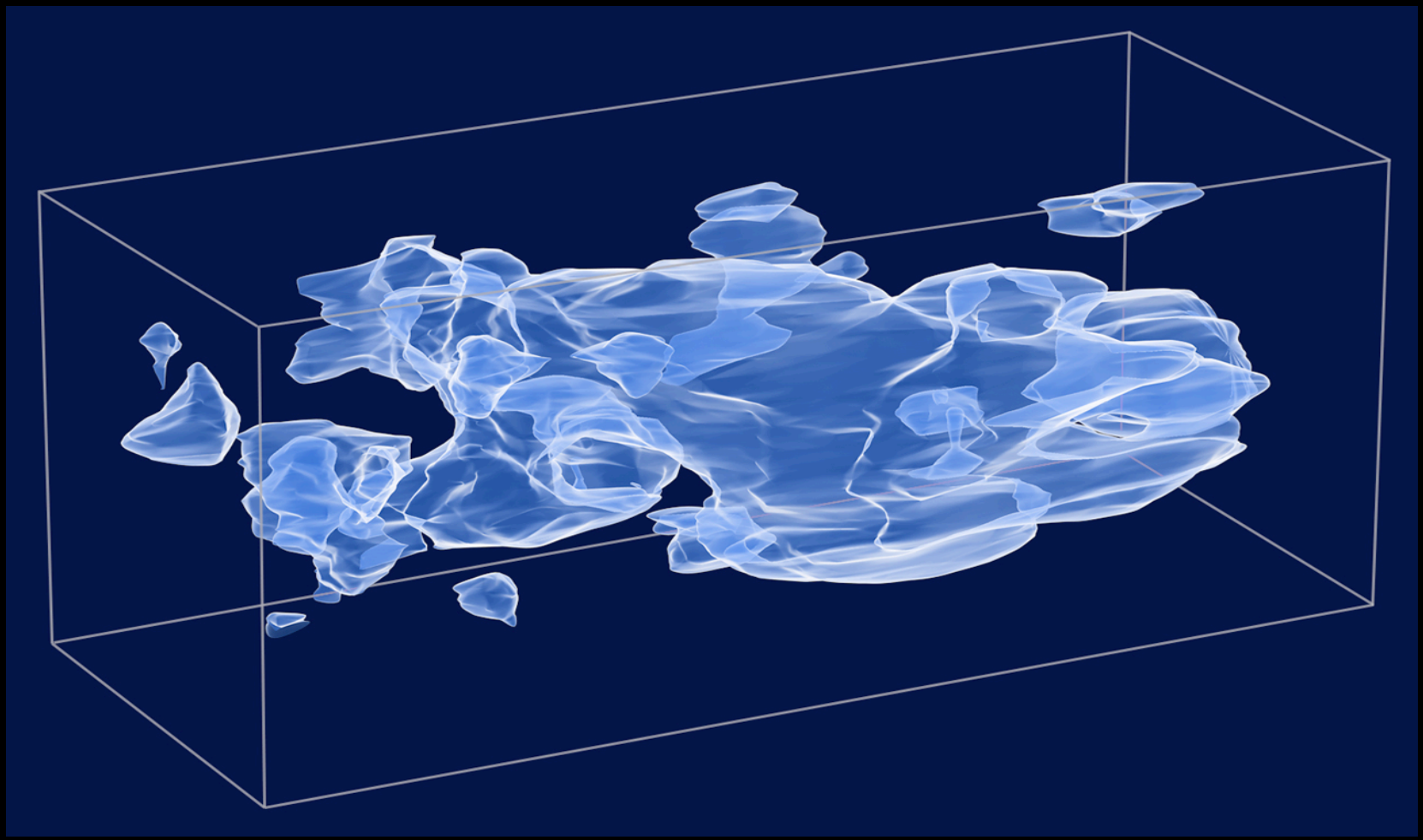

Cosmic Evolution Survey

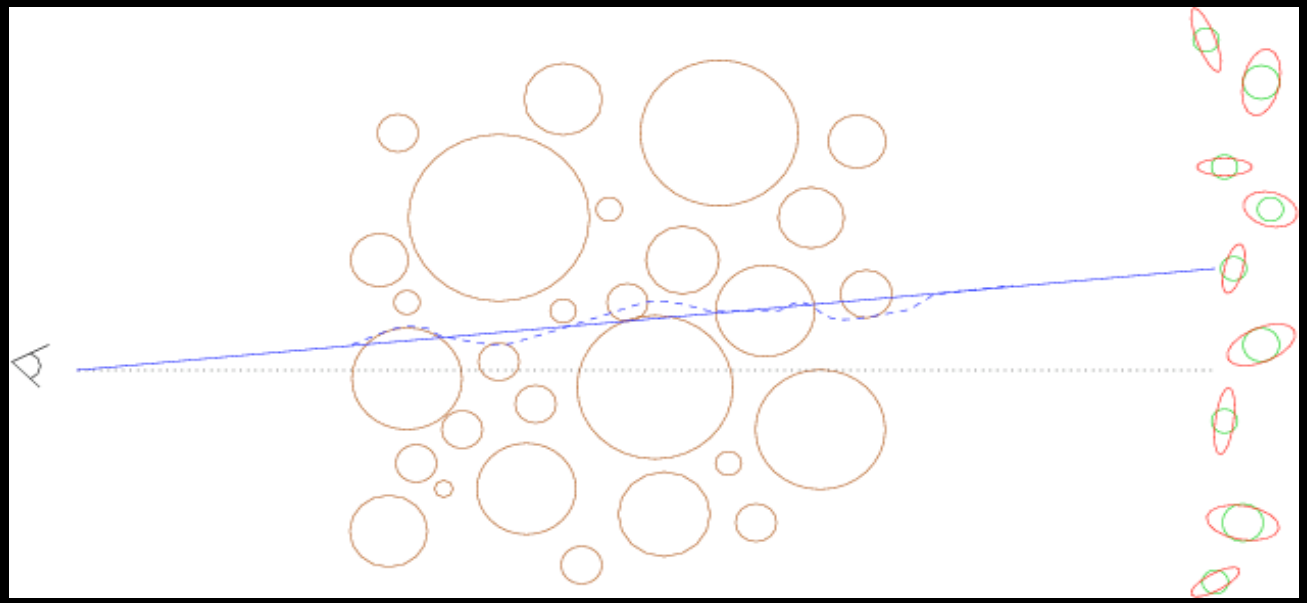

Convergence κ Maps

$$\vec{\theta}_S = \vec{\theta} - \vec{\nabla}_\theta \int_0^{D_S} dz \times \frac{(D_S - z)}{D_S\, z} \times \frac{2\Phi(\vec{\theta} z, z)}{c^2}$$

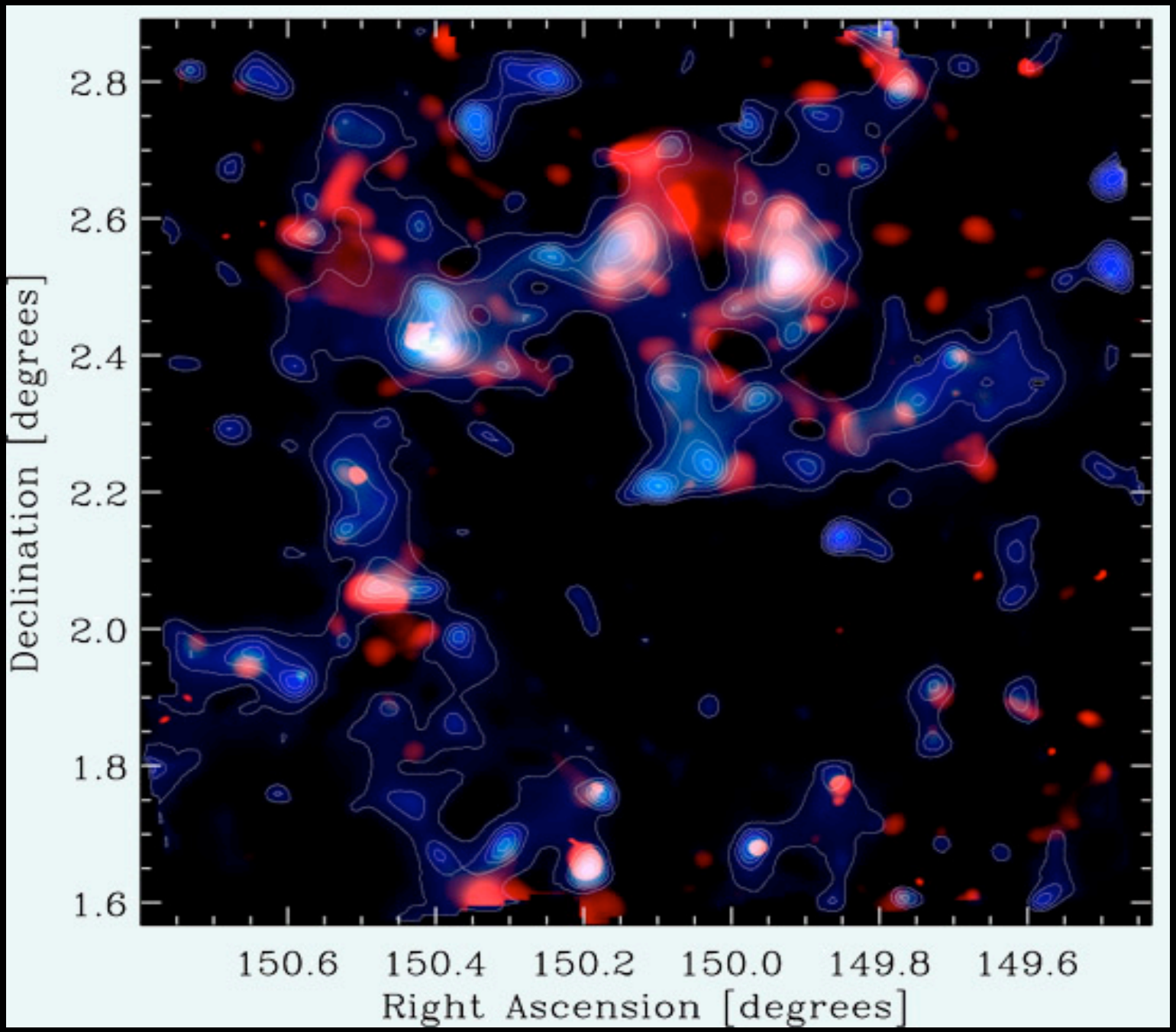
Declination [degrees]
2.8
2.6
2.4
2.2
2.0
1.8
1.6
150.6
150.4
150.2
150.0
149.8
149.6
Right Ascension [degrees]

Convergence κ Maps

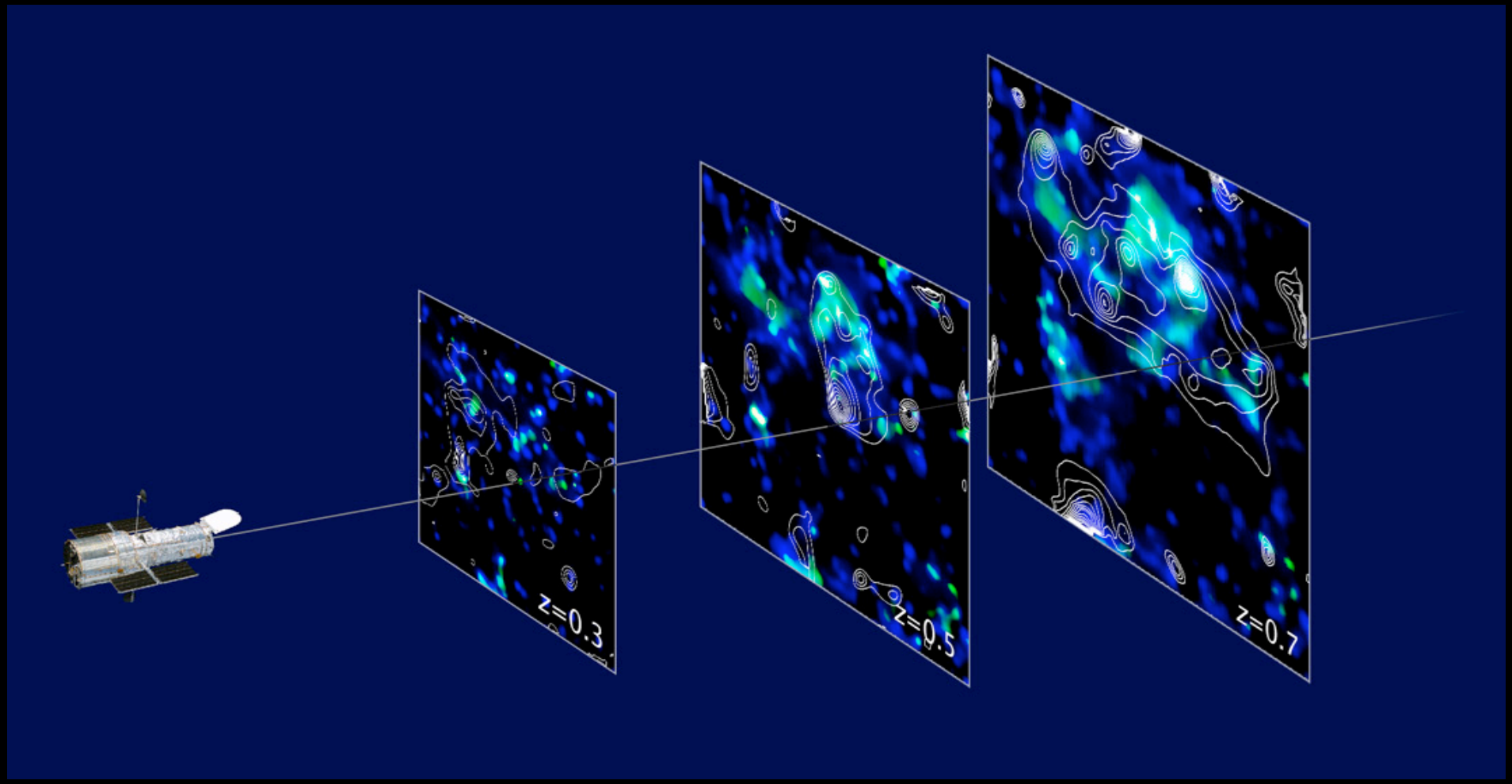

Several depths D_S are selected

Distribution of Dark Matter

HST ▪ ACS/WFC

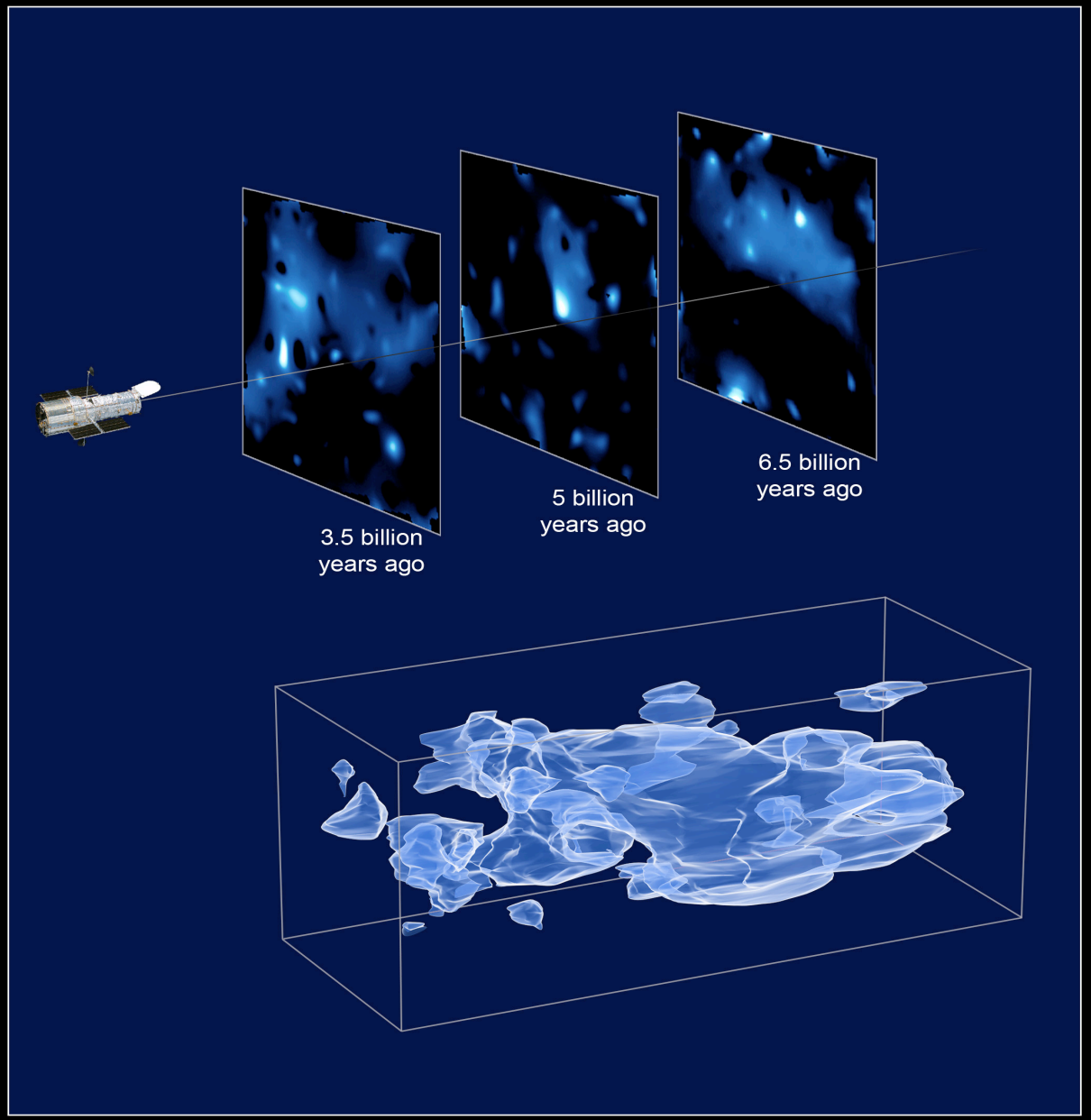

NASA, ESA, and R. Massey (California Institute of Technology)

STScI-PRC07-01a

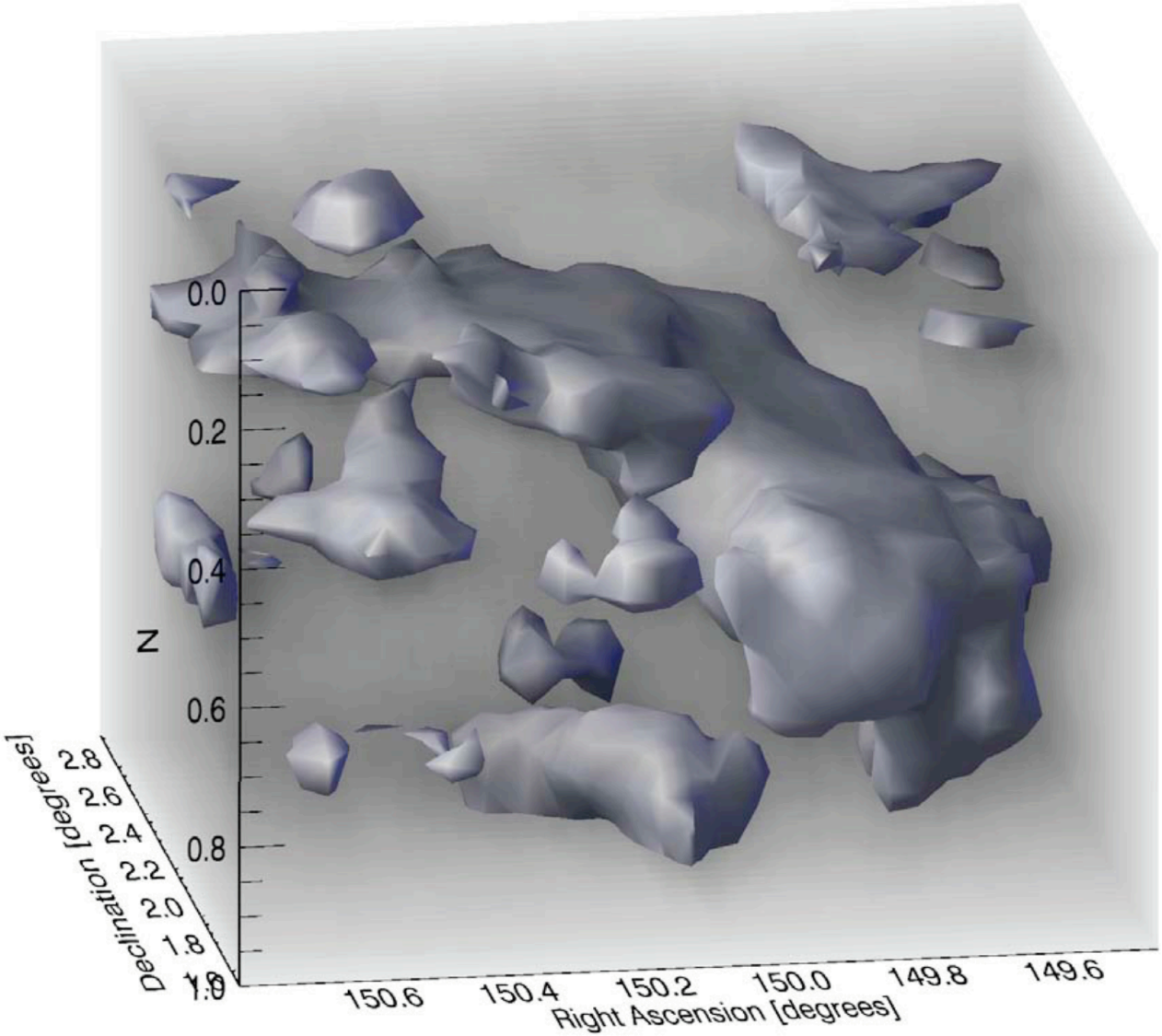

Figure 5 | 3D reconstruction of the dark matter distribution. The three axes correspond to Right Ascension, Declination, and redshift: with distance from the Earth increasing towards the bottom. The redshift scale is highly compressed, and the survey volume is really an elongated cone. An isodensity contour has been drawn at a level of 1.6×10^{12} M_{sun} within a circle of radius 700 *kpc* and Δz=0.05. This was chosen arbitrarily to highlight the filamentary structure. The faint background shows the full distribution, with the level of the grey scale corresponding to the local density. Additional views are provided in supplementary Fig. 7.

THE 3D SKELETON OF THE SDSS

Thierry Sousbie[1], Christophe Pichon[1,2], Hélène Courtois[1], Stéphane Colombi[2], Dmitri Novikov[3]

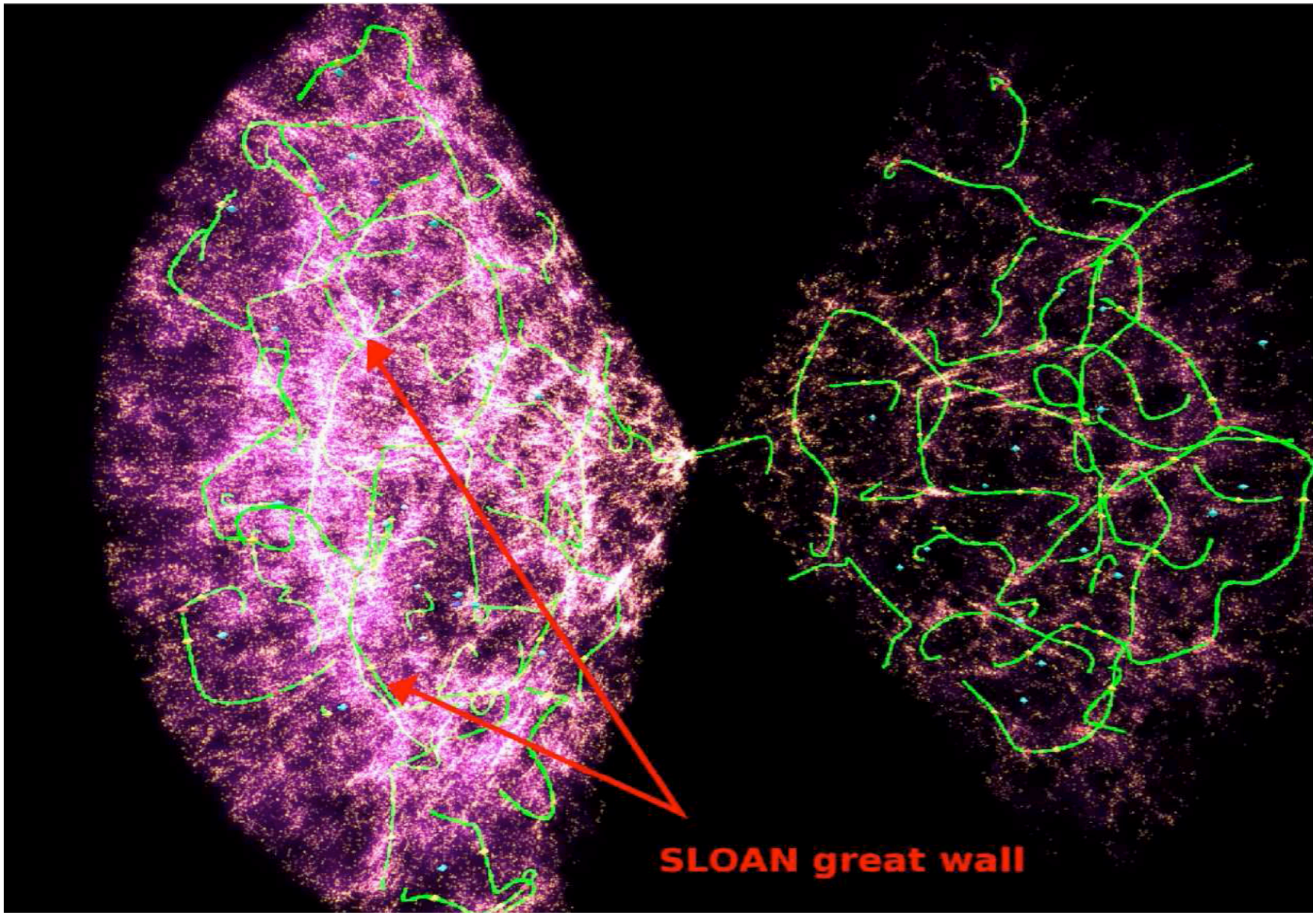

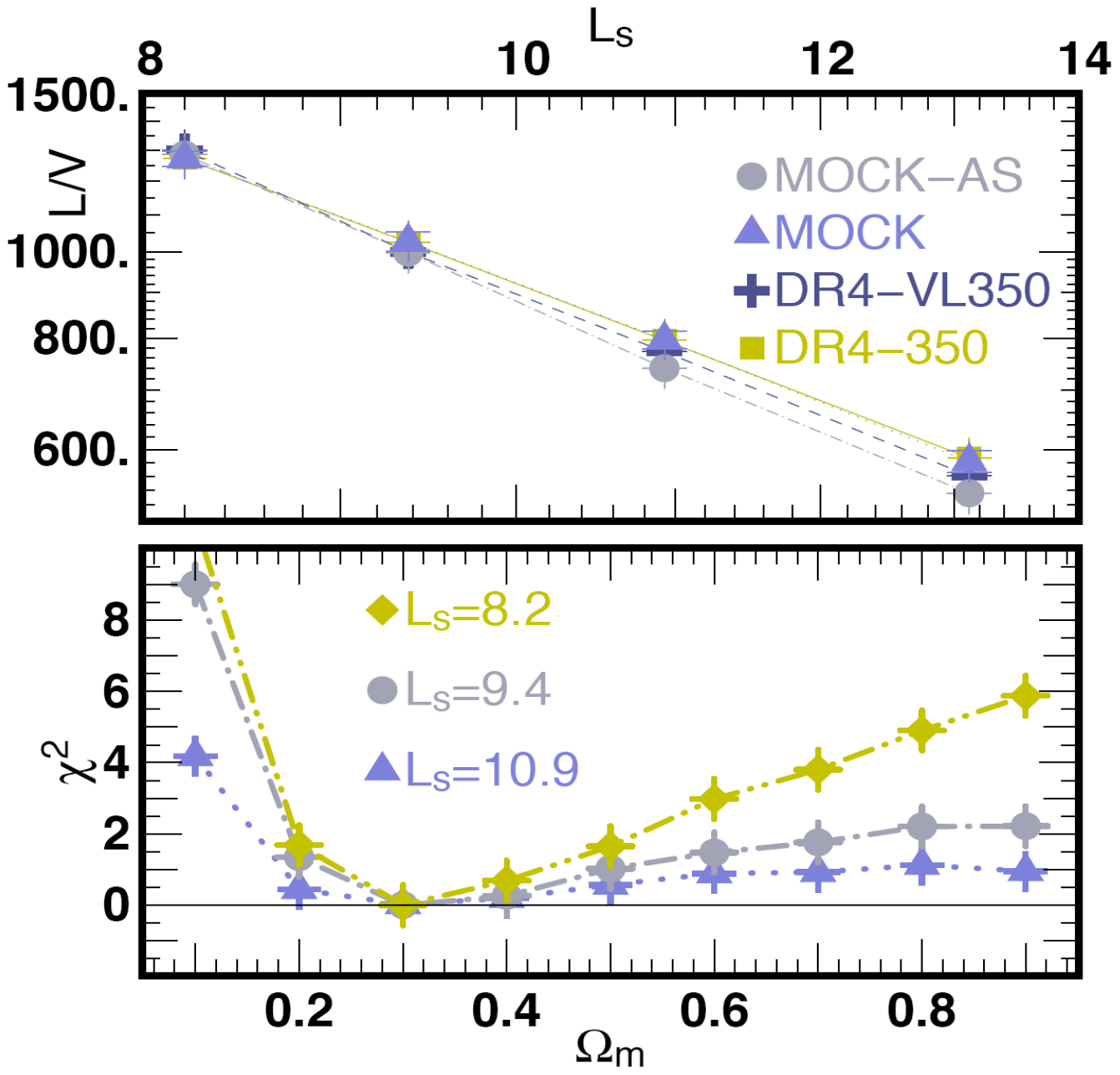

$[0.25, 0.4]$ at one-σ level

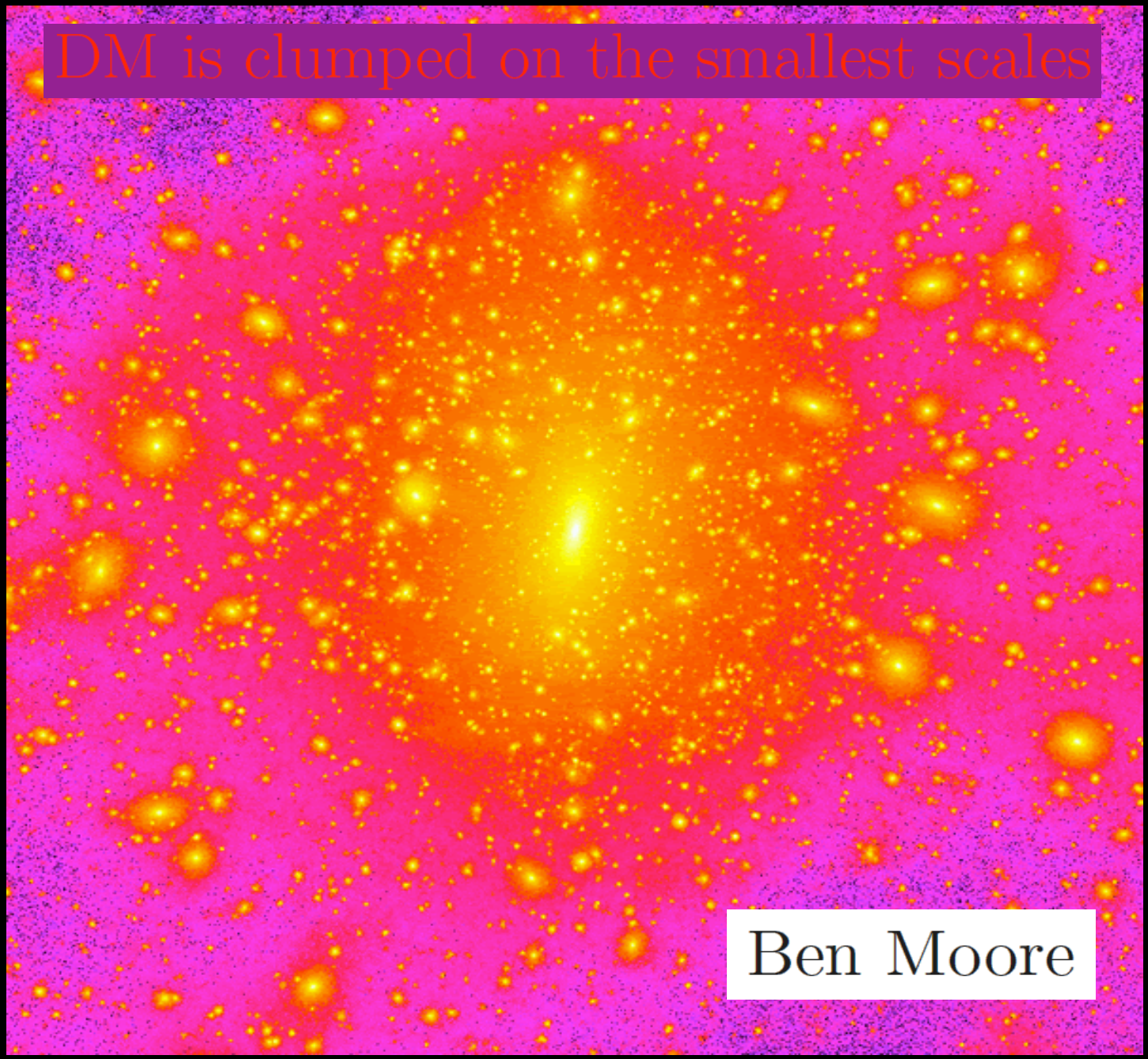
DM is clumped on the smallest scales
Ben Moore

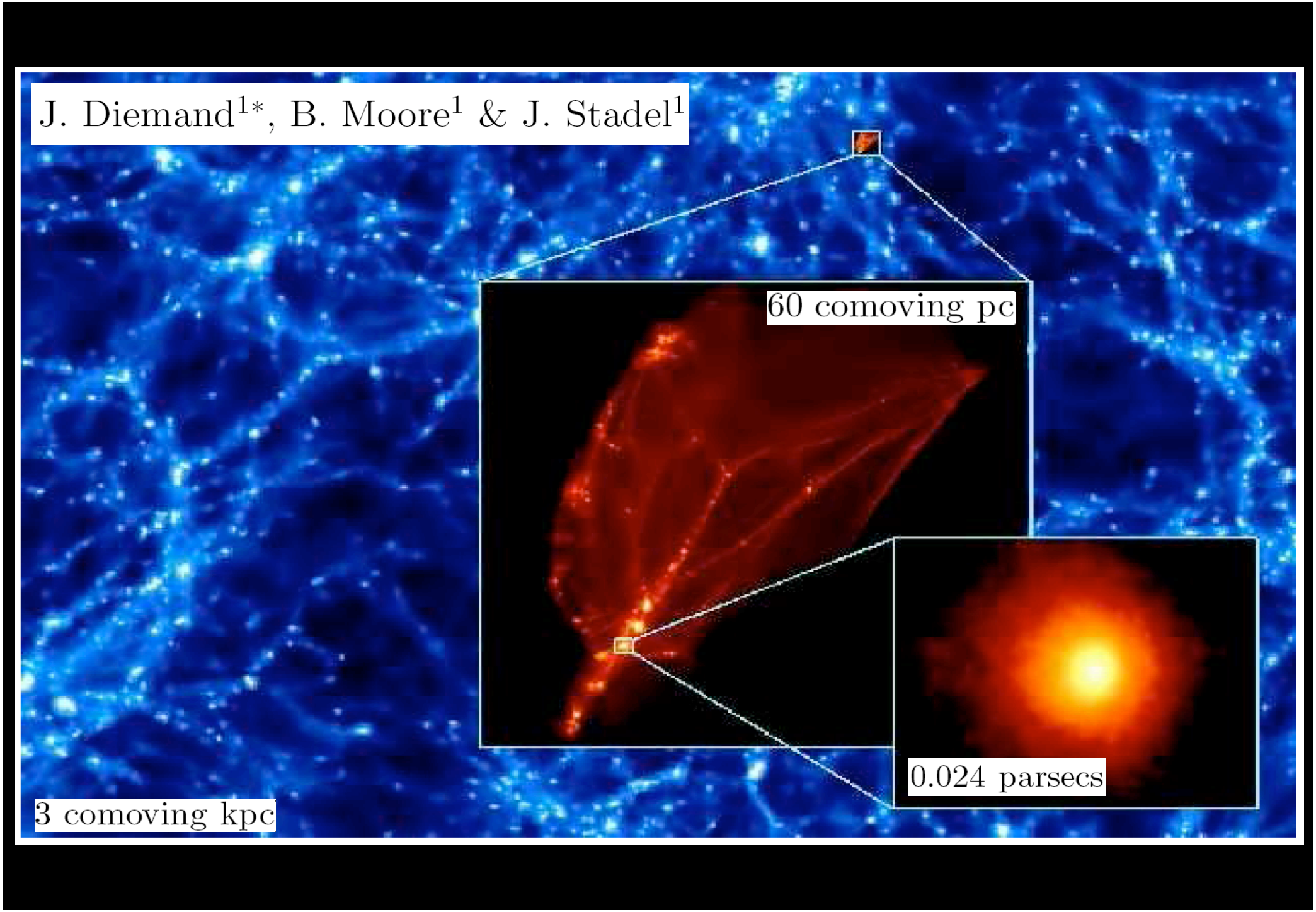
J. Diemand[1*], B. Moore[1] & J. Stadel[1]
60 comoving pc
0.024 parsecs
3 comoving kpc

Jürg Diemand[1,2], Michael Kuhlen[1,3], & Piero Madau[1,4]

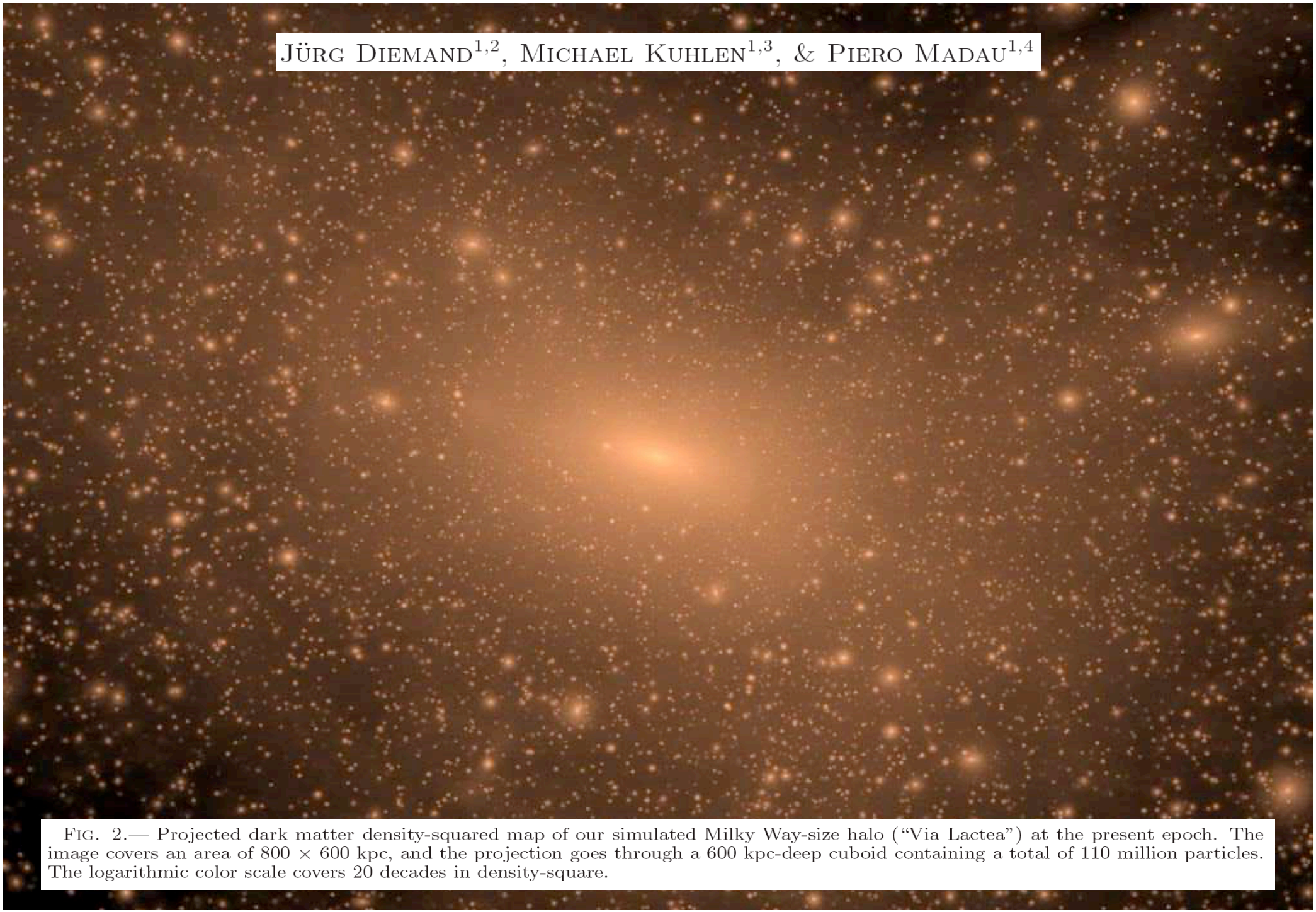

Fig. 2.— Projected dark matter density-squared map of our simulated Milky Way-size halo ("Via Lactea") at the present epoch. The image covers an area of 800 × 600 kpc, and the projection goes through a 600 kpc-deep cuboid containing a total of 110 million particles. The logarithmic color scale covers 20 decades in density-square.

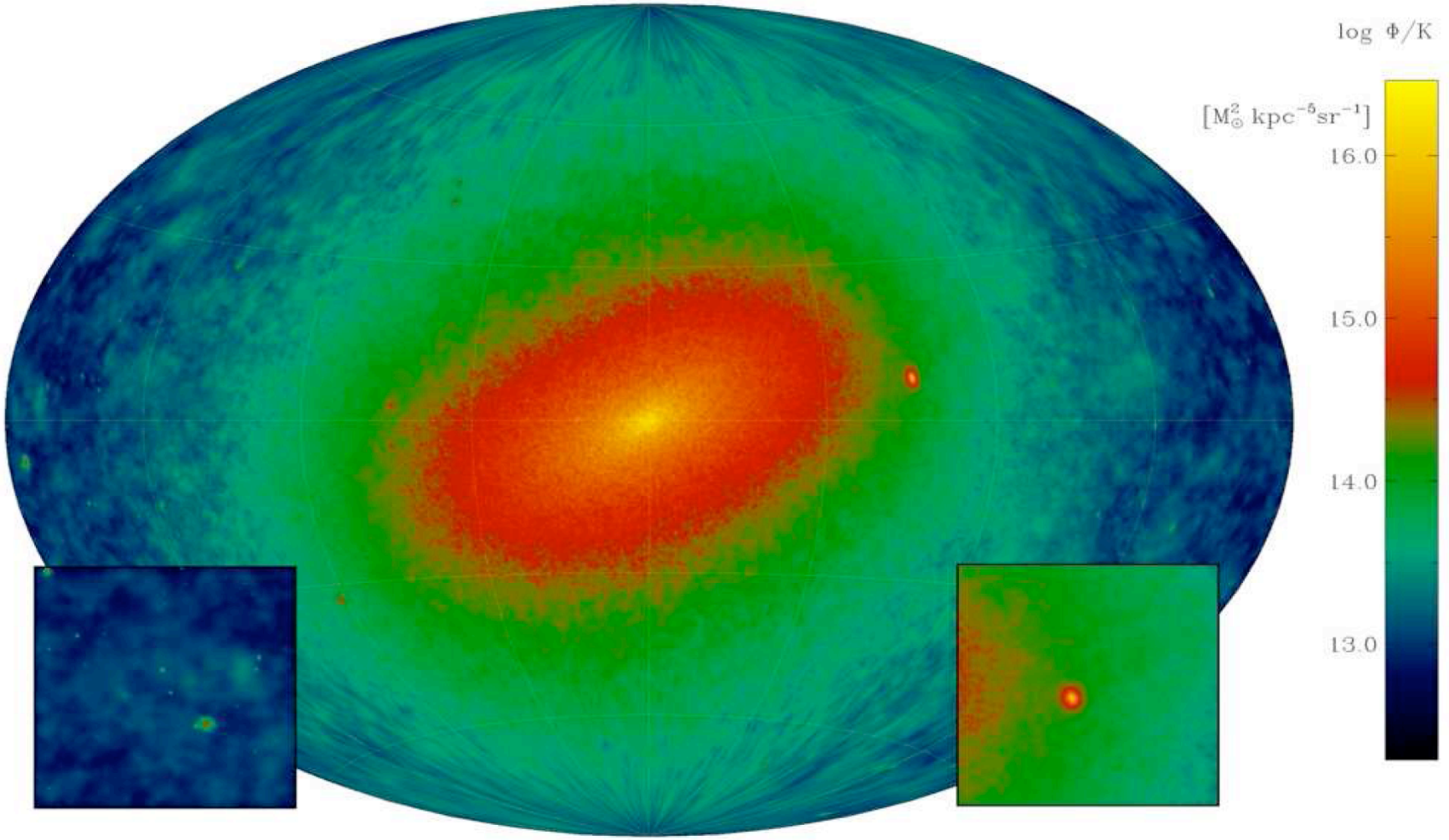

FIG. 9.— All-sky map of the DM annihilation flux Φ/K ($M_\odot^2 kpc^{-5}$ sr^{-1}) in our Via Lactea halo, for an observer located 8 kpc from the Galactic center. The insets show zoom-in's of a $40^\circ \times 40^\circ$ region around the anticenter (*left*) and the brightest subhalo (*right*).

Tobias Goerdt[1⋆], Oleg Y. Gnedin[2], Ben Moore[1], Jürg Diemand[3] & Joachim Stadel[1]

ABSTRACT

If the dark matter particle is a neutralino then the first structures to form are cuspy cold dark matter (CDM) haloes collapsing after redshifts $z \approx 100$ in the mass range $10^{-6} - 10^{-3}\,\mathrm{M}_{\odot}$. We carry out a detailed study of the survival of these micro-haloes in the Galaxy as they experience tidal encounters with stars, molecular clouds, and other dark matter substructures. We test the validity of analytic impulsive heating calculations using high resolution N-body simulations. A major limitation of analytic estimates is that mean energy inputs are compared to mean binding energies, instead of the actual mass lost from the system. This energy criterion leads to an overestimate of the stripped mass and underestimate of the disruption timescale since CDM haloes are strongly bound in their inner parts. We show that a significant fraction of material from CDM micro-haloes can be unbound by encounters with Galactic substructure and stars, however the cuspy central regions remain relatively intact. Furthermore, the micro-haloes near the solar radius are those which collapse significantly earlier than average and will suffer very little mass loss. Thus we expect a fraction of surviving bound micro-haloes, a smooth component with narrow features in phase space, which may be uncovered by direct detection experiments, as well as numerous surviving cuspy cores with proper motions of arc-minutes per year, which can be detected indirectly via their annihilation into gamma-rays.

3) Computing the odds of the galactic lottery

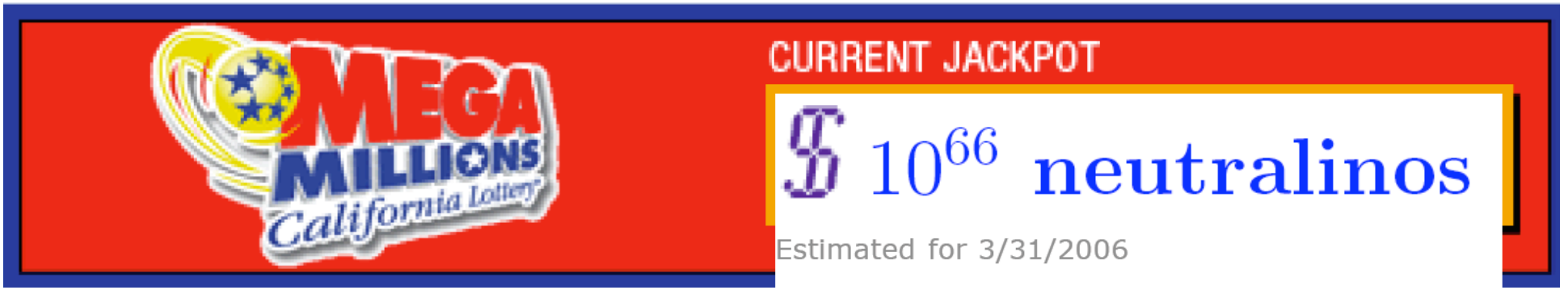

Julien Lavalle[1], Jonathan Pochon[2], Pierre Salati[3,4], and Richard Taillet[3,4]

astro-ph/0603796 – accepted in A&A

Torsten Bringmann and Pierre Salati

astro-ph/0612514 – accepted in PRD

G. Bertone, P. Brun, J. Lavalle, P. Salati and R. Taillet

IMBHs – in preparation

3.1) Motivations for this analysis

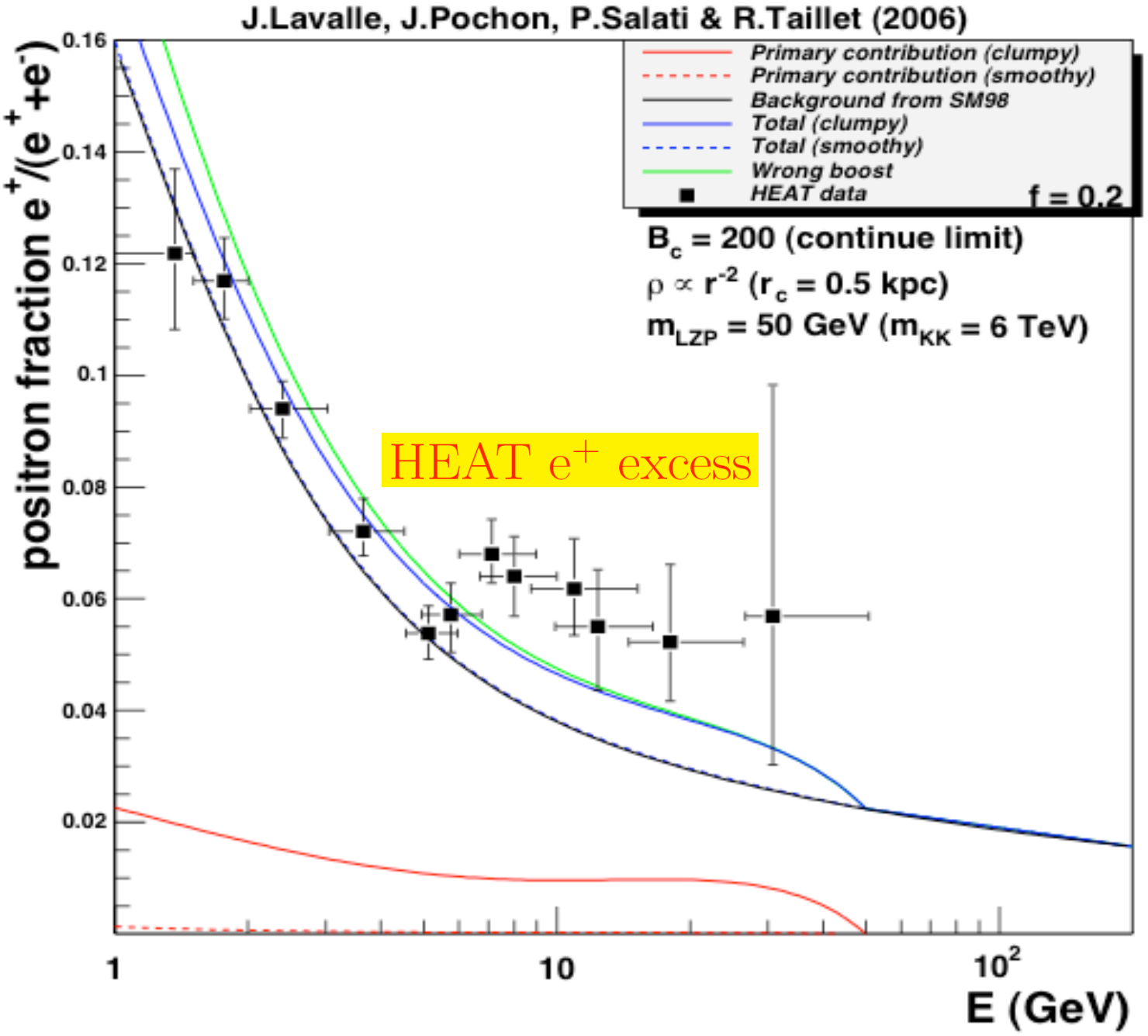

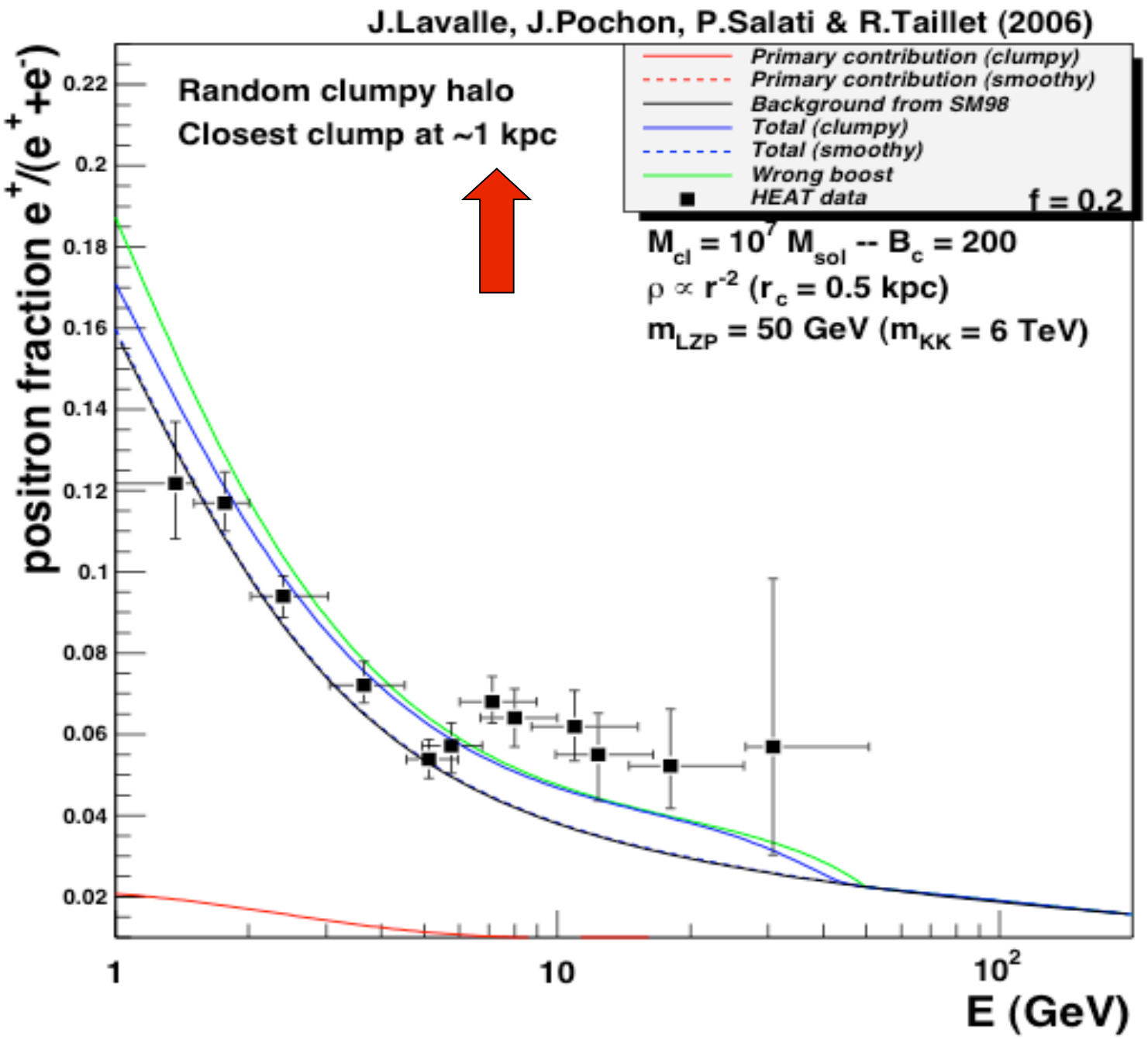
J.Lavalle, J.Pochon, P.Salati & R.Taillet (2006)
Random clumpy halo
Closest clump at ~1 kpc
Primary contribution (clumpy)
Primary contribution (smoothy)
Background from SM98
Total (clumpy)
Total (smoothy)
Wrong boost
HEAT data
f = 0.2
M_cl = 10^7 M_sol -- B_c = 200
ρ ∝ r^-2 (r_c = 0.5 kpc)
m_LZP = 50 GeV (m_KK = 6 TeV)
positron fraction e+/(e+ +e-)
E (GeV)
0.22
0.2
0.18
0.16
0.14
0.12
0.1
0.08
0.06
0.04
0.02
1
10
10^2

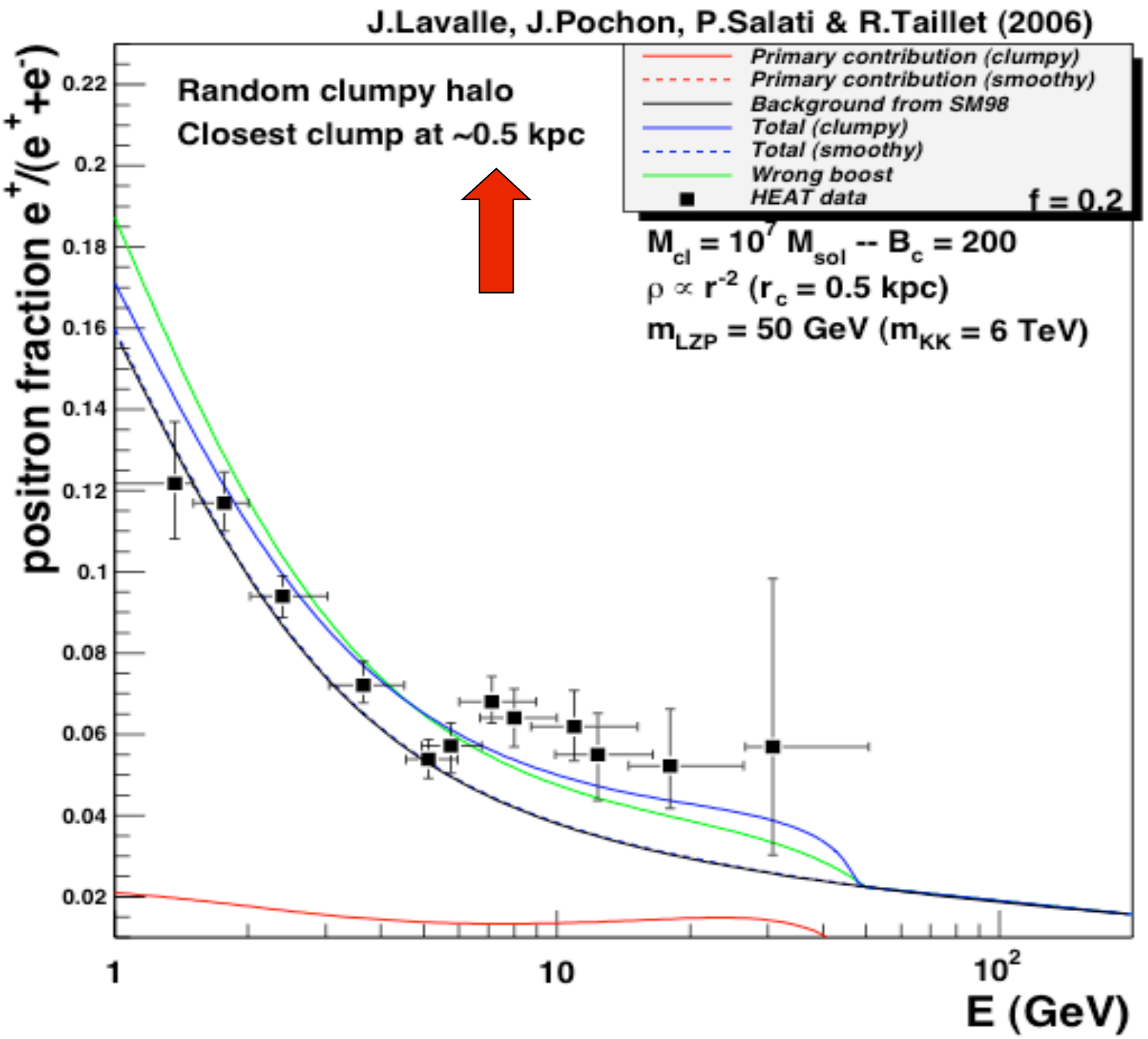
J.Lavalle, J.Pochon, P.Salati & R.Taillet (2006)
Random clumpy halo
Closest clump at ~0.5 kpc
Primary contribution (clumpy)
Primary contribution (smoothy)
Background from SM98
Total (clumpy)
Total (smoothy)
Wrong boost
HEAT data
f = 0.2
M_cl = 10^7 M_sol -- B_c = 200
ρ ∝ r^-2 (r_c = 0.5 kpc)
m_LZP = 50 GeV (m_KK = 6 TeV)
positron fraction e+/(e+ +e-)
E (GeV)
0.22
0.2
0.18
0.16
0.14
0.12
0.1
0.08
0.06
0.04
0.02
1
10
10^2

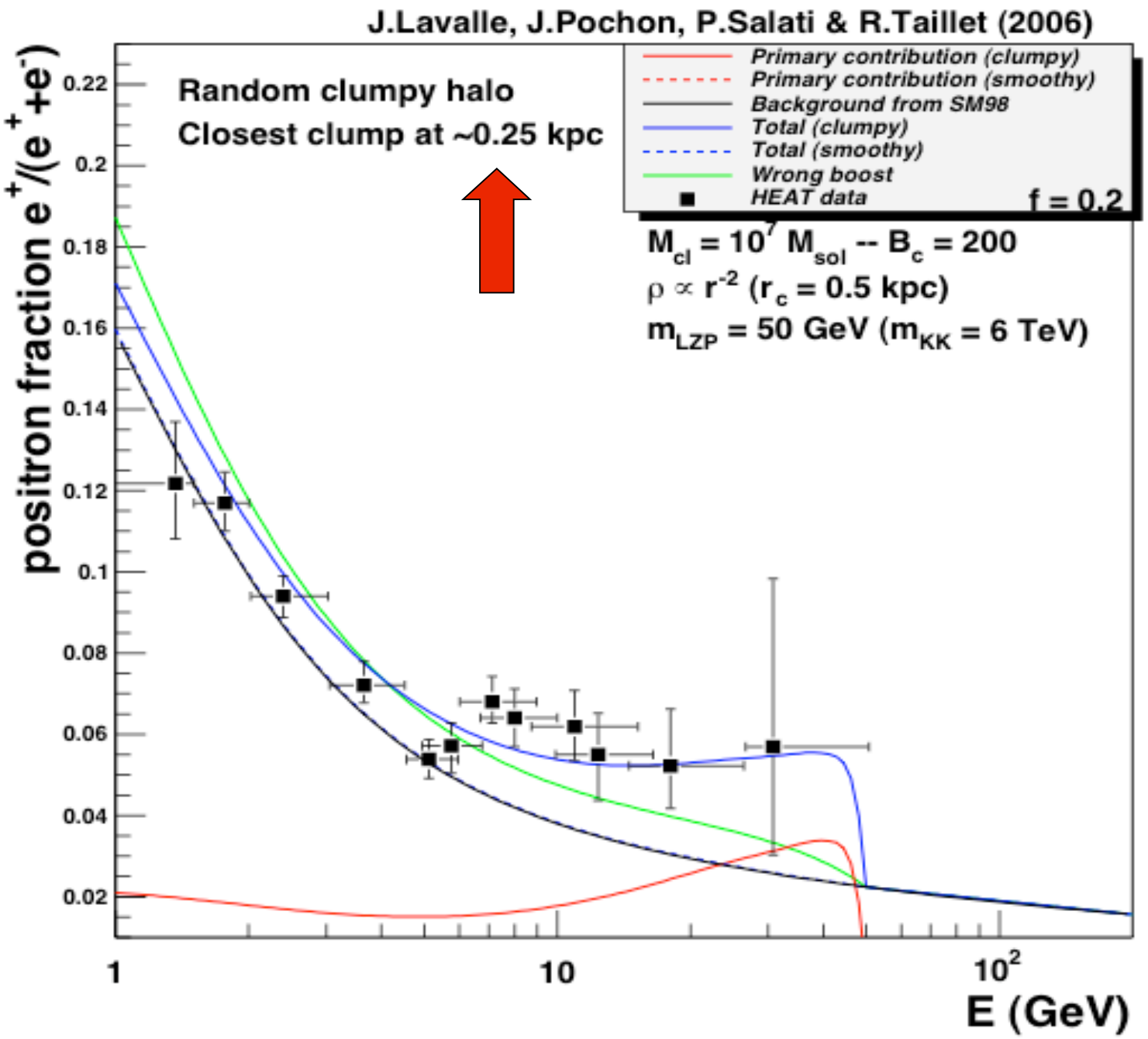
J.Lavalle, J.Pochon, P.Salati & R.Taillet (2006)
Random clumpy halo
Closest clump at ~0.25 kpc
Primary contribution (clumpy)
Primary contribution (smoothy)
Background from SM98
Total (clumpy)
Total (smoothy)
Wrong boost
HEAT data
f = 0.2
M_cl = 10^7 M_sol -- B_c = 200
ρ ∝ r^-2 (r_c = 0.5 kpc)
m_LZP = 50 GeV (m_KK = 6 TeV)
positron fraction e+/(e+ +e-)
E (GeV)
0.22
0.2
0.18
0.16
0.14
0.12
0.1
0.08
0.06
0.04
0.02
1
10
10^2

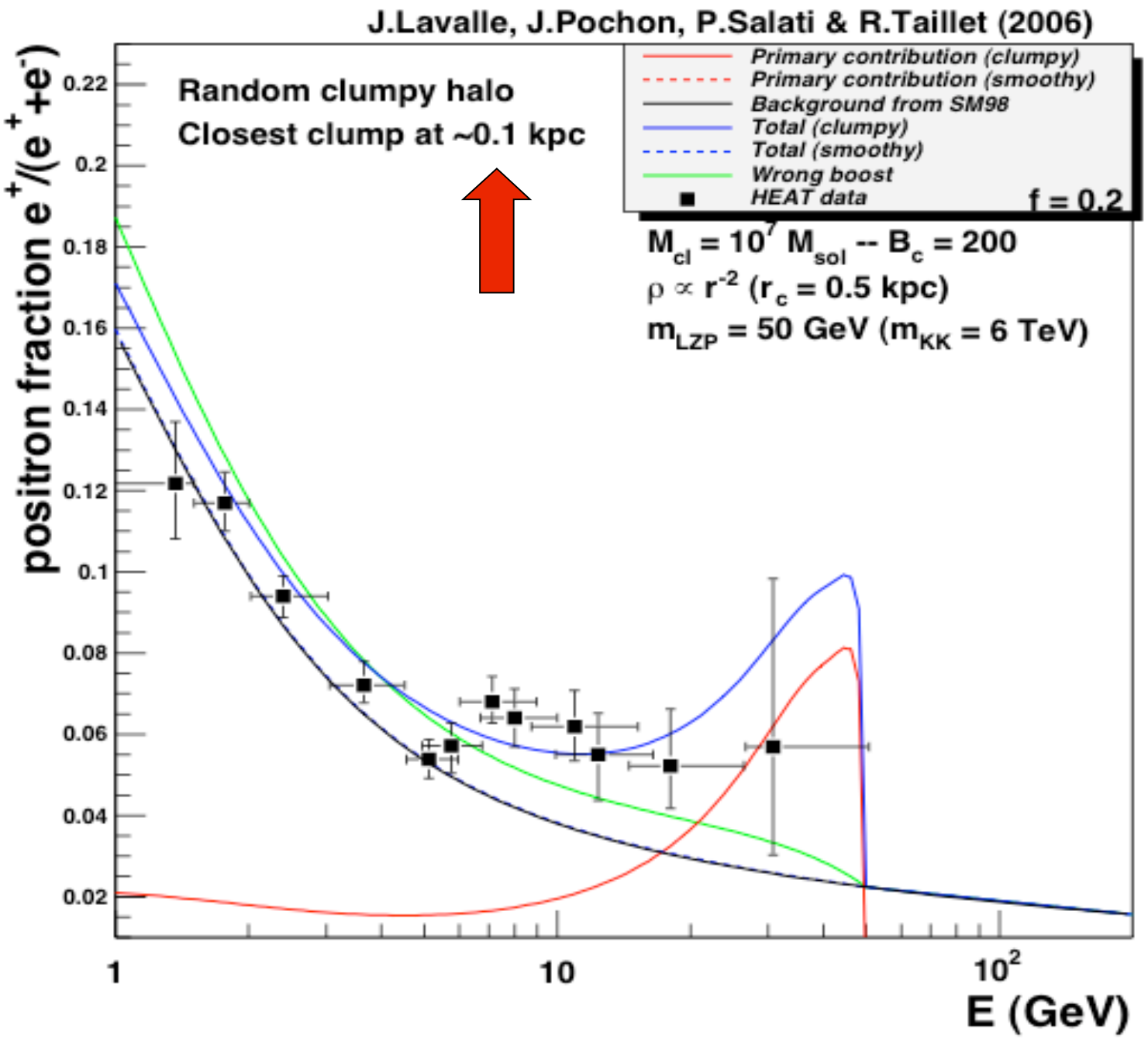
J.Lavalle, J.Pochon, P.Salati & R.Taillet (2006)
Random clumpy halo
Closest clump at ~0.1 kpc
Primary contribution (clumpy)
Primary contribution (smoothy)
Background from SM98
Total (clumpy)
Total (smoothy)
Wrong boost
HEAT data
f = 0.2
M_cl = 10^7 M_sol -- B_c = 200
ρ ∝ r^-2 (r_c = 0.5 kpc)
m_LZP = 50 GeV (m_KK = 6 TeV)
positron fraction e+/(e+ +e-)
E (GeV)
0.22
0.2
0.18
0.16
0.14
0.12
0.1
0.08
0.06
0.04
0.02
1
10
10^2

How probable is that ?

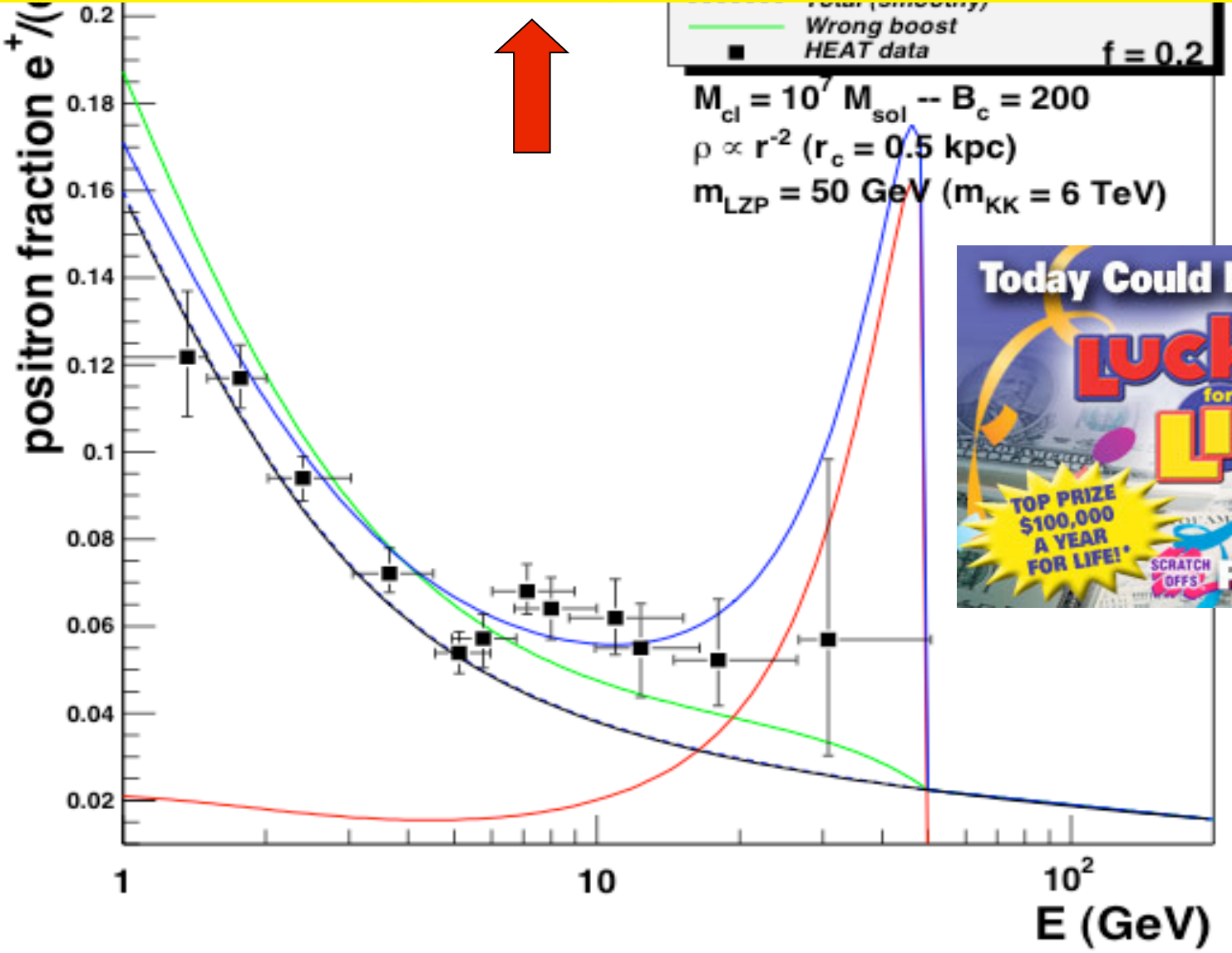

Positron line as the DM signal $\chi + \chi \to e^+ e^-$

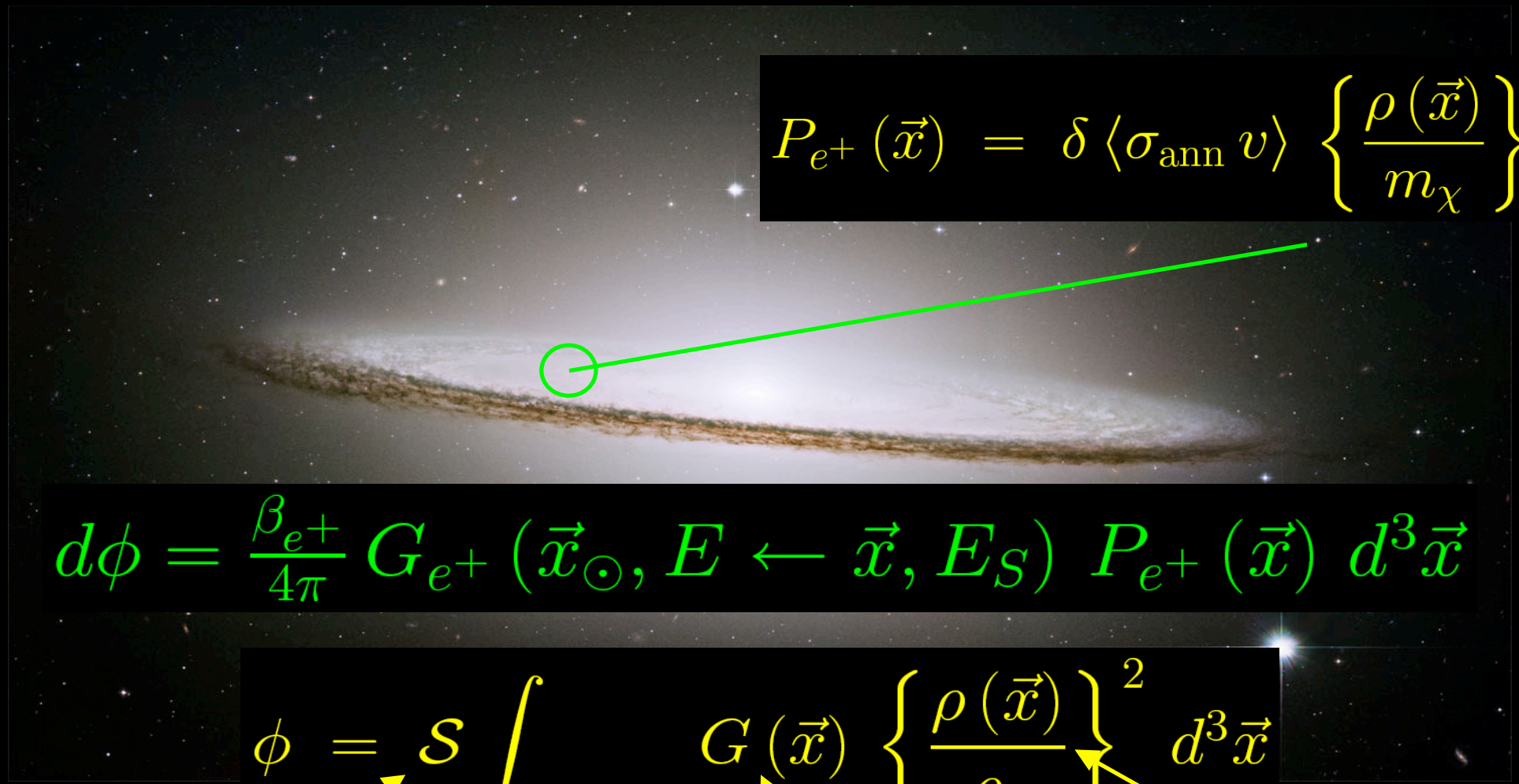

$$P_{e^+}(\vec{x}) = \delta \langle \sigma_{\rm ann}\, v \rangle \left\{ \frac{\rho(\vec{x})}{m_\chi} \right\}^2$$

$$d\phi = \frac{\beta_{e^+}}{4\pi} G_{e^+}(\vec{x}_\odot, E \leftarrow \vec{x}, E_S)\; P_{e^+}(\vec{x})\; d^3\vec{x}$$

$$\phi = \mathcal{S} \int_{\rm DM\,halo} G(\vec{x}) \left\{ \frac{\rho(\vec{x})}{\rho_0} \right\}^2 d^3\vec{x}$$

your favorite model

e^+ propagation

$\rho = \rho'_s + \delta\rho$

- Without clumps – with the smooth DM distribution $\rho(\vec{x}) = \rho_s$

$$\phi_s = \mathcal{S} \int_{\text{DM halo}} G(\vec{x}) \left\{ \frac{\rho_s(\vec{x})}{\rho_0} \right\}^2 d^3\vec{x}$$

- With clumps – with the DM distribution $\rho(\vec{x}) = \rho'_s + \delta\rho$

$$\phi = \phi'_s + \left(\phi_r = \sum_i \varphi_i \right)$$

$$\varphi_i = \mathcal{S} \int_{\text{ith clump}} G(\vec{x}) \left\{ \frac{\delta\rho(\vec{x})}{\rho_0} \right\}^2 d^3\vec{x}$$

random behaviour !

$\Downarrow$

Boost factor $B \equiv \dfrac{\phi}{\phi_s}$

Issues in the presence of DM clumps

- Typical length for positron propagation $\Rightarrow G(\vec{x})$
- Definition of the clump boost factor B_c at the **source**
- Statistical law and distribution of probability for B ?
- What is the average boost $\langle B \rangle \equiv B_{\rm eff}$ and the variance σ_B ?
- Do $B_{\rm eff}$ and σ_B depend on the energy ?

3.2) Positron Galactic propagation – a reminder

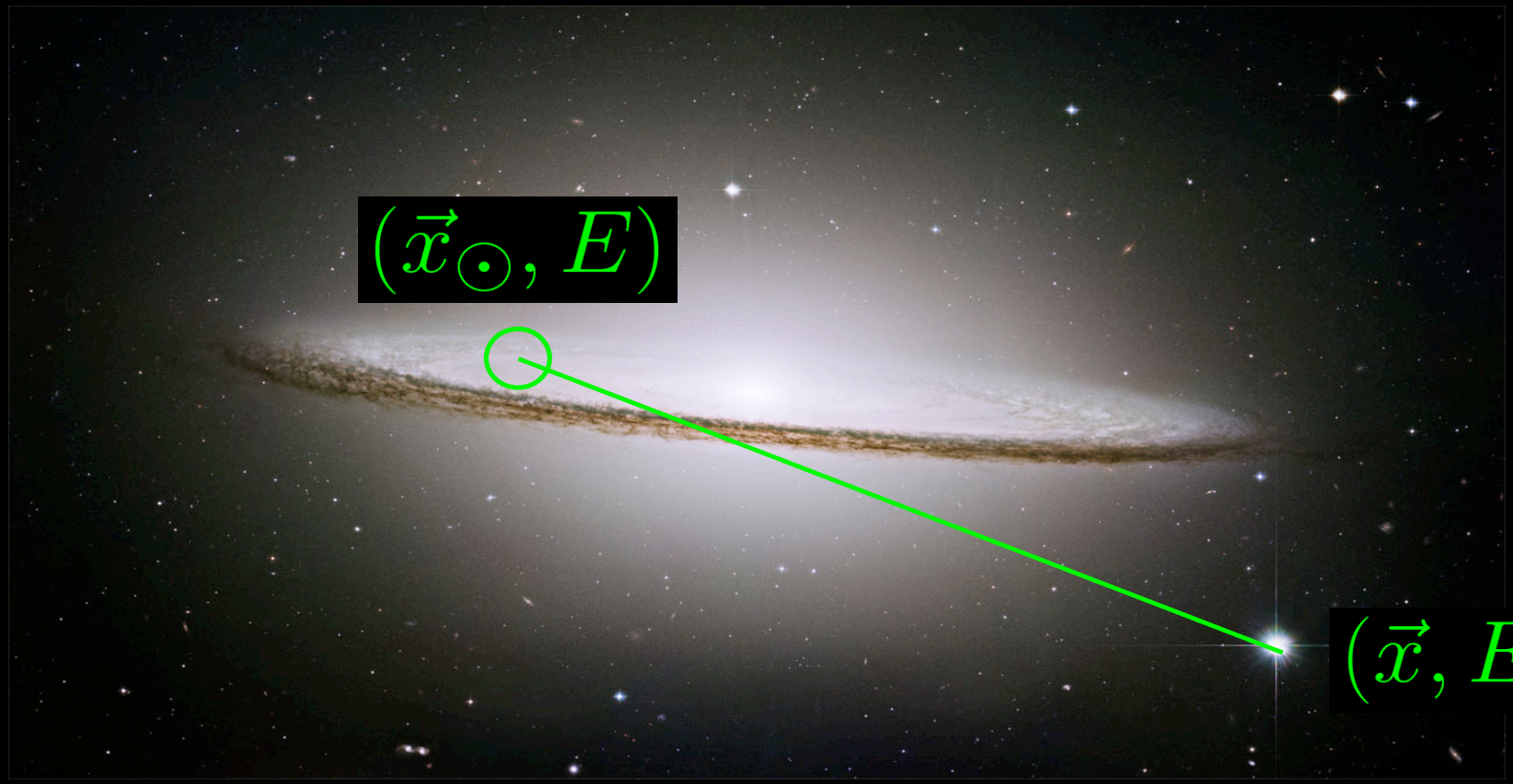

$$G_{e^+}\left(\vec{x}_\odot, E \leftarrow \vec{x}, E_S\right)$$

$$\frac{\partial \psi}{\partial t} - \vec{\nabla} \cdot \left\{ K\left(\vec{x}, E\right) \vec{\nabla} \psi \right\} - \frac{\partial}{\partial E} \left\{ b(E)\, \psi \right\} = Q\left(\vec{x}, E\right)$$

$$K\left(E\right) = K_0 \left\{ \frac{E}{E_0} \right\}^{\alpha} = K_0\, \epsilon^{\alpha} \qquad b(E) = \frac{E^2}{E_0\, \tau_E}$$

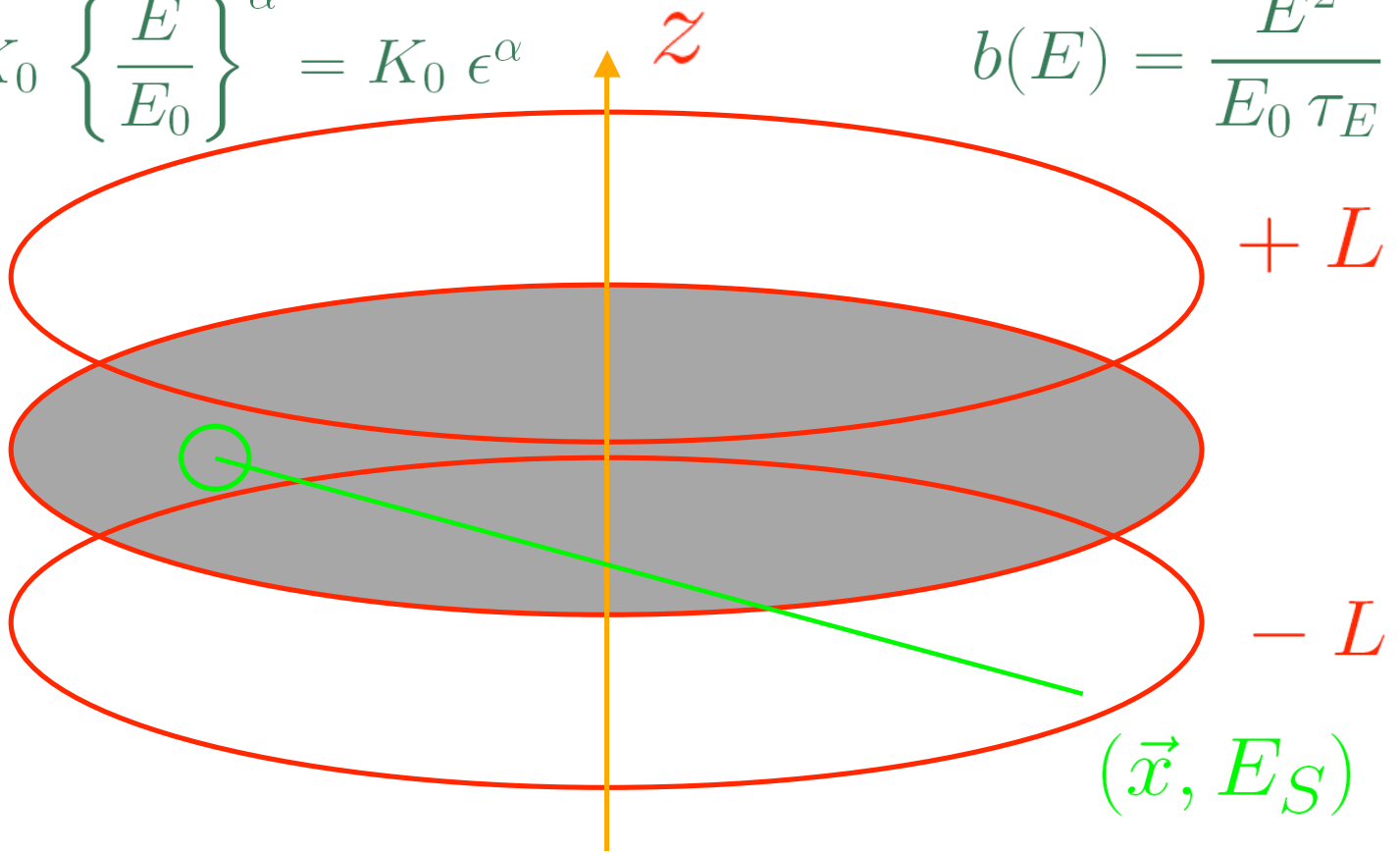

$$K_0\, \epsilon^{\alpha}\, \Delta \psi + \frac{\partial}{\partial \epsilon} \left\{ \frac{\epsilon^2}{\tau_E} \psi \right\} + Q = 0$$

Baltz & Edsjo trick

$$\tilde{\psi} = \epsilon^2\,\psi \quad \text{and} \quad \tilde{Q} = \epsilon^{2-\alpha}\,Q \quad \text{and} \quad \tilde{t}(E) = \tau_E \left\{ v(E) \;=\; \frac{\epsilon^{\alpha-1}}{1-\alpha} \right\}$$

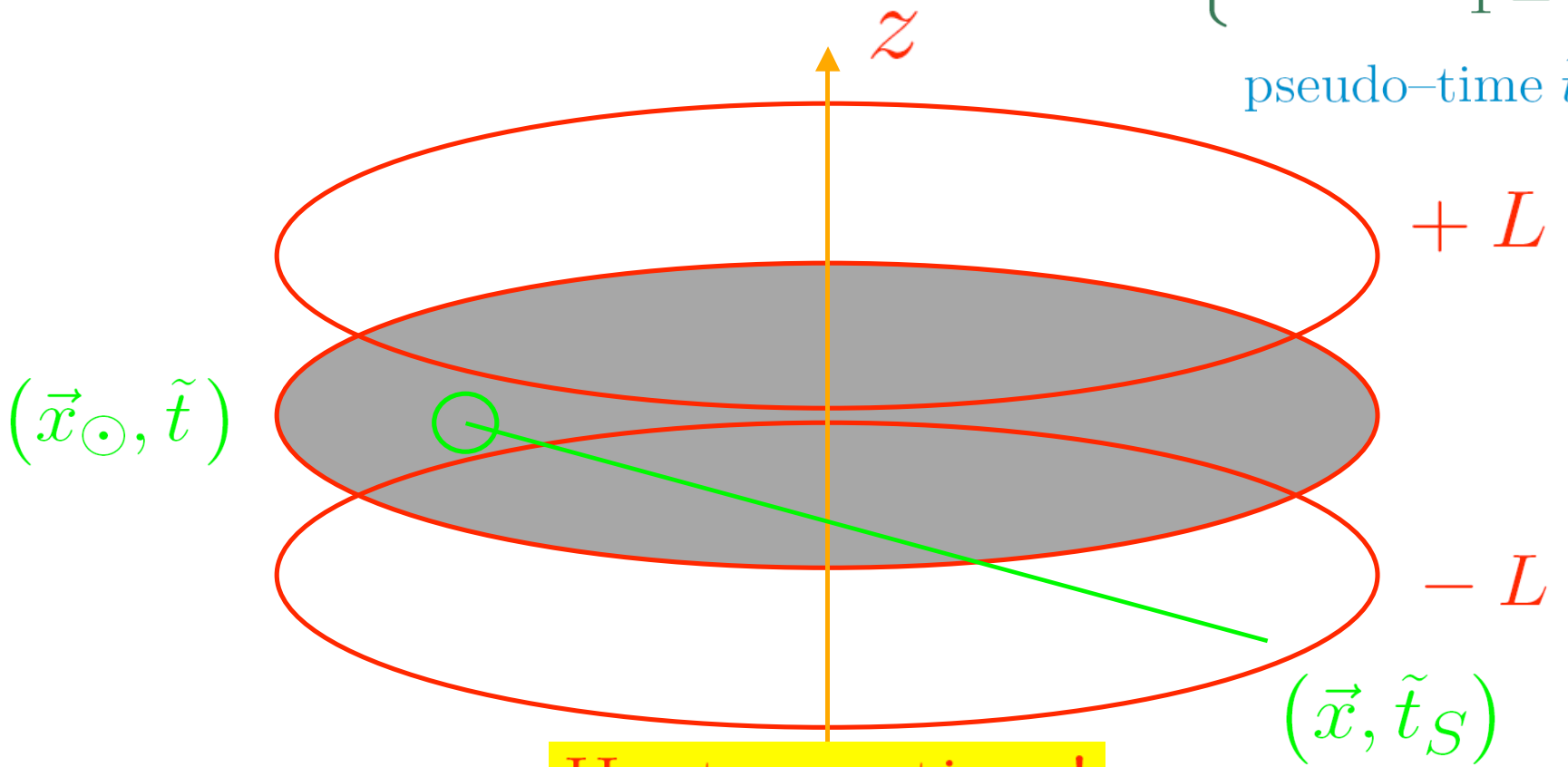

Heat equation !

$$\frac{\partial \tilde{\psi}}{\partial \tilde{t}} \;-\; K_0\,\Delta\tilde{\psi} \;=\; \tilde{Q}\,(\vec{x}, \tilde{t}\,)$$

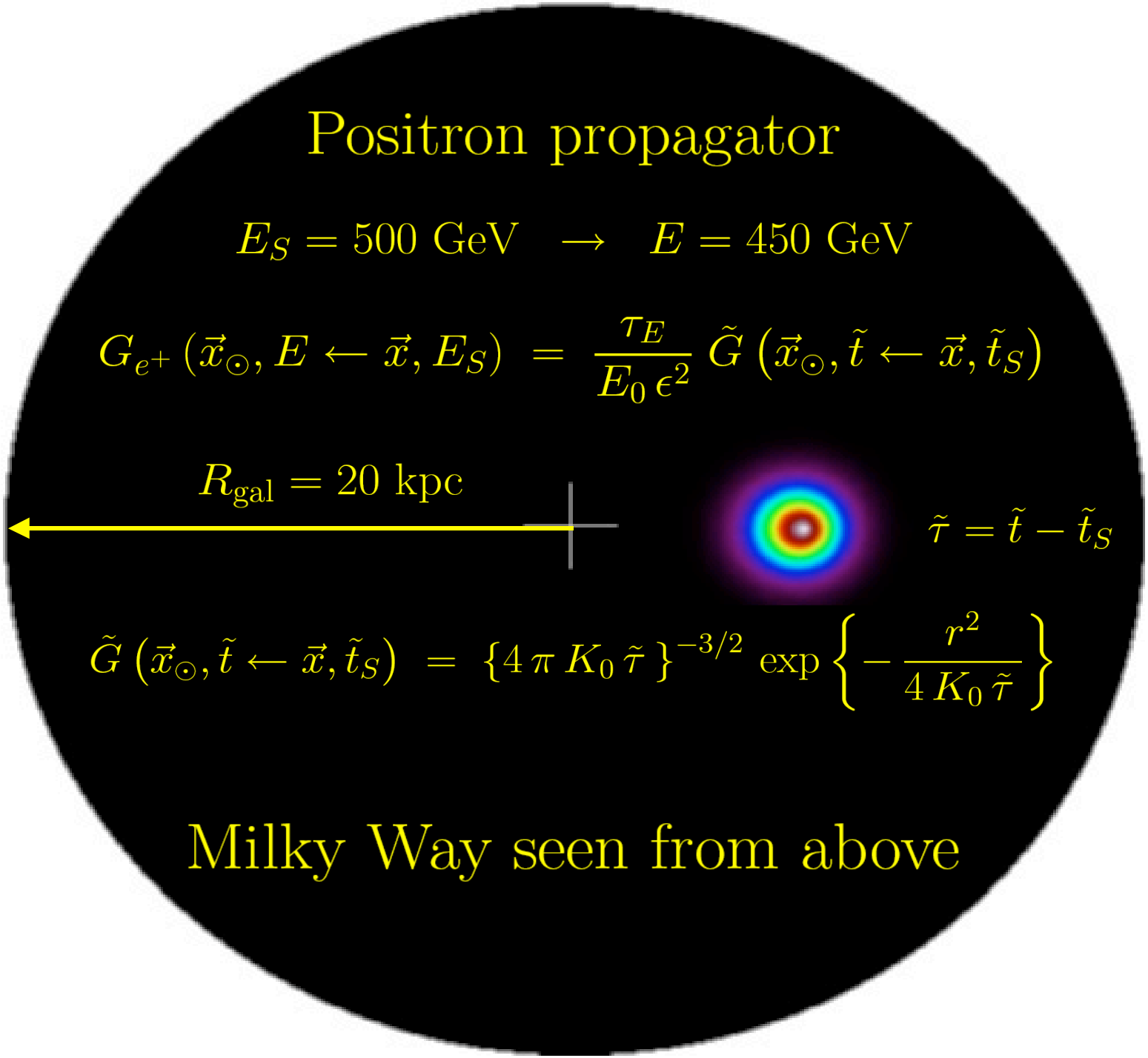
Positron propagator
$E_S = 500$ GeV $\rightarrow$ $E = 450$ GeV
$G_{e^+}(\vec{x}_\odot, E \leftarrow \vec{x}, E_S) = \frac{\tau_E}{E_0\,\epsilon^2}\,\tilde{G}(\vec{x}_\odot, \tilde{t} \leftarrow \vec{x}, \tilde{t}_S)$
$R_{\rm gal} = 20$ kpc
$\tilde{\tau} = \tilde{t} - \tilde{t}_S$
$\tilde{G}(\vec{x}_\odot, \tilde{t} \leftarrow \vec{x}, \tilde{t}_S) = \{4\,\pi\,K_0\,\tilde{\tau}\}^{-3/2}\,\exp\left\{-\frac{r^2}{4\,K_0\,\tilde{\tau}}\right\}$
Milky Way seen from above

Positron propagator

$$E_S = 500 \text{ GeV} \quad \rightarrow \quad E = 450 \text{ GeV}$$

$$G_{e^+}\left(\vec{x}_\odot, E \leftarrow \vec{x}, E_S\right) = \frac{\tau_E}{E_0\,\epsilon^2}\,\tilde{G}\left(\vec{x}_\odot, \tilde{t} \leftarrow \vec{x}, \tilde{t}_S\right)$$

$$\tilde{G}\left(\vec{x}_\odot, \tilde{t} \leftarrow \vec{x}, \tilde{t}_S\right) = \frac{\theta(r_S - r)}{V_S}$$

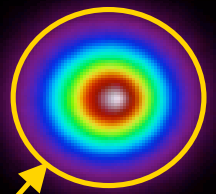

$$\tilde{\tau} = \tilde{t} - \tilde{t}_S$$

$$\frac{1}{V_S} = \int \tilde{G}^2\, d^3\vec{x}$$

Typical range $\lambda_{\rm D} = \sqrt{4\,K_0\,\tilde{\tau}}$

$$V_S = \left(\sqrt{2\pi}\,\lambda_{\rm D}\right)^3$$

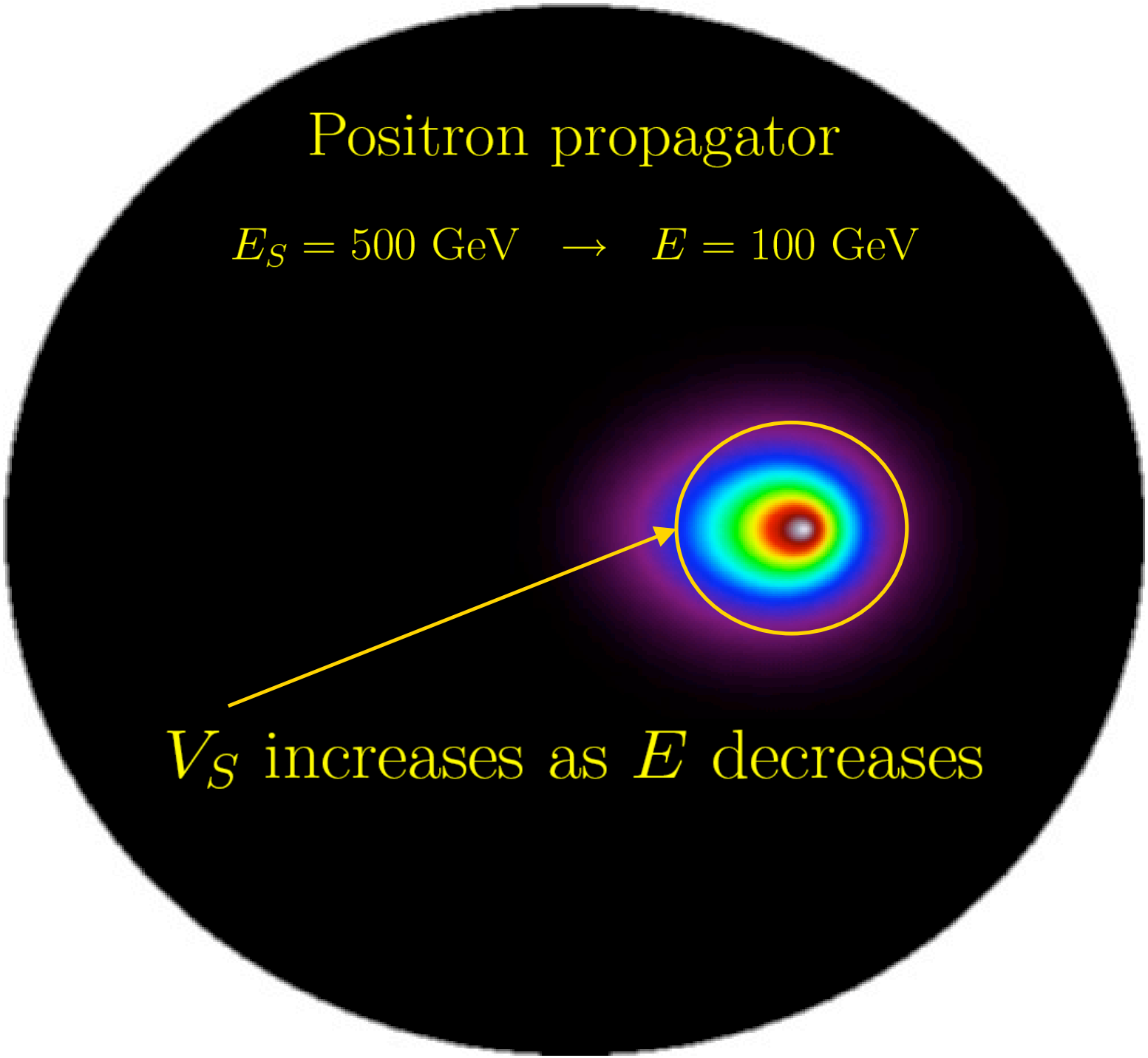
Positron propagator
$E_S = 500$ GeV $\rightarrow$ $E = 100$ GeV
V_S increases as E decreases

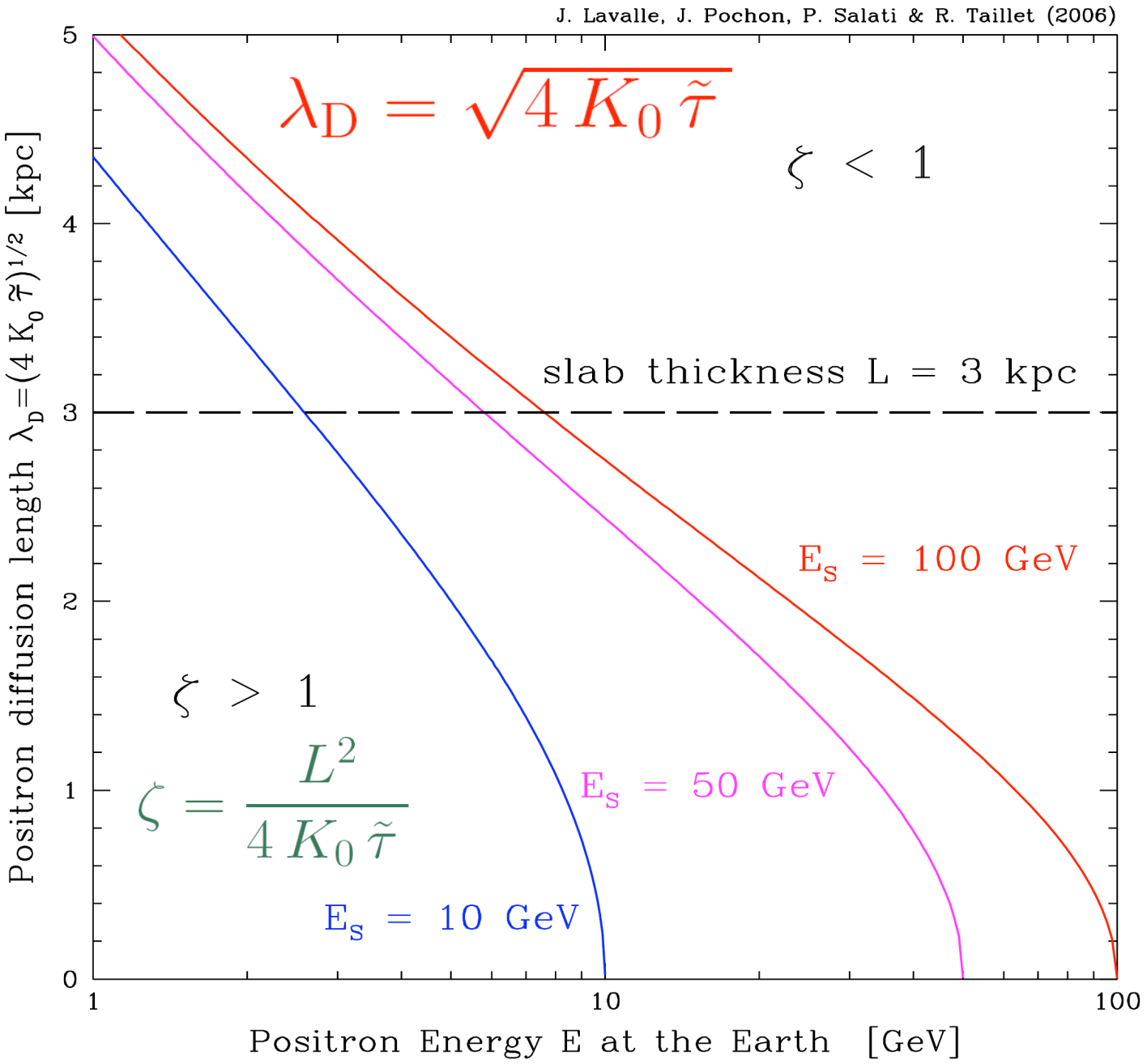
J. Lavalle, J. Pochon, P. Salati & R. Taillet (2006)
$\lambda_D = \sqrt{4\,K_0\,\tilde{\tau}}$
$\zeta < 1$
slab thickness L = 3 kpc
E_s = 100 GeV
E_s = 50 GeV
E_s = 10 GeV
$\zeta > 1$
$\zeta = \frac{L^2}{4\,K_0\,\tilde{\tau}}$
Positron diffusion length $\lambda_D=(4\,K_0\,\tilde{\tau})^{1/2}$ [kpc]
Positron Energy E at the Earth [GeV]
0
1
2
3
4
5
1
10
100

Clumps are small with respect to $\lambda_{\rm D}$

$$\Downarrow$$

$$\varphi_i \;=\; \mathcal{S} \times G(\vec{x}_i) \times \int_{\text{ith clump}} \left\{ \frac{\delta\rho(\vec{x})}{\rho_0} \right\}^2 \, d^3\vec{x}$$

The clump boost factor B_c

$$\int_{\text{clump}} d^3\vec{x}\ \ \delta\rho(\vec{x}) = \boxed{M_c} \quad \text{and} \quad \int_{\text{clump}} d^3\vec{x}\ \ \delta\rho^2(\vec{x}) = \boxed{B_c\ \rho_0}\, M_c$$

Self–gravitating system

$B_0 = 1$

B_c

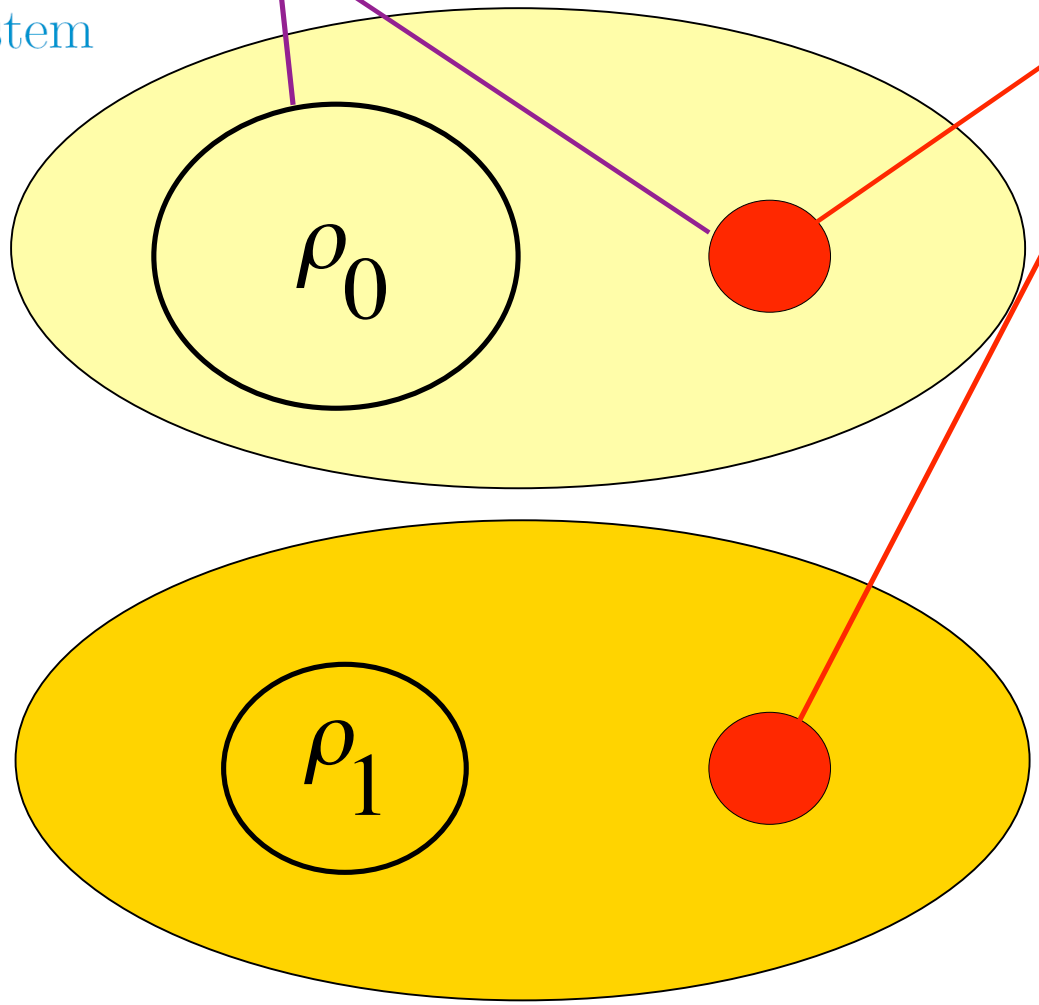

$$B_1 = \frac{\rho_1}{\rho_0}$$

B_c

Clumps are small with respect to $\lambda_{\rm D}$

$$\Downarrow$$

$$\varphi_i \;=\; \mathcal{S} \times G(\vec{x}_i) \times \int_{\text{ith clump}} \left\{ \frac{\delta\rho(\vec{x})}{\rho_0} \right\}^2 \, d^3\vec{x}$$

$$\Downarrow$$

$$\varphi_i \;=\; \mathcal{S} \times \left\{ \xi_i \equiv \frac{B_i \, M_i}{\rho_0} \right\} \times G(\vec{x}_i)$$

Clumps are small with respect to $\lambda_{\rm D}$

$$\Downarrow$$

$$\varphi_i \;=\; \mathcal{S} \times G(\vec{x}_i) \times \int_{\text{ith clump}} \left\{ \frac{\delta\rho(\vec{x})}{\rho_0} \right\}^2 \, d^3\vec{x}$$

$$\Downarrow$$

$$\varphi_i \;=\; \mathcal{S} \times \left\{ \xi_i \equiv \frac{B_i \, M_i}{\rho_0} \right\} \times G(\vec{x}_i)$$

$$\Downarrow$$

If clumps are identical $\varphi_i \;=\; \mathcal{S} \times \left\{ \xi_c \equiv \dfrac{B_c \, M_c}{\rho_0} \right\} \times G(\vec{x}_i)$

3.3) Statistical analysis of the positron signal fluctuations

(i) To simplify the discussion – without loss of generality – we assume that clumps are identical.

$$\phi = \phi'_s \; + \; \left(\phi_r = \sum_i \varphi_i = \mathcal{S} \times \frac{B_c \, M_c}{\rho_0} \times \sum_i G_i \right)$$

(ii) The actual distribution of DM substructures is one particular realization $\in$ statistical ensemble of all the possible **random** distributions.

$$\langle \phi_r \rangle \quad \text{and} \quad \sigma_r^2 = \langle \phi_r^2 \rangle \, - \, \langle \phi_r \rangle^2$$

$$B_{\text{eff}} = \langle B = \phi / \phi_s \rangle \quad \text{and} \quad \sigma_B = \sigma_r / \phi_s$$

(iii) Clumps are distributed independently of each other. Therefore, we just need to determine how a single clump is distributed inside the galactic halo in order to derive the statistical properties of an entire constellation of N_H such substructures.

$$\langle \phi_r \rangle = N_H \, \langle \varphi \rangle \quad \text{and} \quad \sigma_r^2 = N_H \, \sigma^2 = N_H \left\{ \langle \varphi^2 \rangle \, - \, \langle \varphi \rangle^2 \right\}$$

(iv) The set of the random distributions of one single clump inside the domain $\mathcal{D}_H$ forms the statistical ensemble $\mathcal{T}$ which we need to consider. An event from that ensemble consists in a clump located at position $\vec{x}$ within the elementary volume $d^3\vec{x}$.

$$\mathcal{P}\left(\varphi\right)\, d\varphi \;=\; dP \;=\; \int_{\mathcal{D}_\varphi} p\left(\vec{x}\right)\, d^3\vec{x}$$

$$\left\langle \mathcal{F} \right\rangle \;=\; \int \mathcal{F}(\varphi)\, \mathcal{P}\left(\varphi\right)\, d\varphi \;=\; \int_{\mathcal{D}_H} \mathcal{F}\left\{\varphi\left(\vec{x}\right)\right\}\, p\left(\vec{x}\right)\, d^3\vec{x}$$

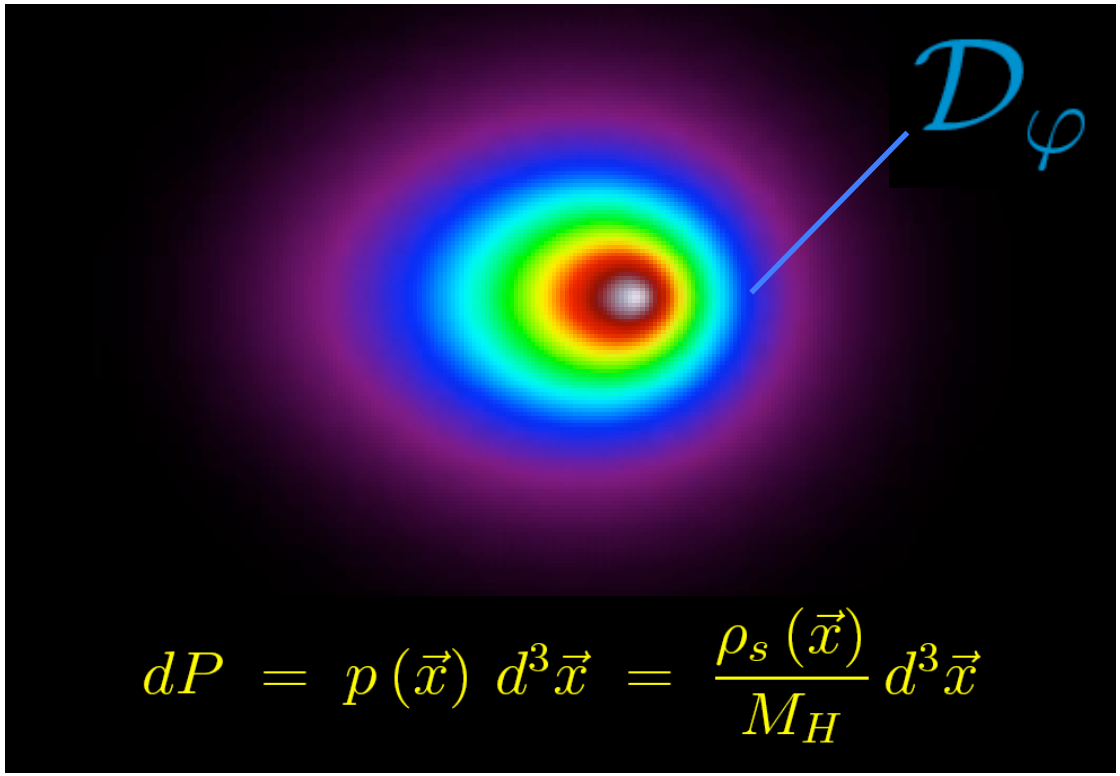

(v) In the following analysis we have furthermore assumed that clumps trace the smooth DM distribution. **This is not generally correct – see IMBHs !**

$$dP \;=\; p\,(\vec{x})\;d^3\vec{x} \;=\; \frac{\rho_s\,(\vec{x})}{M_H}\,d^3\vec{x}$$

(vi) We have finally assumed that $\rho_s' \equiv (1-f)\times\rho_s$ so that

$$\phi = (1-f)^2\,\phi_s \;+\; \left(\phi_r = \mathcal{S}\times\frac{B_c\,M_c}{\rho_0}\times\sum_i G_i\right)$$

$$\Downarrow$$

Analytical determination of $B_{\rm eff}$ and σ_B

Comparison between analytical and Monte-Carlo

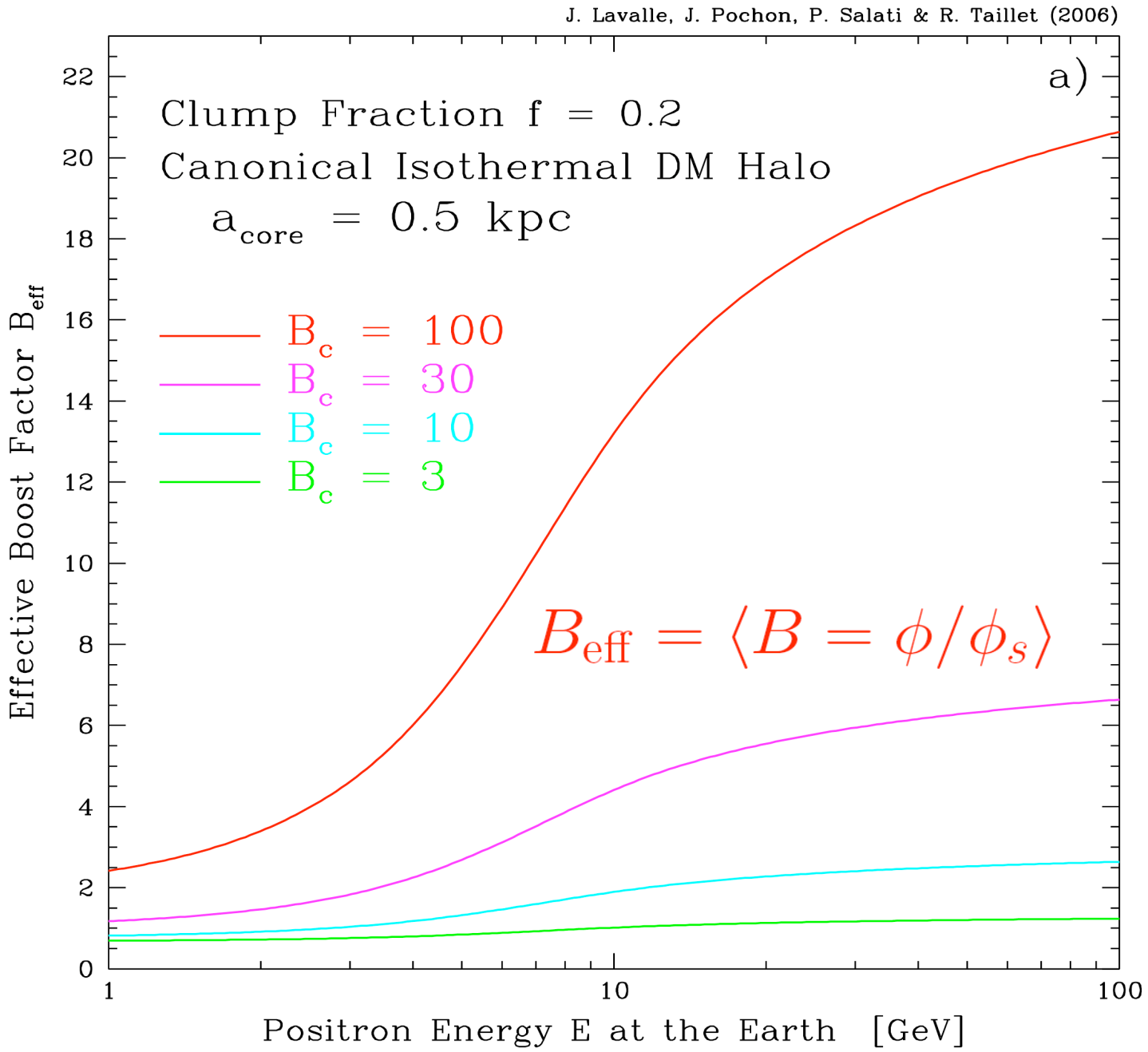
J. Lavalle, J. Pochon, P. Salati & R. Taillet (2006)
a)
Clump Fraction f = 0.2
Canonical Isothermal DM Halo
a_{core} = 0.5 kpc
B_c = 100
B_c = 30
B_c = 10
B_c = 3
$B_{\rm eff} = \langle B = \phi/\phi_s \rangle$
Effective Boost Factor B_{eff}
Positron Energy E at the Earth [GeV]
0
2
4
6
8
10
12
14
16
18
20
22
1
10
100

The clump boost factor B_c

$$\int_{\text{clump}} d^3\vec{x}\ \ \delta\rho(\vec{x}) = \boxed{M_c} \quad \text{and} \quad \int_{\text{clump}} d^3\vec{x}\ \ \delta\rho^2(\vec{x}) = \boxed{B_c\ \rho_0}\, M_c$$

Self–gravitating system

$B_0 = 1$

B_c

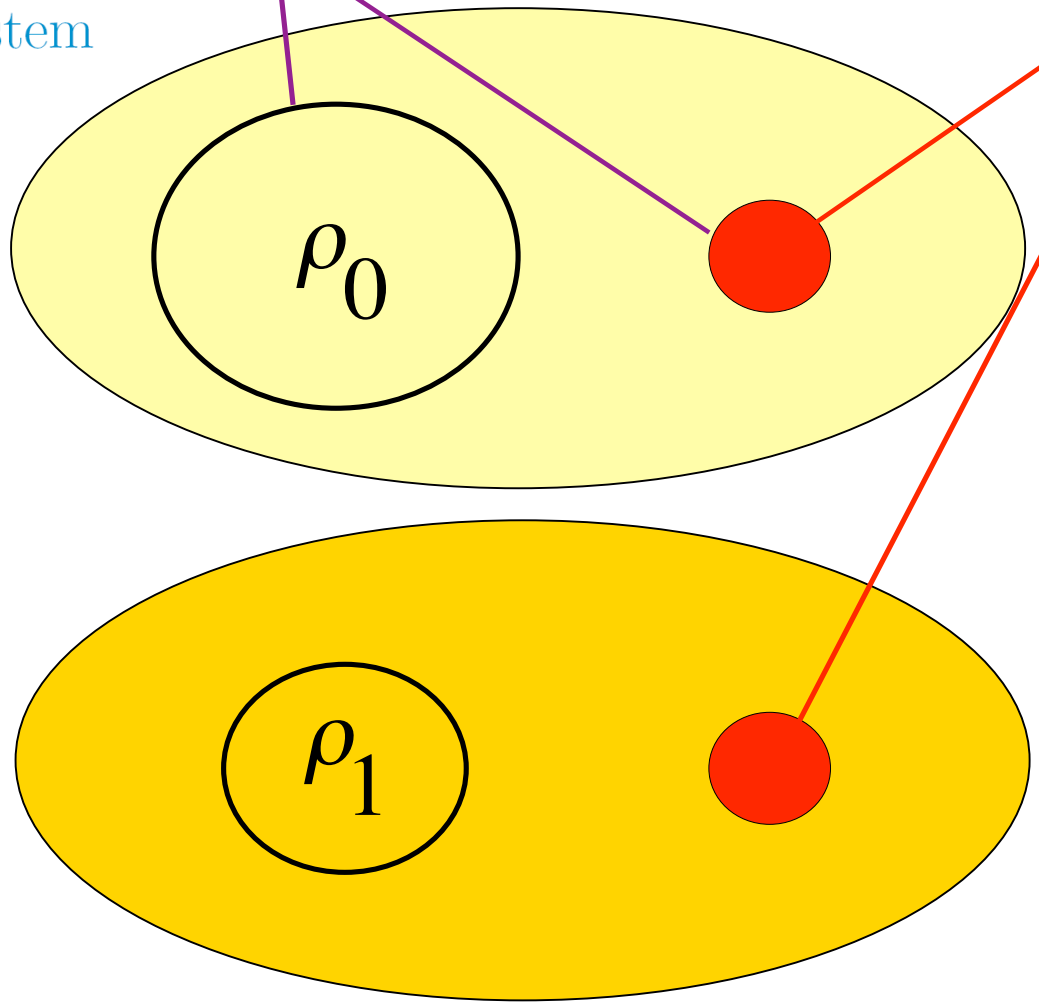

$$B_1 = \frac{\rho_1}{\rho_0}$$

B_c

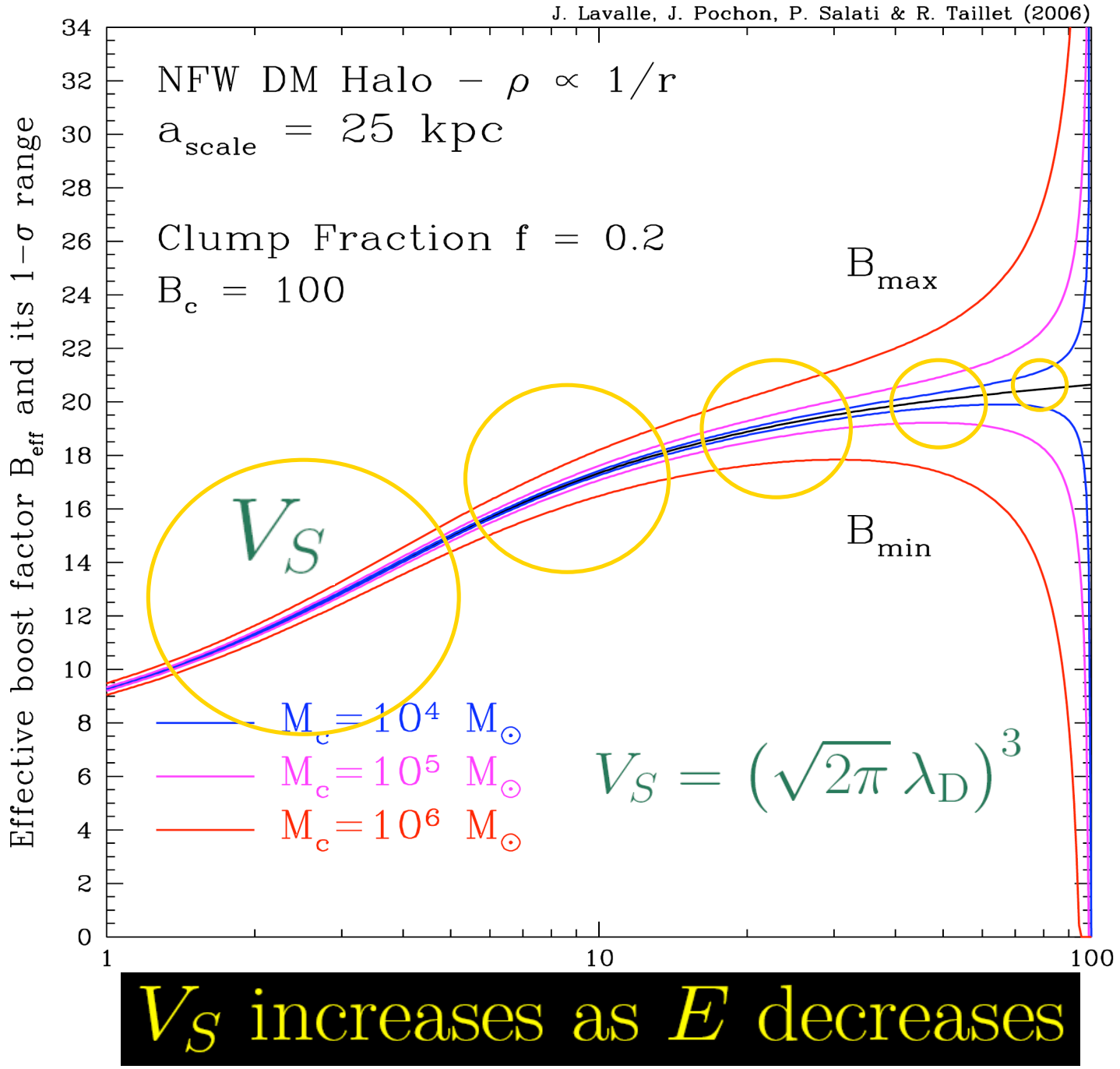

V_S increases as E decreases

The hard–sphere approach

The signal originates from the volume $V_S = \left(\sqrt{2\pi}\,\lambda_{\rm D}\right)^3$

Binomial density of probability for one clump

$$\mathcal{P}(\varphi) \;=\; p\,\delta(\varphi - \varphi_{\rm max}) \;+\; (1-p)\;\delta(\varphi)$$

n clumps inside

$$p = \frac{M_S}{M_H} = \frac{V_S\,\rho_s(\odot)}{M_H}$$

$(1-p)$

Poisson distribution

$$P(n) \;=\; \frac{{N_S}^n}{n!}\,\exp\left(-N_S\right) \text{ where } N_S \equiv p\,N_H$$

On average $\langle n \rangle$ clumps generate the signal

$$\langle n \rangle = N_S = \frac{V_S f \rho_s(\odot)}{M_c} \text{ and } \frac{\sigma_r}{\langle \phi_r \rangle} = \frac{\sigma_n}{\langle n \rangle} = \frac{1}{\sqrt{N_S}}$$

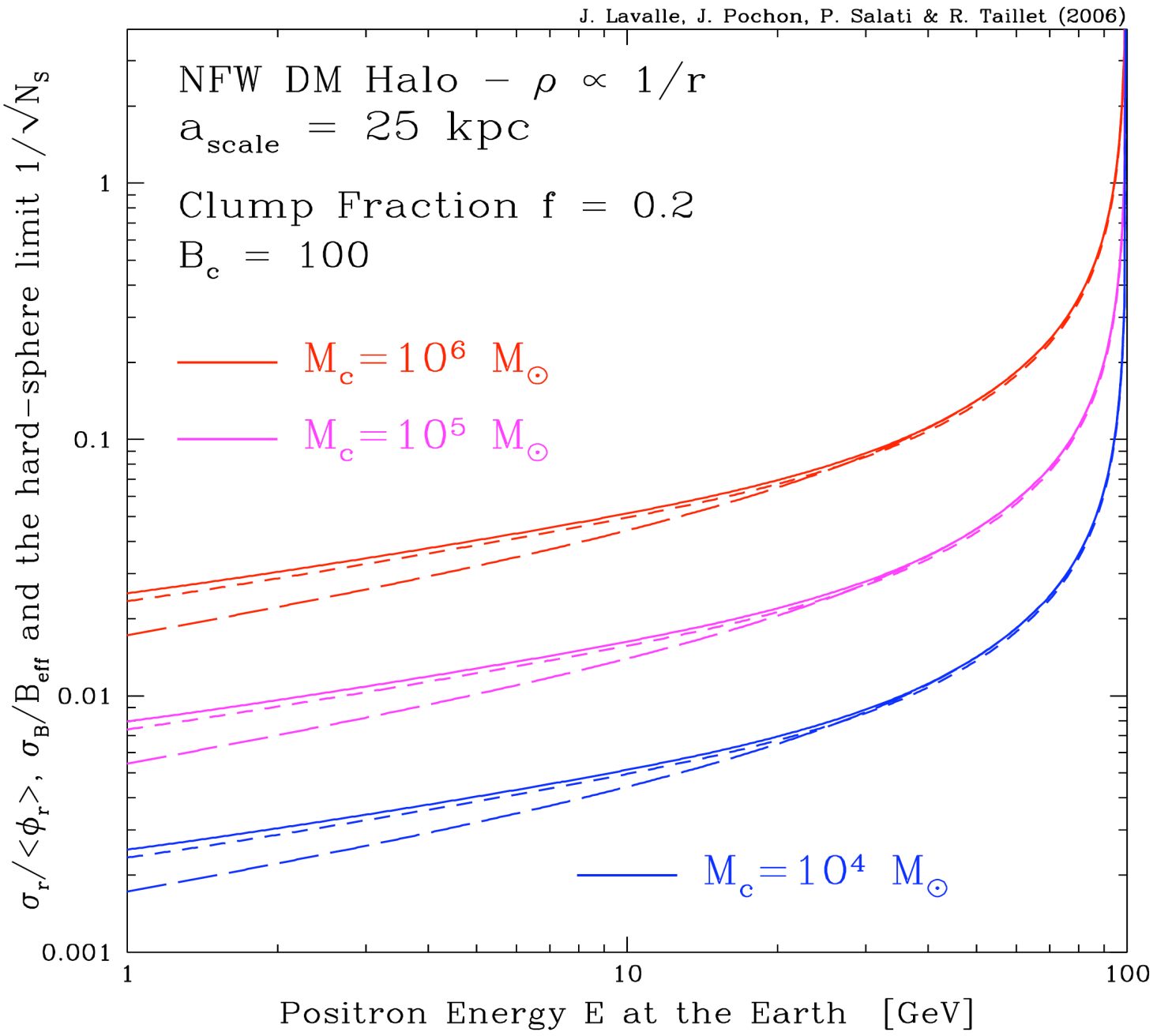
J. Lavalle, J. Pochon, P. Salati & R. Taillet (2006)
NFW DM Halo – ρ ∝ 1/r
a_scale = 25 kpc
Clump Fraction f = 0.2
B_c = 100
M_c = 10^6 M_⊙
M_c = 10^5 M_⊙
M_c = 10^4 M_⊙
σ_r/<φ_r>, σ_B/B_eff and the hard-sphere limit 1/√N_S
1
0.1
0.01
0.001
1
10
100
Positron Energy E at the Earth [GeV]

The large N_S limit

The Poisson statistics becomes Maxwellian

$$P\left(\delta \equiv n - N_S\right) \;=\; \frac{1}{\sqrt{2\pi N_S}}\,\exp\left(-\,\delta^2/2N_S\right)$$

The 1–clump distribution $\mathcal{P}(\varphi)$ is continuous !

The theorem of the central limit

$$\mathcal{P}\left\{\phi_r = \sum_i \varphi_i\right\} \;=\; \frac{1}{\sqrt{2\pi\sigma_r^2}}\,\exp\left\{-\,\frac{\left(\phi_r - \langle\phi_r\rangle\right)^2}{2\sigma_r^2}\right\}$$

$$\mathcal{P}\{B \equiv \phi/\phi_s\} \;=\; \frac{1}{\sqrt{2\pi\sigma_B^2}}\,\exp\left\{-\,\frac{\left(B - B_{\rm eff}\right)^2}{2\sigma_B^2}\right\}$$

$$\mathcal{P}\{\eta \equiv B/B_{\rm eff}\} \;=\; \frac{1}{\sqrt{2\pi\sigma_\eta^2}}\,\exp\left\{-\,\frac{\left(\eta - 1\right)^2}{2\sigma_\eta^2}\right\}$$

Analytical versus Monte Carlo

- Substructures contribute a fraction $f = 0.2$ to the mass of the Milky Way dark matter halo.
- A NFW profile is assumed with typical scale 25 kpc.
- Each clump has a mass of 10^5 $M_\odot$.
- 10^3 different Monte–Carlo realizations of the distribution of substructures.
- Each Monte–Carlo realization involves 271,488 clumps.
- The positron injection energy is $E_S = 100$ GeV.

To be compared to the analytical results

E	$B_{\rm eff}$	$\sigma_\eta = \sigma_B / B_{\rm eff}$	N_S
50	20.09	0.04338	498.0
65	20.32	0.06472	223.5
80	20.48	0.10966	78.0
90	20.57	0.19680	24.2

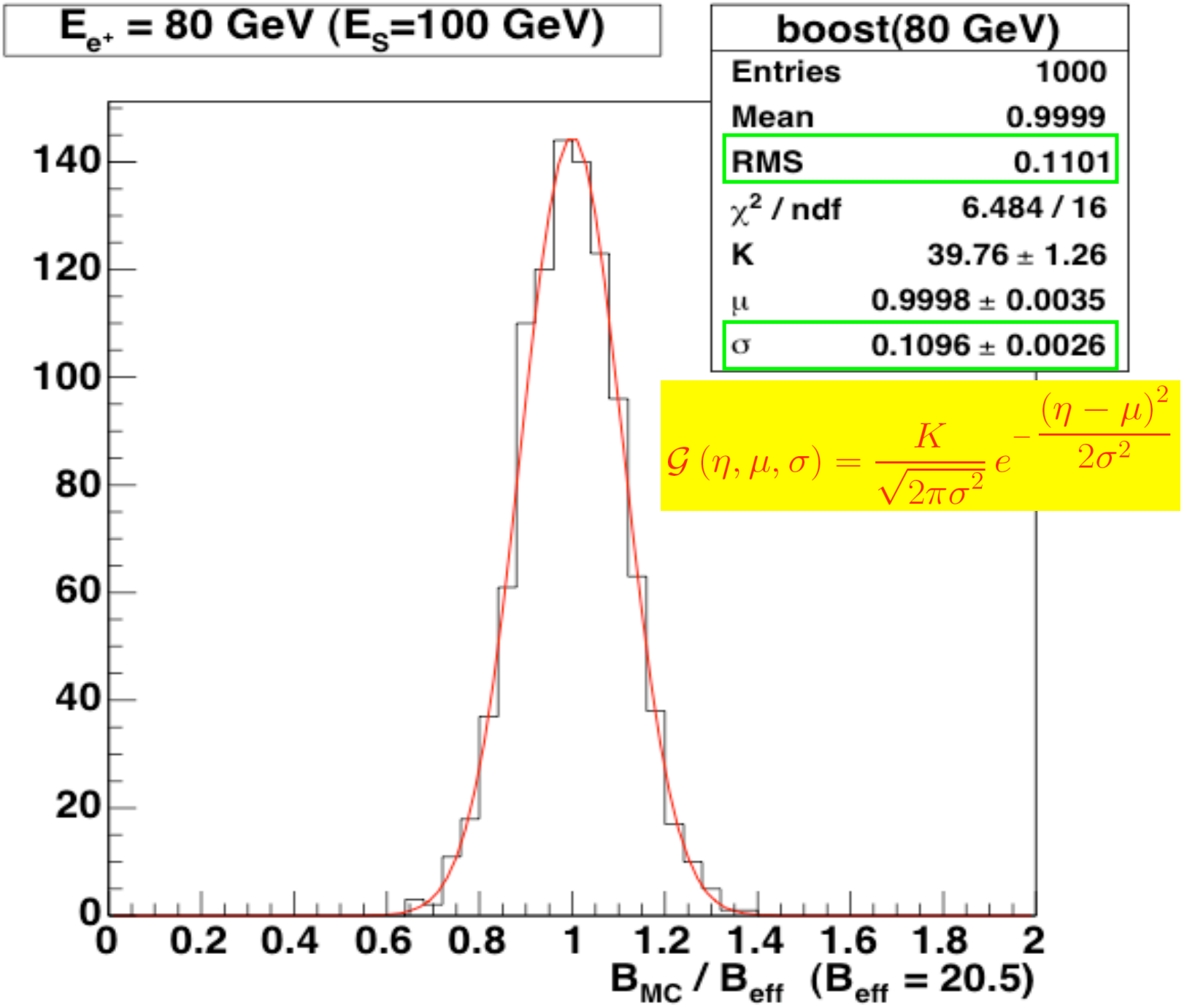
E_{e^+} = 80 GeV (E_S=100 GeV)
boost(80 GeV)
Entries 1000
Mean 0.9999
RMS 0.1101
χ^2 / ndf 6.484 / 16
K 39.76 ± 1.26
μ 0.9998 ± 0.0035
σ 0.1096 ± 0.0026
$\mathcal{G}(\eta,\mu,\sigma) = \frac{K}{\sqrt{2\pi\sigma^2}} e^{-\frac{(\eta-\mu)^2}{2\sigma^2}}$
0 20 40 60 80 100 120 140
0 0.2 0.4 0.6 0.8 1 1.2 1.4 1.6 1.8 2
B_{MC} / B_{eff} (B_{eff} = 20.5)

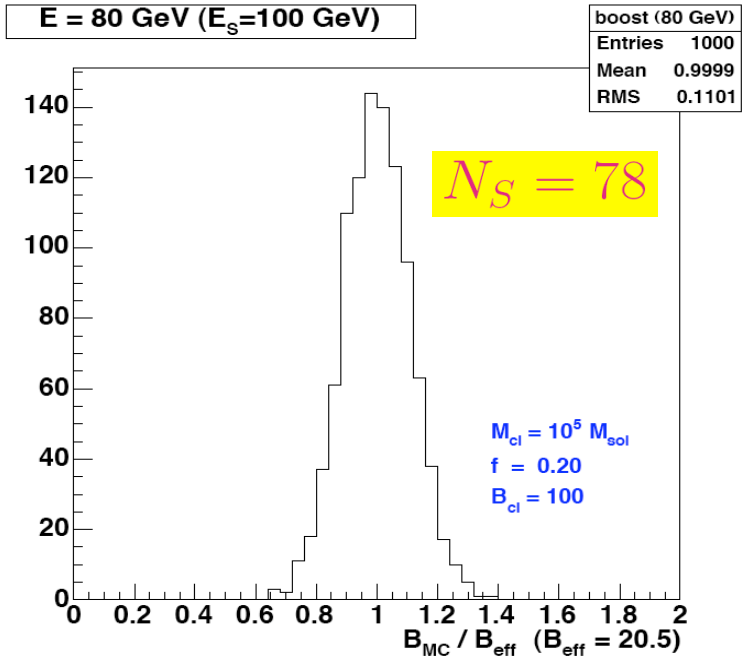
E = 80 GeV (E_S=100 GeV)
boost (80 GeV)
Entries 1000
Mean 0.9999
RMS 0.1101
N_S = 78
M_cl = 10^5 M_sol
f = 0.20
B_cl = 100
B_MC / B_eff (B_eff = 20.5)

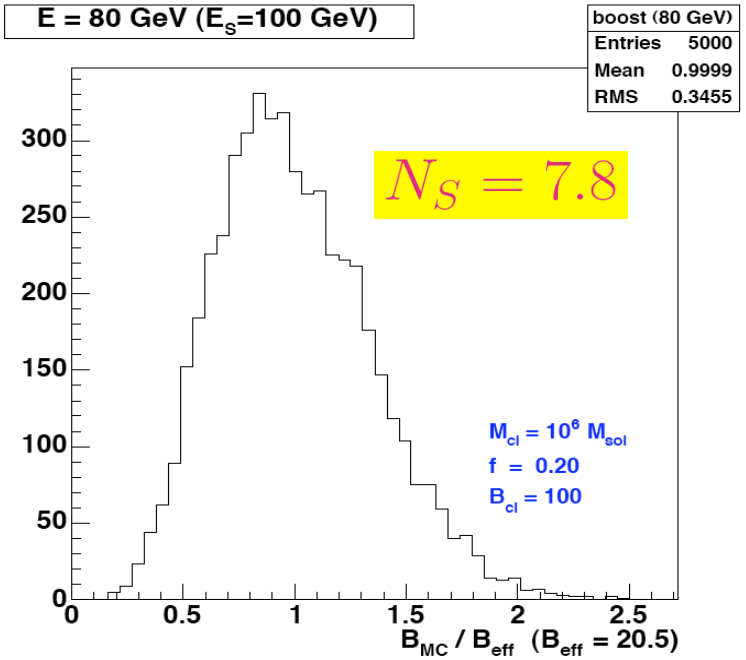
E = 80 GeV (E_S=100 GeV)
boost (80 GeV)
Entries 5000
Mean 0.9999
RMS 0.3455
N_S = 7.8
M_cl = 10^6 M_sol
f = 0.20
B_cl = 100
B_MC / B_eff (B_eff = 20.5)

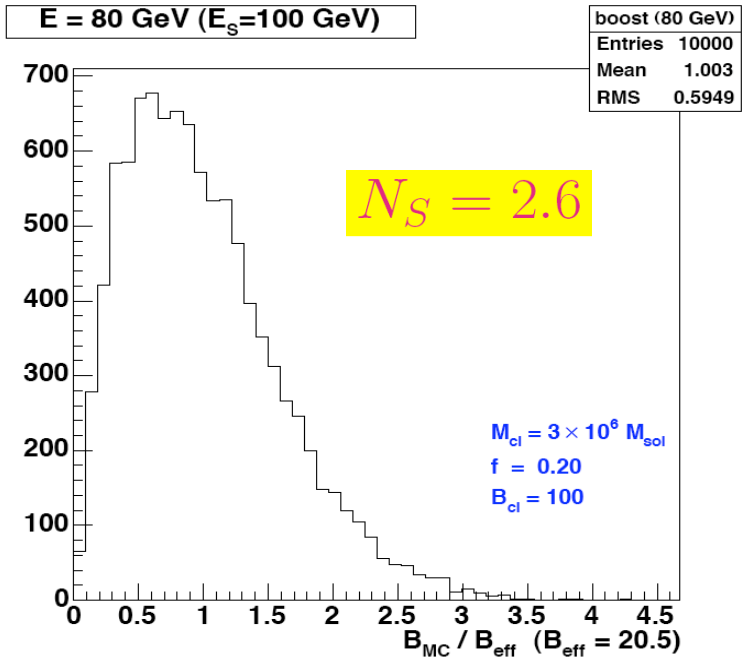
E = 80 GeV (E_S=100 GeV)
boost (80 GeV)
Entries 10000
Mean 1.003
RMS 0.5949
N_S = 2.6
M_cl = 3 × 10^6 M_sol
f = 0.20
B_cl = 100
B_MC / B_eff (B_eff = 20.5)

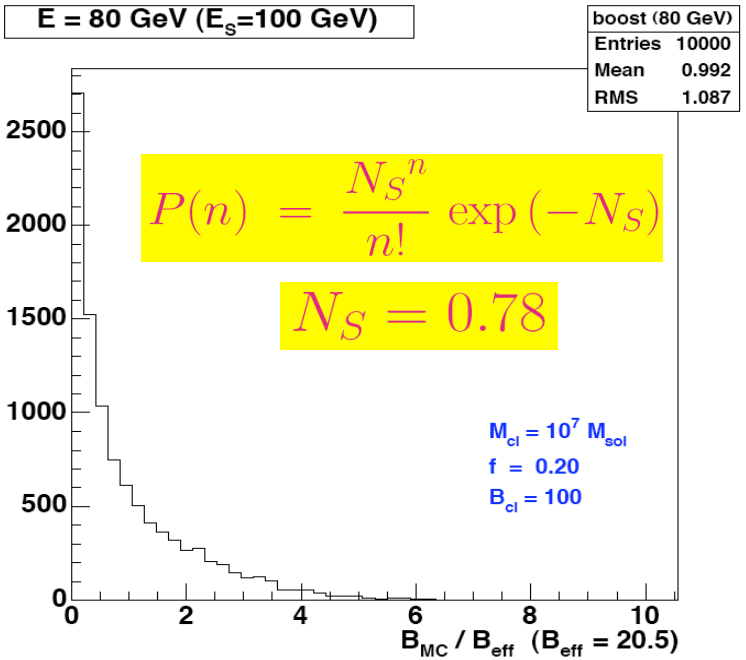
E = 80 GeV (E_S=100 GeV)
boost (80 GeV)
Entries 10000
Mean 0.992
RMS 1.087
$P(n) = \frac{{N_S}^n}{n!} \exp(-N_S)$
N_S = 0.78
M_cl = 10^7 M_sol
f = 0.20
B_cl = 100
B_MC / B_eff (B_eff = 20.5)

The small N_S limit

The distribution of probability is the product of convolution

$$\mathcal{P}_{N_H} = \mathcal{P}_1 * \mathcal{P}_1 * \ldots * \mathcal{P}_1$$

$$\mathcal{P}_{N_H}\left\{0 \leq \varphi \leq \varphi_{\max}\right\} \simeq N_H \times \mathcal{P}_1\left(\varphi\right)$$

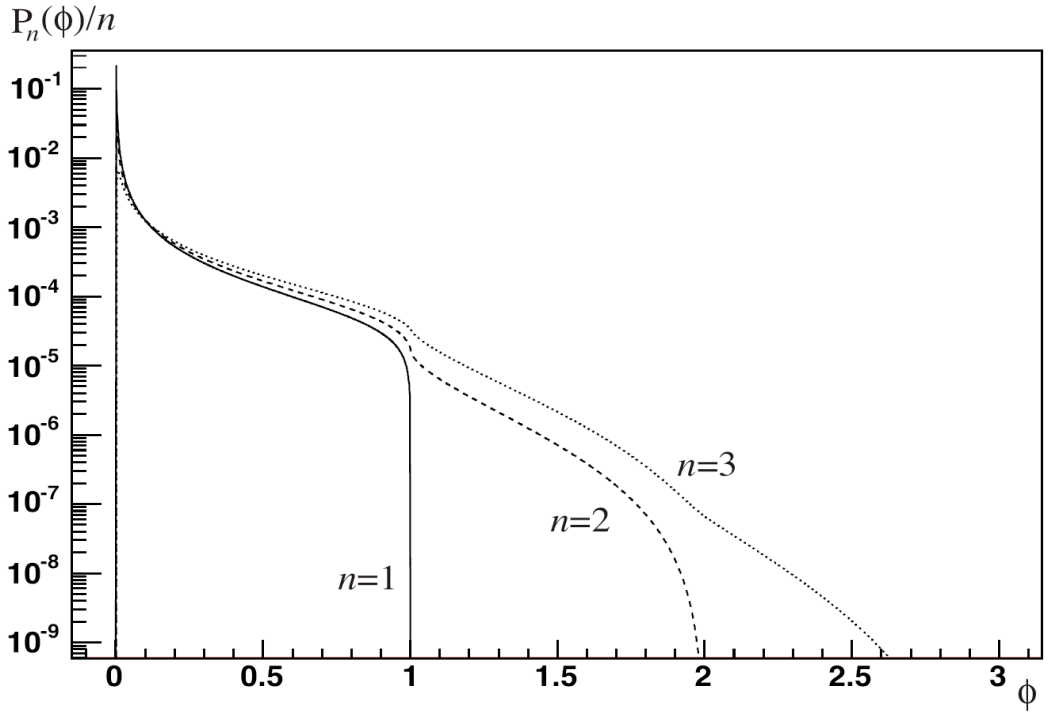

Fig. 10. Probability distribution $\mathcal{P}_n(\phi)/n$ for $n = 1$, 2 and 3, obtained by consecutive convolutions of $\mathcal{P}_1(\phi)$.

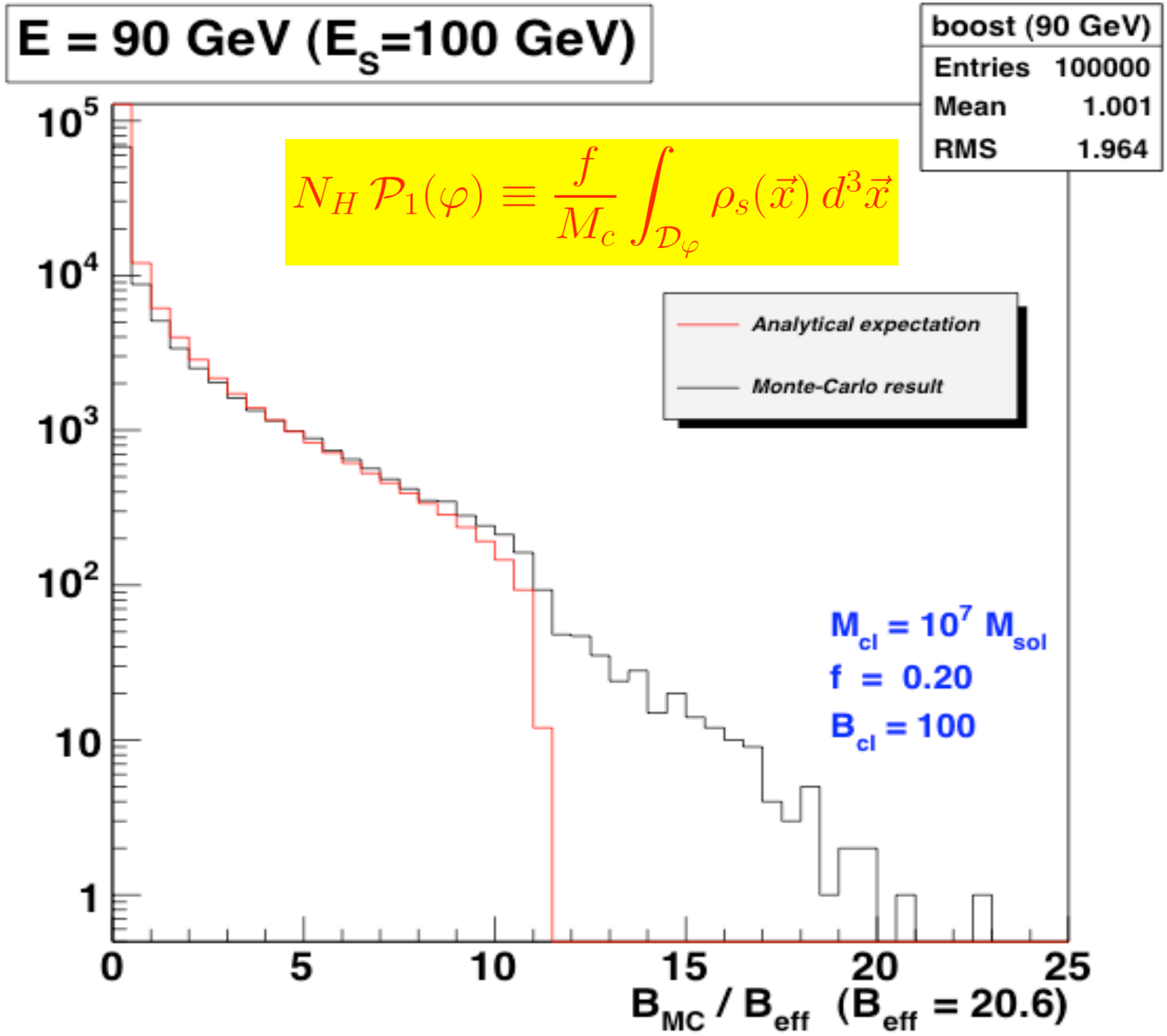
E = 90 GeV (E_S=100 GeV)
boost (90 GeV)
Entries 100000
Mean 1.001
RMS 1.964
$N_H \mathcal{P}_1(\varphi) \equiv \frac{f}{M_c} \int_{\mathcal{D}_\varphi} \rho_s(\vec{x})\, d^3\vec{x}$
Analytical expectation
Monte-Carlo result
M_cl = 10^7 M_sol
f = 0.20
B_cl = 100
10^5
10^4
10^3
10^2
10
1
0
5
10
15
20
25
B_MC / B_eff (B_eff = 20.6)

3.4) Intermediate mass black holes – IMBHs

Scenario 1 :

Remnants of first stars (pop. III)

$M_\bullet \approx 10^2\, M_\odot$

Scenario 2 :

Collapse of primordial baryon gas

$M_\bullet \approx 10^5\, M_\odot$

In 2 cases, the over-density increases :

$\gamma = 0$

$\gamma = 1$

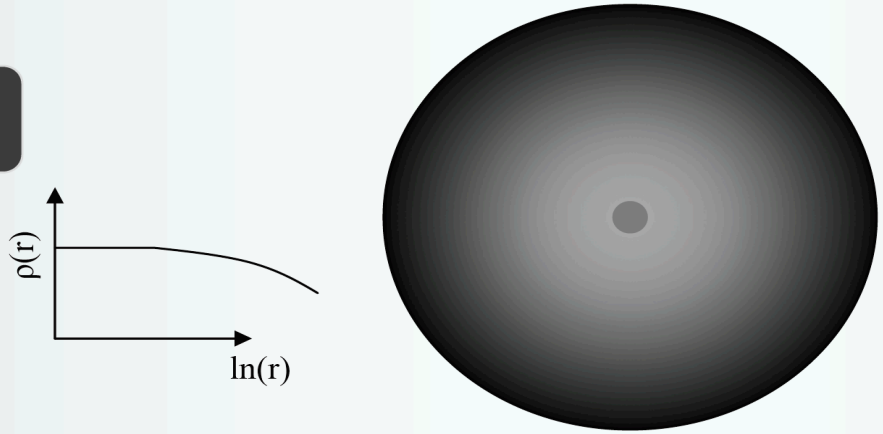

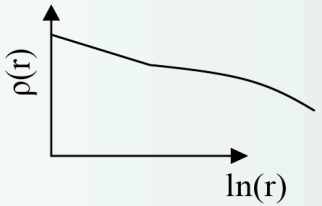

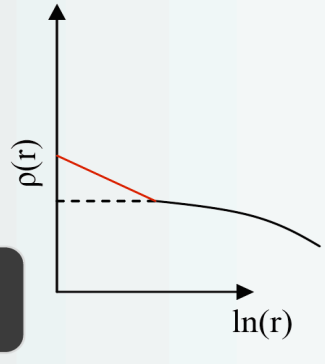

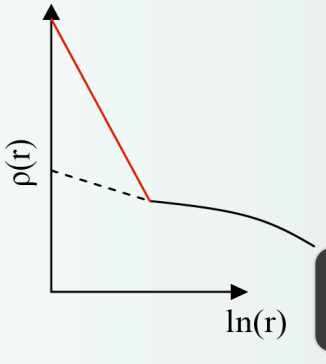

$$\gamma' = \frac{9-2\gamma}{4-\gamma}$$

$\gamma' = 3/2$

$\gamma' = 7/3$

$$\Gamma_{annihilation} \propto \rho^2$$

Mini-Spikes Features

Dark matter density around a type 2 IMBH :

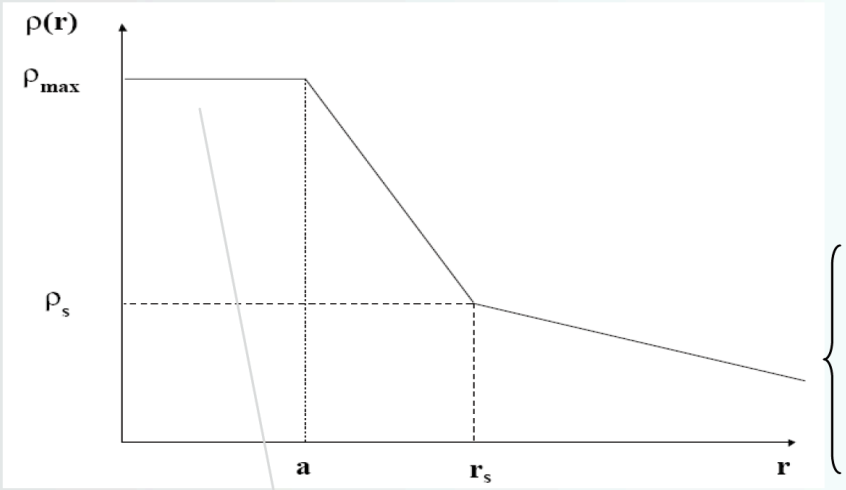

$$\rho_{max} = \frac{m_\chi}{\sigma v \, \tau}$$

Each Black hole is described by M_s, ρ_s, a, r_s

$$\int_{bh} d^3\vec{x}\,(\delta\rho_\chi)^2 = \frac{12\pi}{5} r_s^3 \rho_s^2 \left(\frac{14}{9}\mu - 1\right)$$

- $r_s \approx 1$ pc
- $a \approx 0.1$ pc
- $R_{schwartzchild} \approx 10^{-8}$ pc

with $\mu = \left(\frac{\rho_{max}}{\rho_s}\right)^{\frac{5}{7}}$

⇒ The annihilation rate has not the usual dependence on σv and m_χ :

Intuitively,

$$\Gamma \propto \frac{\sigma v}{m_\chi^2}$$

Because of the ρ_{max} dependence,

$$\Gamma \propto (\sigma v)^{2/7} m^{-9/7}$$

Less model dependent predictions :

a *decrease of σv*

is partially compensated by the

Increase of density around IMBHs

Number of IMBHs and Spatial Distribution

Antimatter fluxes (P.B., G. Bertone, J. Lavalle, P. Salati, R. Taillet):

convolution between the Green function and the probability density functions

Number of unmerged black holes

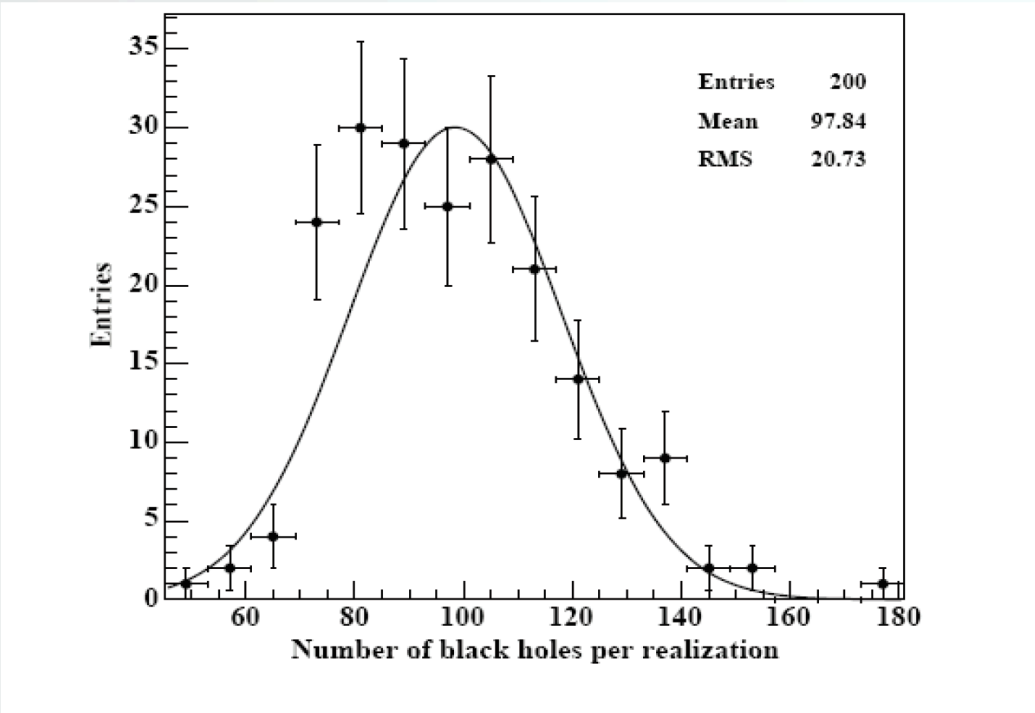

Spatial repartition

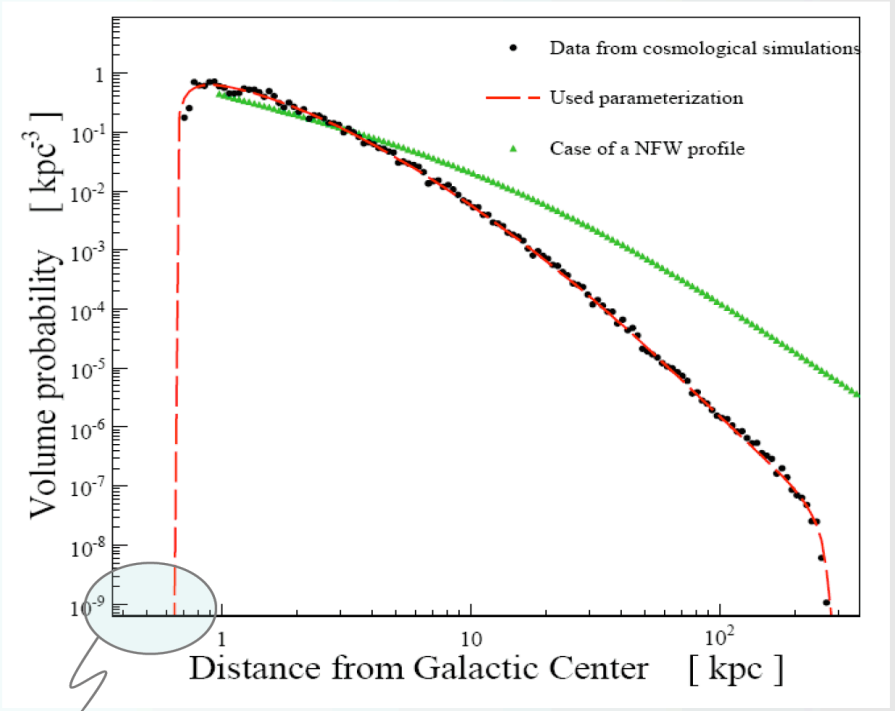

$N_{bh} = 98 \pm 20$

Near Galactic Center, black holes have lost their mini-spikes

G. Bertone, P. Brun, J. Lavalle, P. Salati & R. Taillet

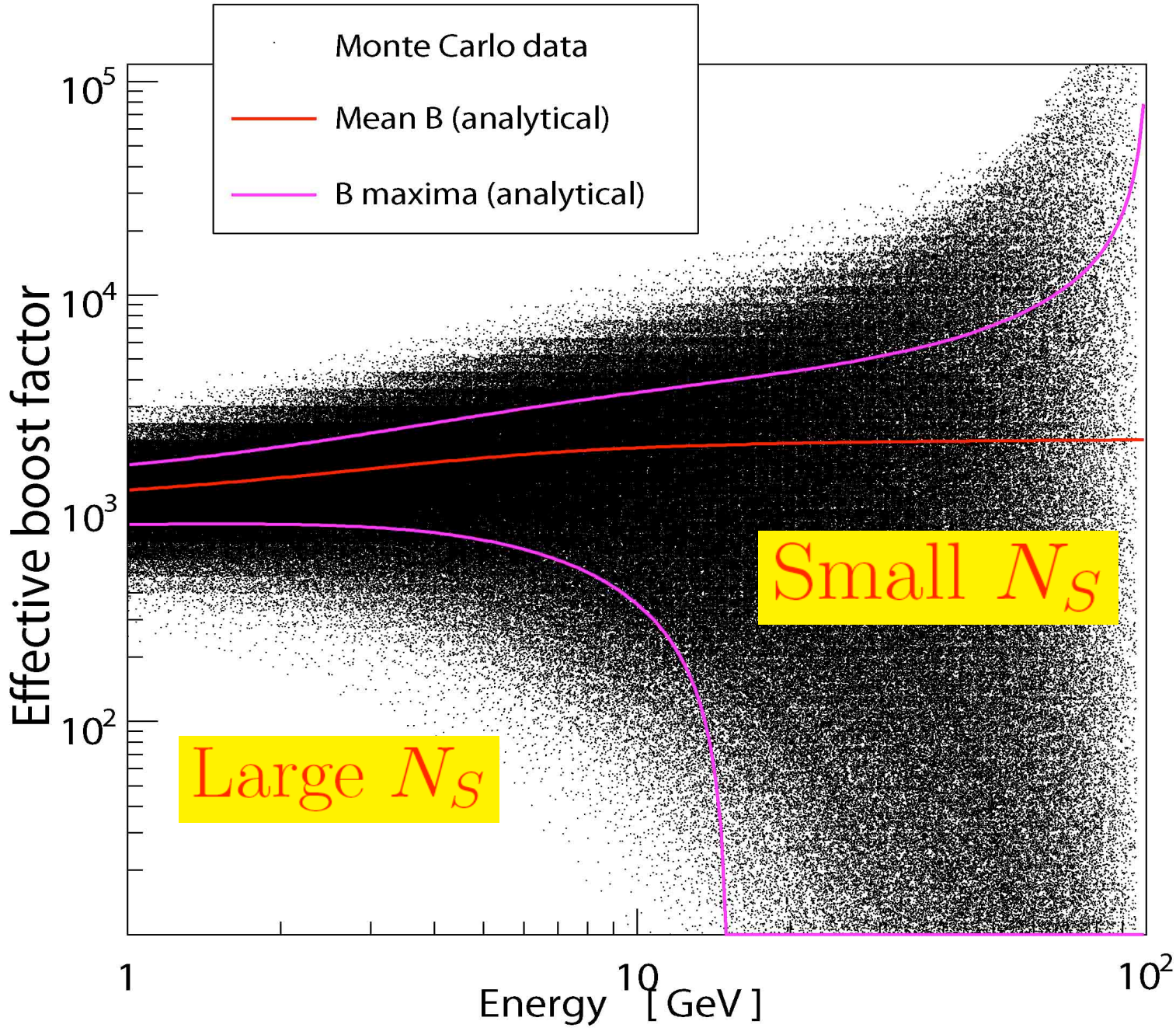

Large N_S regime

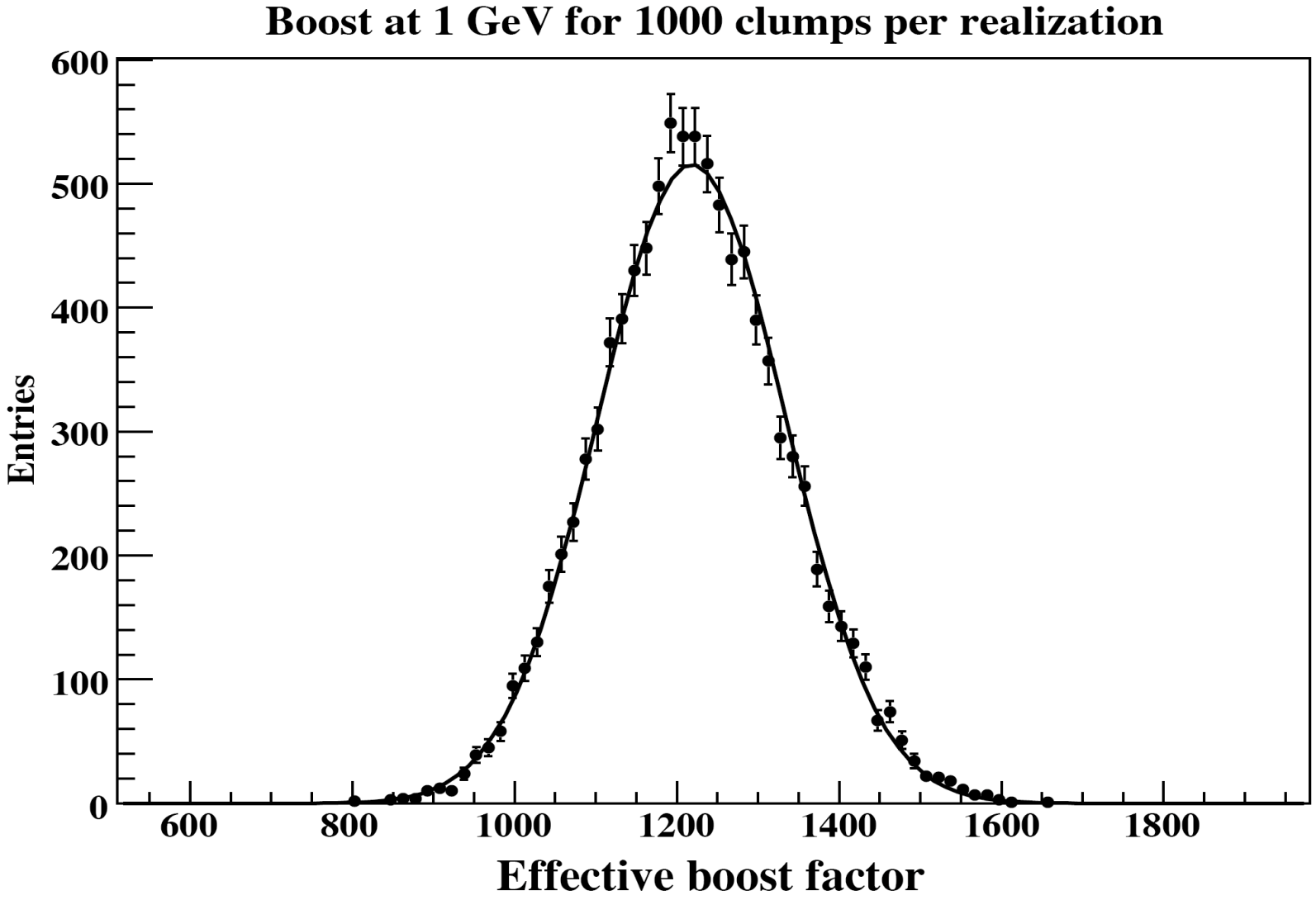

Small N_S regime

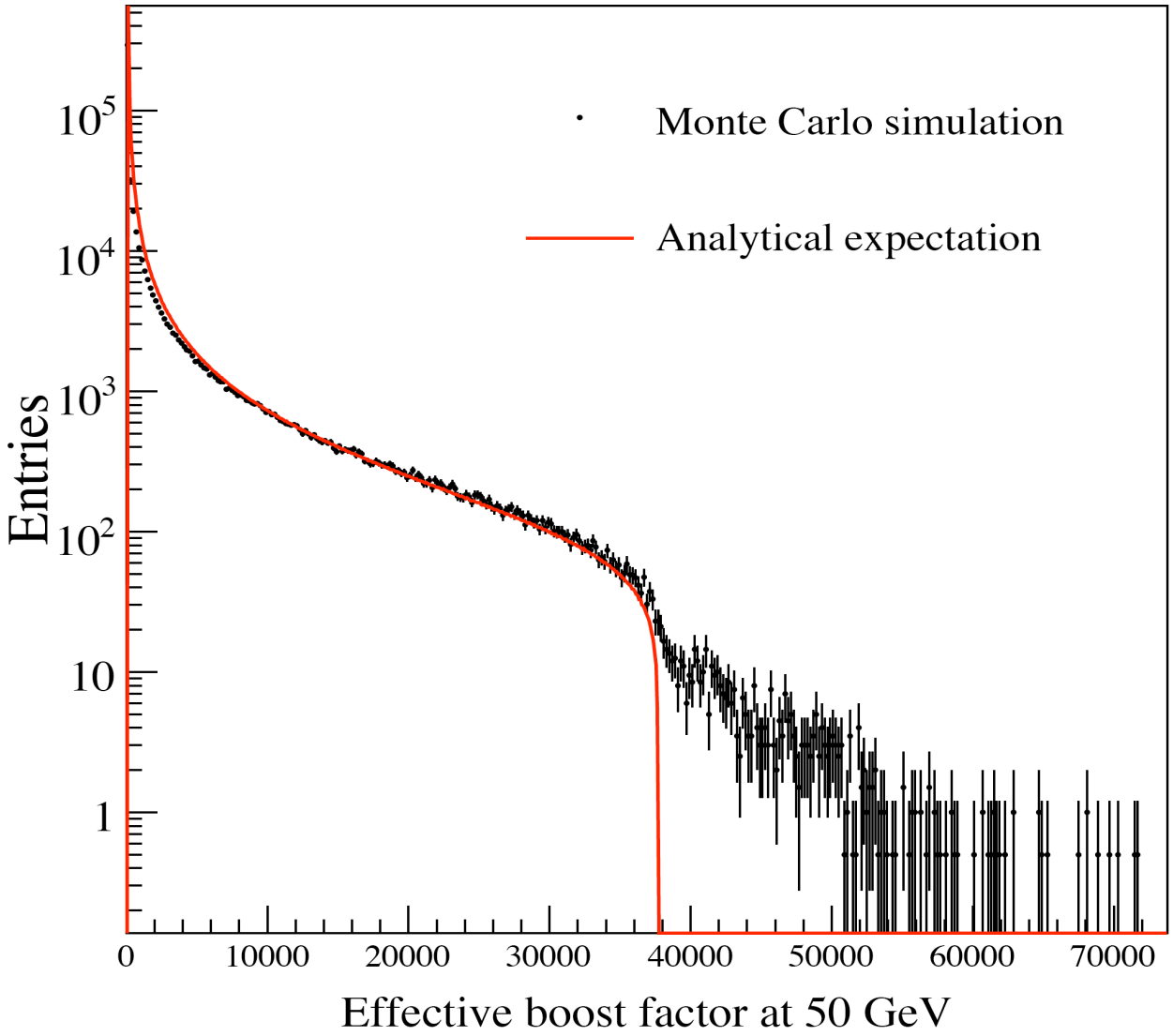

DM model	m	$\langle\sigma_{\rm ann}v\rangle$	$t\bar{t}$	$b\bar{b}$	$c\bar{c}$	$s\bar{s}$	$u\bar{u}$	$d\bar{d}$	ZZ	W^+W^-	HH	gg
LSP1.0	1.0	0.46	-	-	-	-	-	-	-	100	-	-
LKP1.0	1.0	1.60	10.9	0.7	11.1	0.7	11.1	0.7	0.5	1.0	0.5	0.5
LSP1.7	1.7	102	-	-	-	-	-	-	20.1	79.9	-	-
LKP1.7	1.7	0.55	11.0	0.7	11.1	0.7	11.1	0.7	0.5	0.9	0.5	0.5

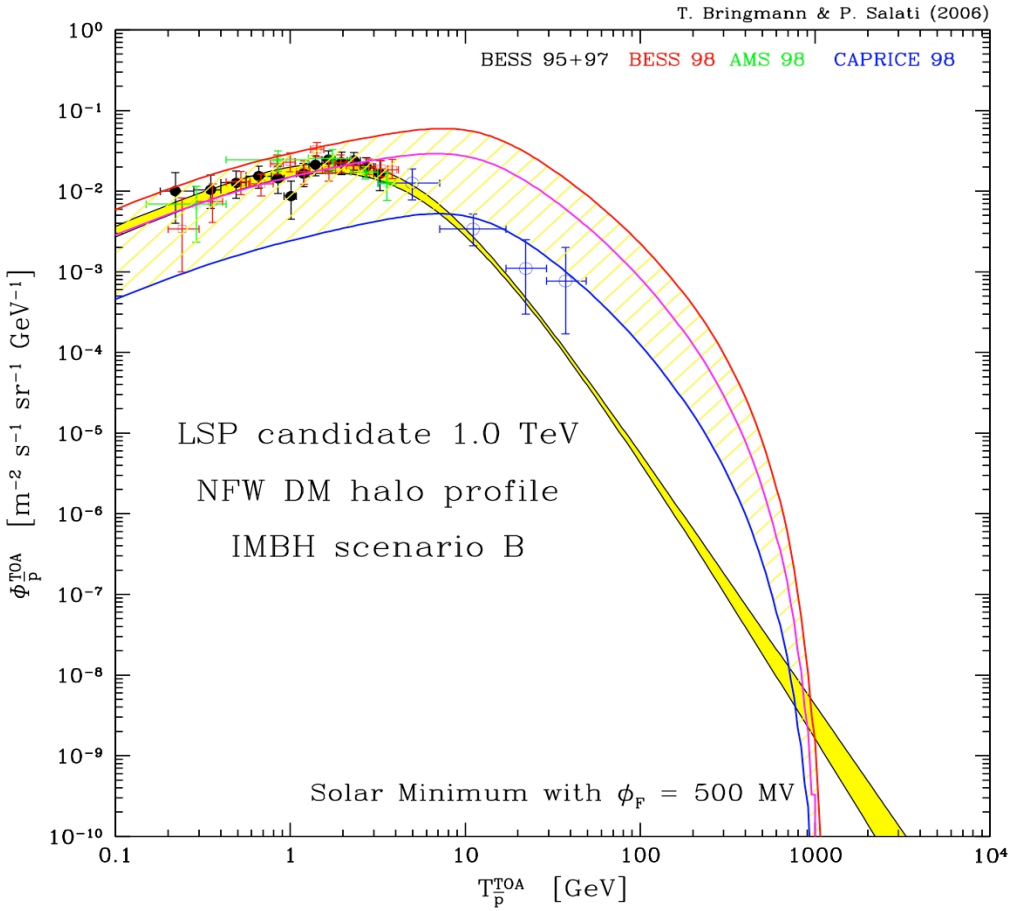

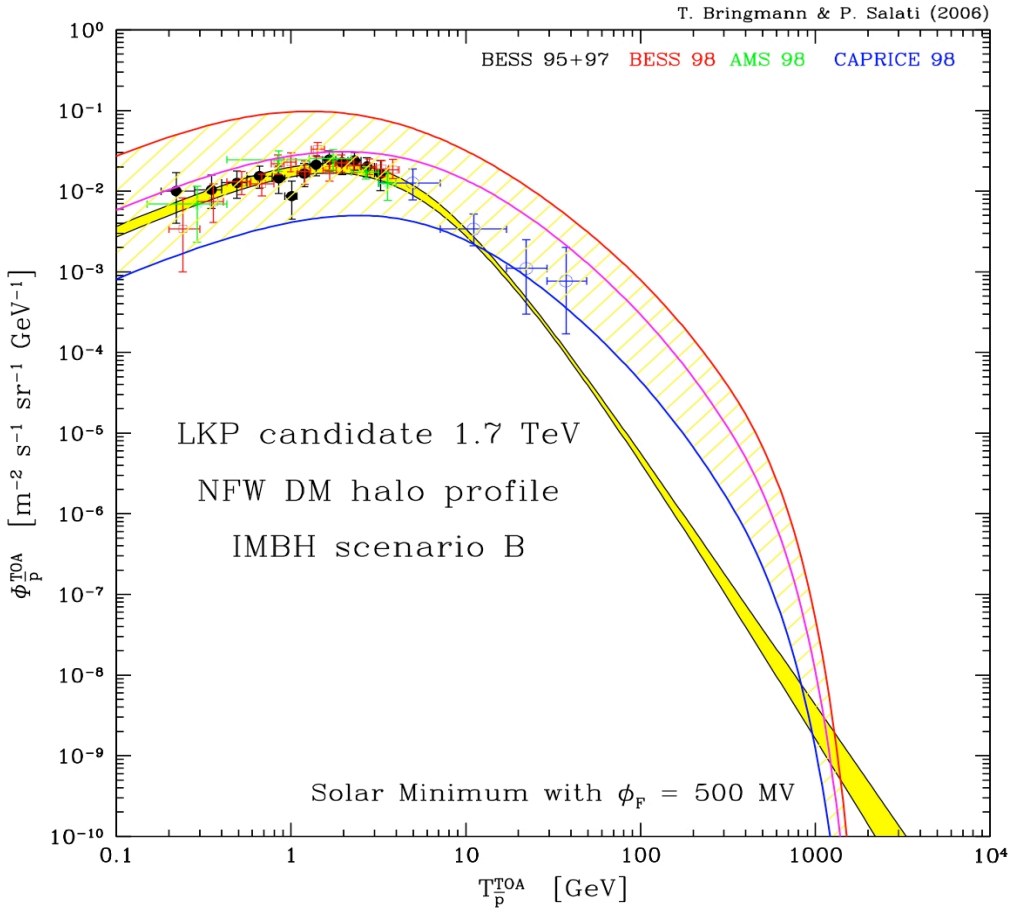

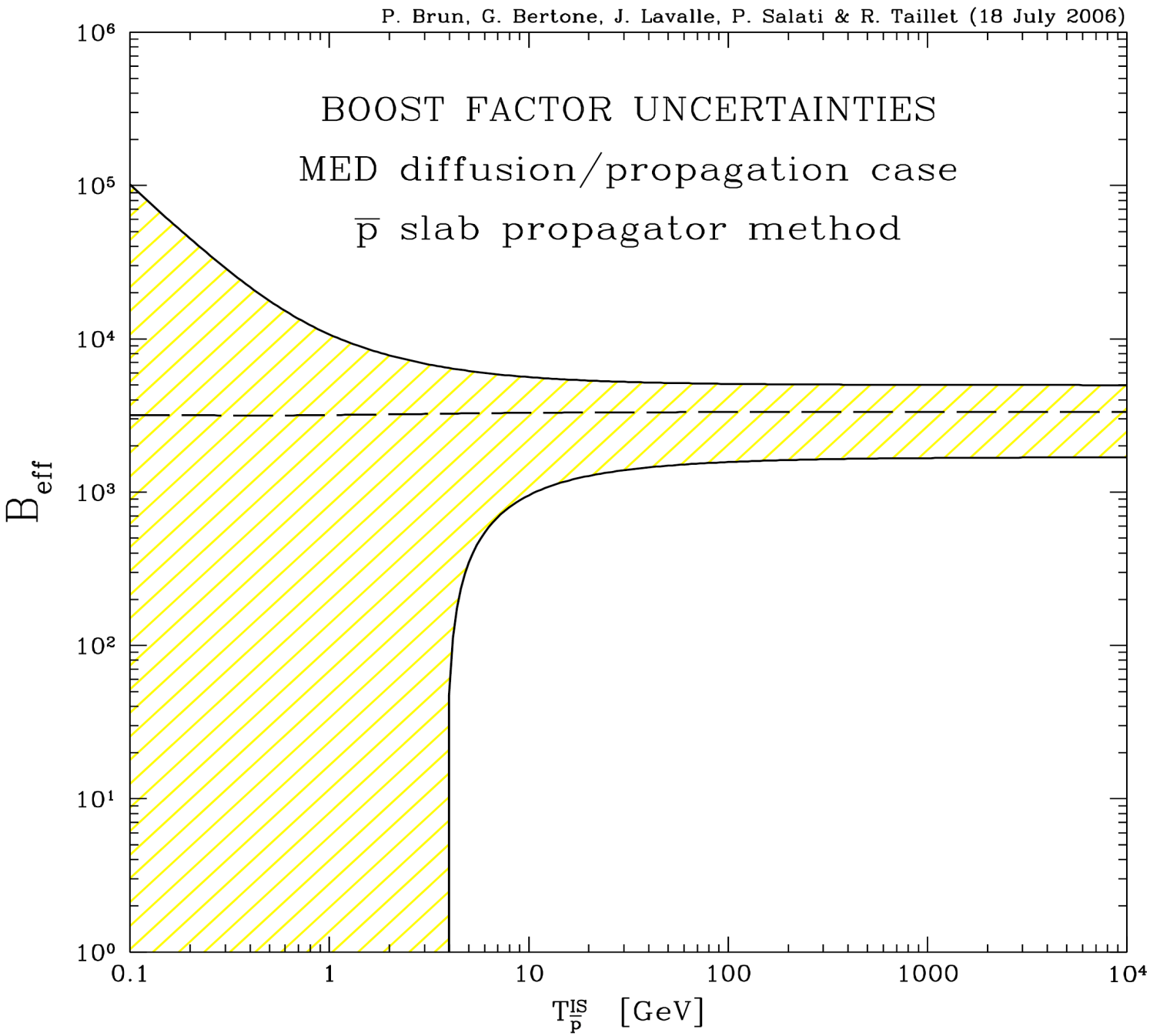
P. Brun, G. Bertone, J. Lavalle, P. Salati & R. Taillet (18 July 2006)
BOOST FACTOR UNCERTAINTIES
MED diffusion/propagation case
$\bar{p}$ slab propagator method
B_{eff}
10^6
10^5
10^4
10^3
10^2
10^1
10^0
0.1
1
10
100
1000
10^4
$T_{\bar{p}}^{IS}$ [GeV]

Positron flux in the IMBHs scenario

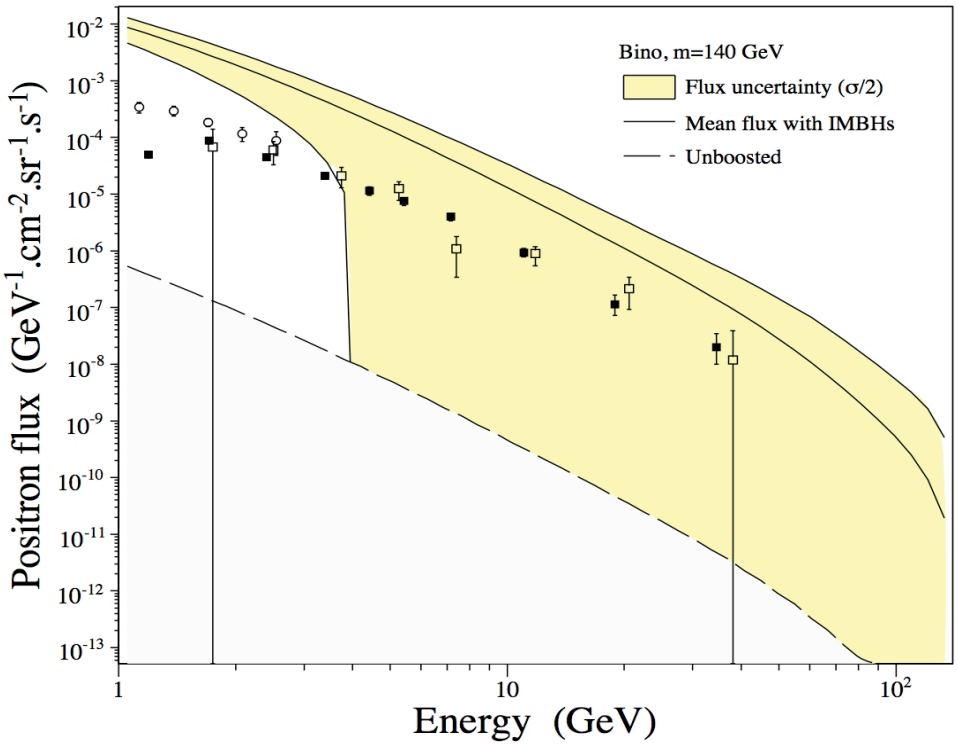

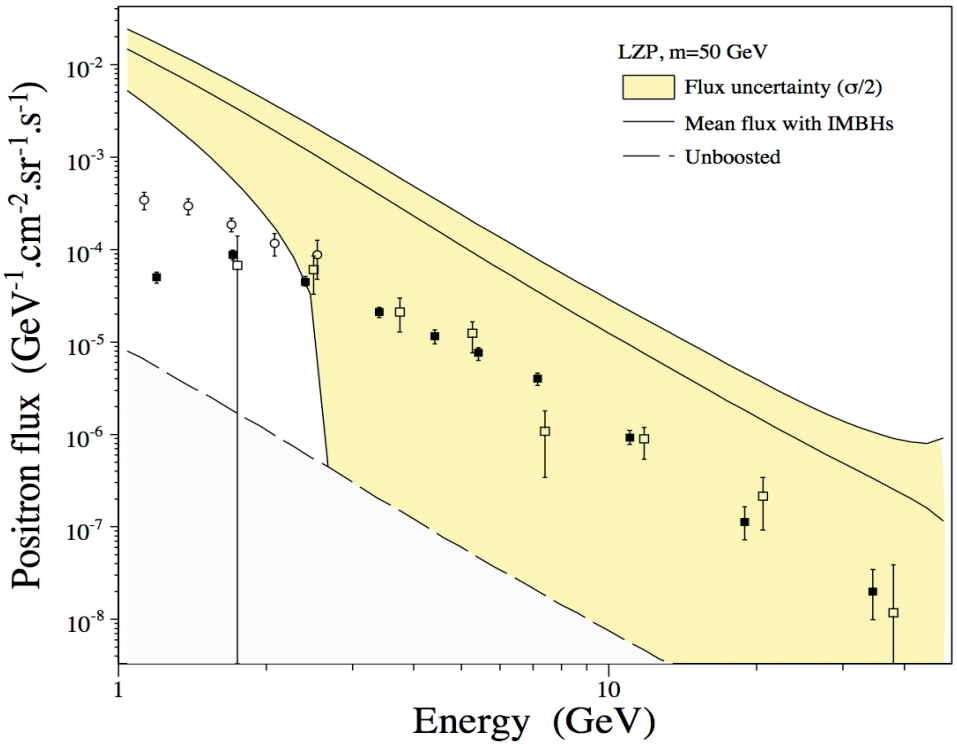

Work in progress !

- Are IMBH clumps detectable with positrons ?
- How far can we probe the SUSY parameter space ?
- Could antiprotons set also stringent constraints ?
- What about Universal Extra Dimensions in that case ?

4) Conclusions and perspectives

MOND has well survived the bullet cluster !

A plausible alternative including neutrinos

3D clear picture of the dark skies has emerged

DM indirect signatures and clumps

We have the tools !

- The boost factor of the **signal** $B_{\rm eff}$ depends on the energy
- Two statistical regimes appear depending on N_S – the average number of clumps that participate in the signal at the Earth.

$$\frac{\sigma_r}{\langle \phi_r \rangle} \simeq \frac{\sigma_B}{B_{\rm eff}} \simeq \frac{1}{\sqrt{N_S}}$$

- Large $N_S \Rightarrow$ maxwellian distribution.
- Small $N_S \Rightarrow \mathcal{P}_{N_H}\left\{0 \leq \varphi \leq \varphi_{\rm max}\right\} \simeq N_H \times \mathcal{P}_1\left(\varphi\right)$